

**Combatting Respiratory Pathogens  
in Cystic Fibrosis:  
Novel Approaches in Bacterial  
Targeting, Biofilm Disruption and  
Sugar Purification**

Karinna Saxby

Masters by Research

University of York

Biology

October 2017

## ABSTRACT

*Pseudomonas aeruginosa*, *Staphylococcus aureus*, *Burkholderia cepacia* and *Stenotrophomonas maltophilia* frequently establish chronic lung infections in Cystic Fibrosis (CF) patients and engender significant morbidity and, in some cases, death. Partially owing to adaptive mechanisms, including the production of biofilms and virulence factors, these pathogens have developed resistance to conventional antimicrobials. To combat these pathogens, novel interventions are required. This pre-clinical study explores three such approaches.

The first approach investigated a novel carbon monoxide releasing molecule (CORM) that had been designed to target the pseudomonal virulence factor, pyocyanin. *In vitro* testing of this drug, termed pyo-CORM, showed non-specific pyocyanin activation and reduced bacterial growth and biofilm formation in *P. aeruginosa*, *S. aureus* and *S. maltophilia*.

The second strategy explored the disruptive capacity of sugar fragments (alginate) against pseudomonal biofilms. We generated and tested alginate fragments, with average degrees of polymerisation within the range of 1-28, against *P. aeruginosa* PA01 *in vitro*. Our study found that the fragments were able to perturb growth and disrupt biofilms in PA01 at concentrations exceeding 5 wt% and that smaller fragments were more effective at biofilm disruption than larger fragments.

Lastly, this project explored novel purification strategies for the synthesis of sugar-based vaccines using the polysaccharide, and virulence factor, poly-*N*-acetylglucosamine (PNAG) as a reference. With the aim of improving purity and efficiency in sugar synthesis, this study investigated a photochemical solid phase cleavage method and a selective bead-mediated recovery strategy. These methods, and the design of a continuous UV flow reactor, achieved successful photocleavage and selective recovery of a tagged *N*-acetylglucosamine (NAG) building block.

The results presented in this project highlight the need for ongoing work in these areas. With new treatments will come new adaptations and therefore it is likely that a combination of novel approaches will be key in combatting CF pathogens in the future.

# LIST OF CONTENTS

<b>Abstract.....</b>	<b>2</b>
<b>List of Contents.....</b>	<b>3</b>
<b>List of Tables.....</b>	<b>8</b>
<b>List of Figures .....</b>	<b>9</b>
<b>Acknowledgements .....</b>	<b>14</b>
<b>Author’s Declaration.....</b>	<b>15</b>
<b>Section 1: Background and Literature Review.....</b>	<b>16</b>
<b>1.1. Cystic Fibrosis.....</b>	<b>16</b>
<b>1.2. Pulmonary Infections and Lung Microbiota .....</b>	<b>17</b>
<b>1.3. Importance and Pathogenesis of <i>P. aeruginosa</i> in CF .....</b>	<b>18</b>
1.3.1. Biofilms.....	19
<b>1.4. Treatment of <i>P. aeruginosa</i> in CF .....</b>	<b>20</b>
1.4.1. Antibiotic Therapy.....	20
1.4.2. Anti-inflammatory Treatment.....	21
<b>1.5. Novel Treatment Strategies .....</b>	<b>21</b>
1.5.1. Ion Channel Modulators .....	21
1.5.2. Novel Antibacterial Compounds .....	22
1.5.3. Anti-virulence Strategies.....	23
1.5.4. Vaccination.....	23
<b>1.6. Project Context and Scope .....</b>	<b>24</b>
<b>Section 2: Targeting <i>P. aeruginosa</i> in CF Pulmonary Infections .....</b>	<b>25</b>
<b>2.1. Background .....</b>	<b>25</b>
2.1.1. Carbon Monoxide Therapy .....	25
2.1.2. CO Releasing Molecules .....	26

2.1.3.	Activation Requirements .....	26
2.1.4.	CORMs with Antibacterial Action.....	27
2.1.5.	Towards a Virulence Factor activated CORM .....	28
2.1.6.	Targeting a Bacterial Virulence Factor .....	29
2.1.7.	CORM Activation by Synthetic Pyocyanin.....	29
<b>2.2.</b>	<b>Aims .....</b>	<b>32</b>
<b>2.3.</b>	<b>Hypothesis .....</b>	<b>32</b>
<b>2.4.</b>	<b>Materials and Methods .....</b>	<b>32</b>
2.3.1.	CORM .....	32
2.3.2.	Strains .....	32
2.3.3.	pyo-CORM Toxicity Assays .....	33
2.3.4.	pyo-CORM Biofilm Assays .....	33
2.3.5.	Data Analysis .....	33
<b>2.5.</b>	<b>Results and Discussion.....</b>	<b>33</b>
2.5.1.	pyo-CORM and PA01 Assays .....	33
2.5.2.	pyo-CORM Assays for PA01 and Phenazine Mutant.....	35
2.5.3.	pyo-CORM Assays for <i>Ralstonia</i> , <i>Staphylococcus</i> and <i>Stenotrophomonas</i> Species	36
<b>2.6.</b>	<b>Conclusions and Future Work .....</b>	<b>37</b>
<b>Section 3: Targeting Biofilms in Model CF Infections.....</b>		<b>39</b>
<b>3.1.</b>	<b>Background .....</b>	<b>39</b>
3.1.1.	Biofilms.....	39
3.1.2.	The Mucoïd Form of <i>P. aeruginosa</i> .....	39
3.1.3.	The Importance of Alginate in <i>P. aeruginosa</i> Pathogenesis .....	40
3.1.4.	Alginate as a Biofilm Disruptor .....	40
<b>3.2.</b>	<b>Aims .....</b>	<b>41</b>
<b>3.3.</b>	<b>Hypothesis .....</b>	<b>41</b>

<b>3.4. Materials and Methods .....</b>	<b>41</b>
3.3.1. Alginate Hydrolysis.....	41
3.3.2. Alginate Viscosity .....	41
3.3.3. Separation of Hydrolysed Alginate .....	42
3.3.4. Growth of PA01 in Hydrolysed Alginate .....	42
3.3.5. Biofilm Assays of PA01 in Hydrolysed Alginate.....	42
3.3.6. Dosing of PA01 in Hydrolysed Alginate.....	42
3.3.7. Hydrolysed Alginate and Separated Hydrolysed Alginate PA01 Assays .	42
3.3.8. Synergistic CORM and Alginate Assays .....	43
3.3.9. Long Term Exposure to Hydrolysed Alginate.....	43
3.3.10. Assessing Pyocyanin Levels in Alginate Treated PA01 Cultures.....	43
<b>3.5. Results and Discussion.....</b>	<b>43</b>
3.4.1. Hydrolysed Alginate Analysis .....	43
3.3.11. Separated and Non-separated Hydrolysed Alginate .....	45
3.3.12. Hydrolysed Alginate Affects Growth and Biofilm Formation.....	47
3.3.13. Dosing with Hydrolysed Alginate .....	49
3.3.14. Long-term Exposure of PA01 to Hydrolysed Alginate.....	49
3.3.15. Synergistic pyo-CORM and Hydrolysed Alginate Assays.....	50
3.3.16. Hydrolysed Alginate Influences Pyocyanin Production .....	52
<b>3.6. Conclusions and Future Work .....</b>	<b>53</b>
<b>Section 4: Optimising Sugar Purification Methods .....</b>	<b>55</b>
<b>4.1. Background .....</b>	<b>55</b>
4.1.1. Towards Bacterial Vaccines.....	55
4.1.2. Making Sugars for Vaccines .....	56
4.1.3. Solid Phase Oligosaccharide Synthesis.....	56
4.1.4. Automated Solid Phase Oligosaccharide Synthesis .....	58
4.1.5. Towards Automated Synthesis of Poly- <i>N</i> -acetylglucosamine .....	59

4.1.6.	Building Block and Protection Strategies .....	59
4.1.7.	Post Synthesis Cleavage and Purification Strategies .....	60
4.1.8.	Choice of Linker.....	61
4.1.9.	Photocleavage in a continuous flow UV reactor.....	62
4.1.10.	Purification by Tagging and Capture.....	62
<b>4.2.</b>	<b>Aims .....</b>	<b>64</b>
<b>4.3.</b>	<b>Hypothesis .....</b>	<b>65</b>
<b>4.4.</b>	<b>Materials and Methods .....</b>	<b>65</b>
4.4.1.	Synthesis of Fmoc Protected 6-aminocaproic acid .....	65
4.4.2.	Removal of Fmoc Protecting Group from NAG Building Block .....	65
4.4.3.	Tagging the NAG Building Block.....	66
4.4.4.	Functionalised Bead Recovery of the NAG Tagged Building Block .....	66
4.4.5.	Construction of a UV Flow Reactor for Photocleavage.....	69
4.4.6.	Calibration of Pump Flow Rates.....	72
4.4.7.	Resin Only Photocleavage Test in Established Reactor Set-up.....	73
<b>4.5.</b>	<b>Results and Discussion.....</b>	<b>73</b>
4.5.1.	Building Blocks .....	73
4.5.2.	Bead Recovery of the Tagged Building Block.....	74
4.5.3.	UV Flow Reactor.....	75
4.5.4.	Resin Photocleavage .....	79
<b>4.6.</b>	<b>Conclusions and Future Work .....</b>	<b>81</b>
<b>Section 5: Project Summary and Future Work .....</b>		<b>82</b>
<b>Appendix.....</b>		<b>84</b>
<b>A1.</b>	<b>Details of Referenced Compounds .....</b>	<b>84</b>
<b>A2.</b>	<b>Details of Referenced Compounds .....</b>	<b>84</b>
<b>A3.</b>	<b>Sample Calculations.....</b>	<b>86</b>
A3.1	Sample calculation for UV flow reactor flow rate at speed 10.0.....	86

<b>A4. Enlarged Mass Spectrometry Results.....</b>	<b>88</b>
Figure A. 6- Photocleavage of Resin.....	94
<b>Bibliography .....</b>	<b>95</b>

## LIST OF TABLES

### Section 1

Table 1. 1 – Mutations in CFTR gene and associated effects. Adapted from Wilschanski <i>et al.</i> (1995) and De Boeck <i>et al.</i> (2014).....	16
--	----

### Section 2

N/A

### Section 3

Table 3. 1 – Viscosity of alginate at different hydrolysis times .....	45
--	----

### Section 4

Table 4. 1 - UV Flow Reactor Specifications obtained for final set-up.....	77
--	----



## LIST OF FIGURES

### Section 1

N/A

### Section 2

- Figure 2. 1- Chemical structure of pyocyanin (right) and green wound discoloration characteristic of *P. aeruginosa* infection (left). Adapted from Mutluoglu and Uzun (2011). ..... 29
- Figure 2. 2- Structure of pyo-CORM comprises a manganese central transition metal and 4 carbonyl groups in a tetraethylammonium salt..... 30
- Figure 2. 3- IR spectra of the reaction of 5 mM of pyo-CORM and 2.5 mM of pyocyanin over 35 mins..... 30
- Figure 2. 4- FTIR spectra of the reaction of 5 mM of pyo-CORM and 2.5 mM of pyocyanin over 35 mins..... 31
- Figure 2. 4- Growth of PA01 for 24 hours at 37°C in either 10 or 100vol% LB. Bacteria were grown in increasing concentrations of pyo-CORM. .... 34
- Figure 2. 5- Biofilm assay for PA01 for 24 hours at 37°C in either 10 or 100 vol% LB. Assays shown for bacteria grown in increasing concentrations of pyo-CORM..... 34
- Figure 2. 6- Growth of PA01 and the *P. aeruginosa* phezanine mutant ( $\Delta$ phz) for 24 hours at 37°C. Bacteria were grown in 10 vol% LB in concentrations of pyo-CORM ranging from 0 to 800  $\mu$ M. .... 35
- Figure 2. 7- Biofilm assay of PA01 and the *P. aeruginosa* phezanine mutant ( $\Delta$ phz) grown for 24 hours at 37°C. Bacteria were grown in 10 vol% LB in concentrations of pyo-CORM ranging from 0 to 800  $\mu$ M..... 35
- Figure 2. 8 - Growth of microbial species for 24 hours at 37°C in 10 vol% LB. Microbial species were grown in concentrations of pyo-CORM ranging from 0 to 800  $\mu$ M.. 36
- Figure 2. 9- Biofilm assay for of microbial species for 24 hours at 37°C in 10 vol% LB. Microbial species were grown in concentrations of pyo-CORM ranging from 0 to 800  $\mu$ M..... 37

### Section 3

Figure 3. 1 – CORMs that have shown to exert bactericidal activity against <i>Escherichia coli</i> and <i>Staphylococcus aureus</i> . Adapted from Nobre <i>et al.</i> (2007). .....	27
Figure 3. 2 – Image showing non-mucoid (left) and mucoid (right) variants of <i>P. aeruginosa</i> grown on a Petri dish. Mucoid variant shows characteristic production of the viscous substance alginate. (Damron and Goldberg, 2012). .....	39
Figure 3. 3 – Chemical structure of an alginate oligomer comprising mannuronate (M) and guluronate (G) residues joined by $\beta$ -1-4 glycosidic linkages. Image shows an alginate pentamer with residue sequence MGGMM. ....	40
Figure 3. 4- Mass spectrometry analysis of the non-separated hydrolysed alginate mixture. Results obtained in ESI negative mode. ....	44
Figure 3. 5- Mass spectrometry analysis of the separated hydrolysed alginate. Results obtained in ESI negative mode. ....	44
Figure 3. 6- Growth of PA01 for 24 hours at 37°C in 10 and 50 vol% LB. PA01 was exposed to either separated hydrolysed alginate or non-separated hydrolysed alginate... ..	46
Figure 3. 7- Biofilm assay of PA01 grown for 24 hours at 37°C in 10 and 50 vol% LB. PA01 was exposed to either separated hydrolysed alginate or non-separated hydrolysed alginate.....	46
Figure 3. 8- Growth of PA01 in 10 and 100 vol% LB containing varying concentrations of alginate for 24 hours at 28°C. (top left) and for 24 hours at 37°C (top right). Biofilm Assays for PA01 in 10 and 100 vol% LB containing varying concentrations of alginate for 24 hours at 28°C (bottom left) and for 24 hours at 37°C (bottom right). .....	48
Figure 3. 9 – Biofilm Assay for PA01 cultures at 37°C after 1 hour treatment with either water or hydrolysed alginate. ....	49
Figure 3. 10 - PA01 growth at 37°C in 50 vol% LB containing either 0, 5 or 10 wt% hydrolysed alginate. Measurements taken at 48 and 288 hours. ....	50
Figure 3. 11 - PA01 biofilm assay after growth at 37°C in 50 vol% LB containing either 0, 5 or 10 wt% hydrolysed alginate. Assays performed at 48 and 288 hours.....	50
Figure 3. 12 - Growth of PA01 cultures in 10 vol% LB exposed to CORM, hydrolysed alginate (with 500 or 1000 $\mu$ M water treatment), or both. Assays incubated at 28°C for 24 hours.....	51

Figure 3. 13 - Biofilm assays for PA01 cultures grown in 10 vol% LB exposed to CORM, hydrolysed alginate (with 500 or 1000 $\mu$ M water treatment), or both. Assays incubated at 28°C for 24 hours. ....	51
Figure 3. 14 - Image of PA01 growth in 100 vol% LB (top row) and PA01 growing in 100%LB with alginate treatment (bottom row).....	52
Figure 3. 15 - PA01 pyocyanin production and bacterial growth after growth at 37°C in either 10 or 100 vol% LB and containing either 0, 2.5, 5 or 10 wt% hydrolysed alginate. Pyocyanin levels (assumed proportional to absorbance at 691 nm) generated per total bacterial growth. ....	53
<b>Section 4</b>	
Figure 4. 1 - Upon activation of X, A $\beta$ -1-4 Glycosidic linkage is formed between the anomeric centre of the glycosyl donor and the hydroxyl group of the glycosyl acceptor anchored to the resin. 'X' refers to a good leaving group (e.g. I, NHCTA). Adapted from (Davis and Fairbanks, 2002).....	57
Figure 4. 2 - an $\alpha$ -form and $\beta$ -form of a glucose Monosaccharide. Adapted from (Davis and Fairbanks, 2002).....	58
Figure 4. 3 - Monomer of <i>N</i> -acetylglucosamine (NAG).....	59
Figure 4. 4 - The <i>N</i> -acetylglucosamine (NAG) building block; NAG with protecting groups. ....	59
Figure 4. 5 - Selective Deprotection of Glycosyl acceptor with piperidine.....	60
Figure 4. 6 - Activation of Sulphur ether group on glycosyl donor using NIS/TMSOTf. Reactive acyloxonium ion only susceptible to $\beta$ attack. ....	60
Figure 4. 7 - Photocleavable <i>O</i> -benzyl Linker attached to Merrifield Resin (Grey Circle). Adapted from (Calin <i>et al.</i> , 2013a).....	61
Figure 4. 8 - Photocleavage of the Linker liberates the resin and leaves a functional CBz protected amine group attached to the sugar. ....	62
Figure 4. 9 - In the synthesis of oligosaccharide chains, the addition of the building block to Glycosyl accepto will result in a) desired glycosylation and sugar extension or b) unreacted 'deletion sequences'. ....	63

Figure 4. 10 - Acetylation of free hydroxyl groups in NAG by acetic anhydride (AcO <sub>2</sub> ) and a base yields an acetate group at the C6 position, thereby preventing subsequent glycosylation. ....	63
Figure 4. 11 - Aminocaproic acid used as a Tag in catch-and-release strategy. ....	64
Figure 4. 12 - The tag (Fmoc protected aminocaproic acid) is generated from 6-aminocaproic acid (adapted from Kröck <i>et al.</i> (2012)). ....	64
Figure 4. 13 - Polymer bound benzoyl chloride beads used for capturing tag. ....	66
Figure 4. 14 – The functionalised benzoyl chloride beads will react with the amine group present on the full-length sugars. This reaction generates hydrochloric acid and anchors the full-length sugar to the beads. ....	68
Figure 4. 15 – Recovery of NAG Building Block from functionalised beads by sodium methoxide/methanol mediated cleavage of 6-aminocaproic acid tag. ....	68
Figure 4. 16 – Set-up for Continuous Flow UV reactor. ....	69
Figure 4. 17 – Autodesk Inventor Sketches for 3D Printed Peristaltic Pump (Diameter Arrow 4.7 cm). ....	70
Figure 4. 18 – Peristaltic Pump and manual control system. Tygon Tubing is Fed into the pump from a water reservoir and held in place with two red clips. ....	70
Figure 4. 19 – Preliminary Set-up with three way PVDF Connection integrated in to FEP tubing with Needles. ....	71
Figure 4. 20 – Re-purposed Äkta mixing chamber used as FEP tubing and Syringe connector point. Threaded screw fittings allow for tighter, more secure seal. Note small needle insertion at solvent entry point. ....	72
Figure 4. 21- Mass Spectra for Fmoc Protected 6-aminocaproic acid tag containing a sodium ion adduct (See Appendix for more detail). ....	73
Figure 4. 22- MS results after silica column purification of Fmoc removed NAG building block containing a sodium ion adduct (See Appendix for more detail). ....	74
Figure 4. 23- Fmoc protected 6-aminocaproic acid Tagged NAG building block containing a sodium ion adduct (See Appendix for more detail). ....	74
Figure 4. 24- Mass spectrometry results from Sugar recovered from Carboxylated polystyrene beads in Cartridge A (See Appendix for more detail). ....	74

Figure 4. 25- Mass spectrometry results from Sugar recovered from Carboxylated polystyrene beads in Cartridge B (See Appendix more detail). ..... 75

Figure 4. 26- Final UV Flow Reactor set-up. Pump Draws water from reservoir and pumps into Intermediate Solvent container. DCM is then withdrawn and pushed through into FEP Tubing. Resin is injected as the Injection point and pushed through Reactor by Pump Pressure. FEP tubing at Reactor exit is directed into a frit-containing cartridge for immediate filtration and separation of cleaved product. .... 75

Figure 4. 27- Schematic of Intermediate Reservoir container showing biphasic conditions that allow for solvent uptake into FEP tubing. .... 76

Figure 4. 28- Intermediate Container Lid showing Syringe Fitting connected to filter-containing cartridge (Left) or Syringe at the solvent uptake point..... 77

Figure 4. 29- Flow Rates for Peristaltic Pump settings obtained with DCM. .... 78

Figure 4. 30- Graphical representation of the Single-pass Irradiation time ranges that can be achieved in a single pass within the achievable pump flow rates. .... 79

Figure 4. 31- Mass spectra of Product obtained from Resin-only photocleavage showing product present with a sodium ion adduct (See Appendix for more detail) ..... 80

## ACKNOWLEDGEMENTS

I would like to thank my amazing supervisors, Alison Parkin, Ville Friman and Martin Fascione, everyone in the Parkin/Fascione lab, Leo Caves and Julie Knox, my fellow CIDCATS and my partner Liam for being a fantastic source of support and laughter throughout my time in York. I absolutely couldn't have done this work without you.

## AUTHOR'S DECLARATION

I, Karinna Saxby, declare that this thesis is a presentation of original work and I am the sole author. This work has not previously been presented for an award at this, or any other, University. All sources are acknowledged as References.

## SECTION 1: BACKGROUND AND LITERATURE REVIEW

### 1.1. Cystic Fibrosis

Cystic Fibrosis (CF) is the most prevalent genetic disease in the Caucasian population with a carrier rate of 1 in 25 (Troxler *et al.*, 2012). CF is caused by mutations in the cystic fibrosis transmembrane transmembrane-conductance regulator (CFTR) gene which in turn leads to functional irregularities in the CFTR protein (Shah *et al.*, 2016). The CFTR protein is an ion channel (a transmembrane protein) and is important for solute transport and fluid balance across epithelial cells (Hurt and Bilton, 2012, Wood and Ramsey, 1996). In particular, this is important for salt and water balance on the surface of epithelial cells. CFTR protein dysfunction leads to aberrant fluid transport and elevated secretions and levels of mucous in the lungs and other organs (Wood and Ramsey, 1996, Shah *et al.*, 1996). This altered epithelial transport causes reduced mucociliary clearance that predisposes CF sufferers to chronic respiratory infections (Shah *et al.*, 2016, Drevinek and Mahenthalingam, 2010, Kreindler, 2010).

In developed countries, the median survival rate has improved from 14 years, in 1969, to 40 years in 2010 (Döring *et al.*, 2012). However, despite this increase in life expectancy, as CF patients age, their quality of life decreases (De Boeck *et al.*, 2014).

To date, over 1900 mutations of the CFTR gene have been reported (De Boeck *et al.*, 2014). Mutations can be grouped into classes based on the structural change to the CFTR protein and are outlined in Table 1. 1.

**Table 1. 1 – Mutations in CFTR gene and associated effects. Adapted from Wilschanski *et al.* (1995) and De Boeck *et al.* (2014)**

Class	Description Type	Effect on CFTR	Mutation Example
1	Mutations that cause a truncated protein	CFTR protein is non-functional	G621T
2	Aberrantly folded protein is targeted for degradation by cellular machinery.	Absence of CFTR protein at the apical cell membrane	ΔF508
3	Full length CFTR protein is incorporated into membrane but unable to be regulated by cyclic adenosine monophosphate (cAMP)	No chloride ions flow through CFTR protein	G551D



Class	Description Type	Effect on CFTR	Mutation Example
4	CFTR protein has reduced conductance	Movement of chloride ions through the CFTR channel are restricted	R117H
5	Reduced levels of CFTR protein or only partially matured protein	Less functional protein is present at the epithelial cell membrane.	3849 + 10KbC>T, A455E

The most common mutation is  $\Delta F508$  and approximately 50% of all CF patients carry this (Mayer, 2016). The  $\Delta F508$  causes misfolding of the CFTR protein and, often degradation of the misfolded protein (Eckford *et al.*, 2012). The mutation G551D, which leads to a full length CFTR protein but no ion transport, accounts for approximately 4% of all CF cases (Heidi, 2012).

In other mutations, such as R117H, the CFTR protein cannot open as well but still maintains some ion transport activity. In this case, full CF disease does not occur. Some mutations will cause mucous secretion issues in the pancreas but only mildly impact the lungs. This is referred to as atypical CF and can often go undiagnosed for many years (Schram, 2012).

Patients carrying at least one mutation in classes 4 and 5 generally lead to the less severe form of the disease compared to patients who are homozygous for classes 1 – 3 mutations (Castellani *et al.*, 2008).

## 1.2. Pulmonary Infections and Lung Microbiota

Chronic respiratory infection and inflammation in CF patients is the most common cause of morbidity and mortality (Zhao *et al.*, 2012). Pulmonary infections in CF patients are frequently polymicrobial (Goss and Muhlebach, 2011) with common opportunistic pathogens including *Pseudomonas aeruginosa*, *Staphylococcus aureus*, *Stenotrophomonas maltophilia*, *Haemophilus influenzae* and *Burkholderia* species (Drevinek and Mahenthalingam, 2010, Turner *et al.*, 2015, Heijerman *et al.*, 2009a, Goss *et al.*, 2002).

*S. aureus* is often the first bacterium to cause infections in CF patients at a younger age (Marks, 1990). *S. aureus* causes progressive lung damage and has been shown to facilitate coinfection with *P. aeruginosa* (Moigne *et al.*, 2016). The lung microbiota

changes over the lifespan of CF patients, where approximately 27% of CF patients carry *P. aeruginosa* between 2-5 years and over 80% of patients between 25-34 years (Heijerman *et al.*, 2009a). This is partially explained by conventional therapy whereby, with repeated exposure, antibiotic use has been shown to reduce bacterial diversity in the lungs (Zhao *et al.*, 2012). Older CF patients subsequently have predominantly *P. aeruginosa* in their lung microbiota (Zhao *et al.*, 2012). Currently *P. aeruginosa* is the cause of reduced lung function and death in approximately 95% of patients (Stanton, 2017).

As CF patients age, other opportunistic pathogens, such as *Burkholderia cepacia* and *S. maltophilia*, can also become more prevalent (Horsley *et al.*, 2016, Davies and Rubin, 2007). *B. cepacia* infections are associated with poorer health outcomes and earlier mortality rates than non-infected CF patients and *S. maltophilia* has been broadly associated with poor lung function (Chaparro *et al.*, 2001, Davies and Rubin, 2007). Unfortunately, in CF patients, pulmonary infections are inevitable, and between 80 to 95% of CF patients will die from cardiopulmonary failure caused by an infection (Schneider *et al.*, 2016).

### **1.3. Importance and Pathogenesis of *P. aeruginosa* in CF**

Over 80% of CF patients are chronically infected with *P. aeruginosa* (Ratjen *et al.*, 2001). *P. aeruginosa* is a Gram-negative rod-shaped bacterium that is ubiquitous in the environment (Hraiech *et al.*, 2015). Typically, if *P. aeruginosa* is inhaled, innate immune responses, such as phagocytosis, can help clear the invader without initiation of the inflammatory response (Bhagirath *et al.*, 2016, Davies, 2002). In CF patients however, epithelial cells are unable to capture as many *P. aeruginosa* cells and mucociliary clearance is not as effective (Bhagirath *et al.*, 2016, Davies, 2002). Moreover, the airway surface liquid and mucous present in CF airways enables bacteria to adhere to airway cells and establish chronic infections (Davies, 2002).

*P. aeruginosa* has developed resistance to many conventional antibiotics. It is able to do this by undergoing genetic mutations and, within a bacterial population, the occurrence of hypermutable strains that lack effective DNA mismatch repair systems (Heijerman *et al.*, 2009a). Moreover, *P. aeruginosa* possesses multiple efflux pumps in its membrane which enables efflux of antibiotics from within the bacterial cell (Smith *et al.*, 2006).

A broad range of other factors contribute to the persistence of *P. aeruginosa* in CF infections. For example, over the course of a chronic infection, spontaneous mutations occur within the *P. aeruginosa* genome that help it adapt to its environment and persist.

In a study analysing genetic changes in *P. aeruginosa* in a CF patient over 8 years, it was found that several genes underwent mutations (Smith *et al.*, 2006). Mutations in the *mutS* gene were shown to result in hypermutable strains that can rapidly adapt to antibiotic pressure (Smith *et al.*, 2006). The study also found that some virulence factors required for colonisation in acute infections, such as quorum sensing regulators, are not expressed in chronic infections (Smith *et al.*, 2006). This is thought to be associated with immune evasion, whereby the immune system can recognise the virulence factors used in acute infections and kill the bacteria secreting them (Smith *et al.*, 2006). Therefore, through continuous genetic changes, *P. aeruginosa* is able to respond to its changing environment and evade the immune response of the host to establish chronic, ongoing infections in CF patients.

### **1.3.1. Biofilms**

One of the most key mechanisms of pathogenesis for *P. aeruginosa* is the pathogen's ability to grow in biofilms. Biofilms are a structured matrix of bacteria, exopolymeric substances, protein and DNA (Hoiby *et al.*, 2010). Following initial infection, oxygen in the lung mucus is rapidly consumed by bacteria, CF airway cells and immune cells, such as neutrophils (Yoon *et al.*, 2002). This leads to an anaerobic environment, in which *P. aeruginosa* thrives (Yoon *et al.*, 2002). The anaerobic environment supports the secretion of biofilm related molecules, such as polysaccharides, from *P. aeruginosa* and this leads to the development of the dense biofilm structure (Yoon *et al.*, 2002).

The correlation between Pseudomonas biofilm development and persistent infections was first noted in CF patients in 1980 (Lam *et al.*, 1980). Biofilm growth of *P. aeruginosa* in CF lungs causes a slower rate of bacterial growth and is associated with an increased rate of mutations (Hoiby *et al.*, 2010). In addition, the dense polymeric matrix of the biofilm can retard penetration of some antibiotics and thereby prevent the antimicrobial agent 'access' to the bacterial cells (Zhang and Mah, 2008). This reduces antibiotic efficacy as the majority of conventional antibiotics are only effective against readily growing, metabolically active, and accessible, bacteria (Lebeaux *et al.*, 2014). For instance, the minimum inhibitory concentration of tobramycin against *P. aeruginosa* is 50 times higher for biofilms than planktonic cells (Sriramulu, 2013). Moreover, the

polymeric matrix reduces influx and movement of antimicrobial peptides produced by the innate immune response and correspondingly, *P. aeruginosa* in biofilms are more tolerant to host immune responses than their planktonic counterparts (Lebeaux *et al.*, 2014, Sriramulu, 2013).

Together, the increased rate of mutations, impermeable matrix and slower growth rate allow for bacterial adaptation, antibiotic tolerance, immune evasion and the establishment of chronic infections (Hoiby *et al.*, 2010).

#### **1.4. Treatment of *P. aeruginosa* in CF**

##### **1.4.1. Antibiotic Therapy**

To preserve lung function in CF patients with chronic lung infections, antibiotic therapy is commonly used (Döring *et al.*, 2012). Antibiotic eradication therapy (AET) is predominantly used to target *P. aeruginosa* and it has been shown that antibiotic treatment at early stages of *P. aeruginosa* colonisation have positive clinical outcomes for CF patients (Döring *et al.*, 2012). Strategies for AET of *P. aeruginosa* include inhalation of tobramycin, oral ciprofloxacin and inhalation of colistin (Döring *et al.*, 2012).

The efficacy of antibiotic treatment depends on a wide range of factors including method of administration, duration of treatment, different therapeutic combinations, and, of course, bacterial resistance. Subsequently, the success of clearance in CF patients is variable, with the mean efficacy rate ranging between 63 to 100% (Döring *et al.*, 2012).

No standard protocol for AET exists however it has been shown that AET is most effective at clearing *P. aeruginosa* within 12 weeks of initial detection (Döring *et al.*, 2012). This is, in part, explained by the pathogenesis of *P. aeruginosa* as, in the early stages of infection, the bacterial population comprises predominantly non-mucoid strains which are more susceptible to antibiotics than the alginate producing, mucoid variants (Ratjen *et al.*, 2001).

In terms of administration, inhaled tobramycin has been shown to be effective at clearing *P. aeruginosa* but does not reduce lung inflammation (Noah *et al.*, 2010). In addition, a trial comparing intravenous administration of antibiotics to inhaled/oral antibiotic treatment showed that the inhaled and oral antibiotic treatments were more effective at eradication of *P. aeruginosa* in CF patients (Noah *et al.*, 2010). However, this work also demonstrated that the systemic (intravenous) antibiotics were able to reduce inflammation more than the inhaled antibiotic treatments (Noah *et al.*, 2010).

The efficacy of AET is also dependent on the presence of resistant strains in CF patients. To date, *P. aeruginosa* has developed resistance to most modern day antibiotics including carbapenems, fluoroquinolones and aminoglycosides (Fuse *et al.*, 2013). Moreover, the process of AET itself will select for more resistant organisms over time and subsequently, AET is more effective for younger CF patients than older patients. Membrane disruptors, polymyxin B and colistin are often used against multi-drug resistant Gram-negative pathogens however reports of Pseudomonas resistance to these “last in line” antibiotics are becoming more frequent (Schneider *et al.*, 2016).

There are side effects from long-term AET for instance, although azithromycin, a macrolide antibiotic with anti-inflammatory properties, is useful for eradicating bacteria and reducing inflammation, its ability to block autophagy can predispose CF patients to other mycobacterial infections (Renna *et al.*, 2011).

#### **1.4.2. Anti-inflammatory Treatment**

In order to prevent inflammatory-associated lung damage, CF patients are commonly treated with anti-inflammatory medication. Anti-inflammatory treatment can include steroids such as corticosteroids (Smith *et al.*, 2006). High doses of ibuprofen have also shown to slow the progression of lung disease in CF patients (Chmiel and Konstan, 2005). In addition, therapeutics that target and neutralise pro-inflammatory cytokines are being explored as these can cause significant damage in the airways (Chmiel and Konstan, 2005). Antibodies that target TNF-alpha and IL-8 are examples of these. Other therapies that attempt to limit the damage caused by elevated immune response include neutrophil products such as DNase and antioxidants (Chmiel and Konstan, 2005).

### **1.5. Novel Treatment Strategies**

#### **1.5.1. Ion Channel Modulators**

Recently, the combination therapy ivacaftor/lumacaftor (brand name Orkambi) has been approved for treatment of CF patients. In 2012, ivacaftor was approved for use in CF patients with specified mutations – including G551D (Kuk and Taylor-Cousar, 2015). Ivacaftor works by restoring CFTR ion channel activity for channels present at the epithelial cell surface and thereby enabling chloride transport (Eckford *et al.*, 2012). A study on the microbiota changes associated with administration of the drug showed that patients treated with ivacaftor had reduced levels of *P. aeruginosa* and its mucoid variants after one year (Heltshe *et al.*, 2014).

Lumacaftor is used to transport defective CFTR protein to the surface and enhances lung function by increasing the number and function of CFTR channels at the epithelial cell surface (Kuk and Taylor-Cousar, 2015). Clinical studies have found that, when used in combination with ivacaftor, there is significant improvement in patients homozygous for the  $\Delta F508$  mutation (Kuk and Taylor-Cousar, 2015).

Investigation into other modular therapies for patients with heterozygous mutations for F580del and other mutations are currently underway. The possibility of DNA and RNA editing is also an option for future therapies (Kuk and Taylor-Cousar, 2015).

Despite innovative treatments, such as ivacaftor/lumacaftor, the development and persistence of lung infections is still a major threat for CF patients. For instance, the *P. aeruginosa* virulence factor Cif has been found to cause degradation of CFTR rescued by ivacaftor/lumacaftor (Stanton, 2017). In addition, as these drugs are not currently reimbursed in many countries, including Australia and the U.K., treatment cost is a significant issue. For instance, in 2016, the annual cost for Orkambi was approximately £104,000 per patient (Gulland, 2016). Such prices are therefore limiting the use of ion channel modulators in the wider CF population.

### **1.5.2. Novel Antibacterial Compounds**

The majority of conventional antibiotics are ineffective at eradicating *P. aeruginosa* in persistent infections, particularly when the organism is found within a mature biofilm. In response to this problem, the development of novel antibacterial compounds, that are able to disrupt biofilms or target metabolically inactive bacteria (or persisters), has become a priority. To this end, there are a number of studies that have evaluated compounds that can disrupt pseudomonal biofilms (Alexander *et al.*, 2015, Klare *et al.*, 2016, Diaz De Rienzo *et al.*, 2016) and recently researchers have developed novel peptides that were shown to be toxic against both *P. aeruginosa* biofilms and persister cells *in vitro* (Bahar, 2015).

In addition, novel compounds that can specifically target *P. aeruginosa* are being explored. For instance, recently, antimicrobial peptide prodrugs have been developed that are specifically activated by proteases that co-localise with *P. aeruginosa* in the lung (Forde *et al.*, 2014). These prodrugs were shown to be toxic against *P. aeruginosa* in an *in vitro* model and were considered to be, in some ways, more effective than conventional antibiotics in that they could more specifically target the bacterium and

thereby be less toxic to human cells or protective, non-damaging microflora (Forde *et al.*, 2014).

### **1.5.3. Anti-virulence Strategies**

There have been several alternative novel methods proposed to combat multi-drug resistant *P. aeruginosa* in CF patients. One strategy is to target and reduce the effects of virulence factors in order to make the bacteria more innocuous in chronic infections. For instance, targeting a virulence factor that facilitates biofilm production, such as molecules involved in quorum sensing (a method of bacterial communication), could reduce biofilm formation and thereby potentiate antimicrobial therapy or the patient's immune response (Høiby, 2002, Smith and Iglewski, 2003).

### **1.5.4. Vaccination**

Bacterial vaccines have been effective for other important human pathogens including *Streptococcus pneumoniae* and *H. influenzae* type B. Moreover, for CF patients specifically, these vaccines are currently prescribed and have proven effective in preventing invasive infections (Moigne *et al.*, 2016). Given that there are already existing, and clinically effective, bacterial vaccines for CF patients, it is unsurprising that there is a significant drive to develop a vaccine for *P. aeruginosa*.

Efforts to develop an effective vaccine for *P. aeruginosa* have been ongoing since the early seventies when Alexander and Fisher (1970) published results of a trial using a vaccine derived from pseudomonal sugars (lipopolysaccharides expressed on the bacterium's surface). Many pseudomonal vaccines developed since have been based on other *P. aeruginosa* virulence factors including outer membrane proteins and other secreted sugars (Priebe and Goldberg, 2014).

Despite numerous distinct pseudomonal vaccines and clinical trials, a recent Cochrane Review found that the pseudomonal vaccines were not effective at reducing the risk of chronic *P. aeruginosa* infection (Johansen and Gøtzsche, 2015). In part, this is attributed to the diverse virulence factors of the pathogen whereby broad protection against different *P. aeruginosa* strains and subtypes is not consistent (Priebe and Goldberg, 2014). Further research into developing effective vaccination strategies is therefore required and may involve a number of different pathways including specifically tailoring vaccines to specific strains in different CF populations, using multiple immunogenic

factors or focusing on other important CF pathogens where vaccines may be more effective.

## **1.6. Project Context and Scope**

As outlined above, there is an urgent requirement for the development of innovative strategies to combat chronic pseudomonal infections suffered by CF patients. The development of novel antibacterial and/or anti-virulence compounds would augment the current arsenal of classical antibiotics at a clinician's disposal and increase treatment options. Conversely, the development of an effective and safe pseudomonal vaccine has the potential to prevent the organism from establishing chronic infections altogether.

This project aims to make contributions on all three of these fronts through:

- i. Performing a pre-clinical evaluation of a novel antibacterial compound that may hijack a *P. aeruginosa* virulence factor;
- ii. Investigating whether sugar molecules can disrupt pseudomonal biofilms and;
- iii. Establishing methods to facilitate the purification of sugars that have the potential to act as bacterial vaccines.



## SECTION 2: TARGETING *P. AERUGINOSA* IN CF PULMONARY INFECTIONS

### 2.1. Background

#### 2.1.1. Carbon Monoxide Therapy

Lungs of CF patients are chronically inflamed which leads to physiological effects, including decline in lung function, tissue destruction and aberrant metabolism (Heijerman *et al.*, 2009b). Therefore, in order to preserve lung function, anti-inflammatory treatment is often concomitantly used with antibiotic therapy (Heijerman *et al.*, 2009b). Antibiotics that exert anti-inflammatory effects, such as macrolides, have shown to improve lung function in CF patients chronically infected with *P. aeruginosa* (Heijerman *et al.*, 2009b).

Another molecule shown to exert anti-inflammatory effects is the gas carbon monoxide (CO) (Otterbein *et al.*, 2000, Otterbein, 2002). Additionally, CO has been shown to exert antimicrobial activity against a wide range of human pathogens including *Escherichia coli* and *P. aeruginosa* (Desmard *et al.*, 2012, Nobre *et al.*, 2007, Nobre *et al.*, 2009). It is thought to mediate this effect by interfering with the bacterial respiratory chain and subsequently causing cell death (Desmard *et al.*, 2012).

Studies performed *in vitro* have shown that CO can reduce expression of inflammatory cytokines, modulate apoptosis and act as an anti-oxidant (Bathoorn *et al.*, 2007, Otterbein, 2002). CO immunomodulatory effects can protect rodent lungs from exotoxin and asthma and human trials have shown that inhalation of CO gas at low concentrations (100-125ppm) can reduce lung inflammation and eosinophils in chronic obstructive pulmonary disease (Bathoorn *et al.*, 2007, Otterbein, 2002). Inhalation of low concentrations of CO has also been shown to protect against both cellular and tissue damage (Mizuguchi *et al.*, 2010)

Despite these successes, the use of CO gas as a therapeutic agent has been hindered by concerns over toxicity, whereby CO can cause death by hypoxemia by binding with great affinity to the oxygen-carrying protein hemoglobin (240 times higher affinity than oxygen) (Wu and Juurlink, 2014, Ryter and Choi, 2006). Although this asphyxiation can occur at high concentrations, CO itself is endogenously expressed in the human body and remains an important signaling molecule (Bathoorn *et al.*, 2007, Otterbein, 2002).

### 2.1.2. CO Releasing Molecules

A recent advance in CO therapeutic delivery has been developed by embedding CO into transition metal carbonyls. Binding CO into these 'carrier metals', CO can be released in a controlled manner in biological systems (Desmard *et al.*, 2009). These compounds are referred to as CO releasing molecules (CORMs) and allow for the beneficial effects of CO while minimising toxicity (Desmard *et al.*, 2009).

CORMs may be synthesised with different metal centres whereby the choice of transition metal can influence its solubility in water and the CO release kinetics (Desmard *et al.*, 2012). Due to backbonding, the CO-transition metal bond is highly stable (Schatzschneider, 2015).

### 2.1.3. Activation Requirements

The therapeutic potential of CORMs is largely dependent on the controlled release of CO and therefore various chemical structures of CORMs have been developed with the aim to improve CO release and activity. CO can be released from the metal carrier in CORMs by enzymatic activation, photoactivation or ligand exchange (Schatzschneider, 2015). Alternative methods are also being explored such as the magnetic-field activation of CORMs that are bound to magnetic nanoparticles (Schatzschneider, 2015).

The light activated release of CO from the metal carrier occurs when light is absorbed at particular wavelengths and causes electronic excitations that, in turn, reduces the metal charge density and weakens the CO-metal bond (Schatzschneider, 2015). The CORM  $Mn_2(CO_{10})$  is one such molecule (Motterlini and Otterbein, 2010). Visible light activated CORMs are limited by light penetration through tissues (Schatzschneider, 2015) and therefore, are not suitable for intravenous or internal clinical administration.

Enzymatically activated CORMs release CO in the presence of a specific enzyme. This method is beneficial as it is specific and can enable intracellular delivery (Stamellou *et al.*, 2014). For instance, enzymes such as esterase and phosphatase can cleave an ester or phosphate group, generate an unstable metal centre and ultimately trigger CO release (Zobi, 2013). This mechanism of activation is currently limited to a finite group of enzymes (Zobi, 2013).

Other CORMs are able to start releasing CO based on ligand exchange. This can occur in particular solvents and therefore, for some CORMs, upon dissolution, they can begin to release CO immediately. This can be a disadvantage for clinical development of CORMs

as they do not always express desirable pharmacokinetics. Some water soluble CORMs for instance, have release rates that range from 1 minute ( $\text{Ru}(\text{CO})_3\text{Cl}_2$ ) to 21 minutes ( $[\text{H}_3\text{BCO}_2]\text{Na}_2$ ) (Motterlini and Otterbein, 2010). Moreover, some ruthenium-based CORMs (e.g.  $[\text{RuCl}(\text{glycinato})(\text{CO})_3]$ ) have different kinetics based on their solvent system and pH (Schatzschneider, 2015).

There are a wide range of different activation mechanisms being explored, however the need for targeted therapeutic applications is driving demand for CORMs that can be activated by specific stimuli (Schatzschneider, 2015).

#### 2.1.4. CORMs with Antibacterial Action

Various CORMs, with different metal centres, have shown to exert bactericidal activity against both Gram-negative and Gram-positive organisms (Figure 3. 1) (Nobre *et al.*, 2007).

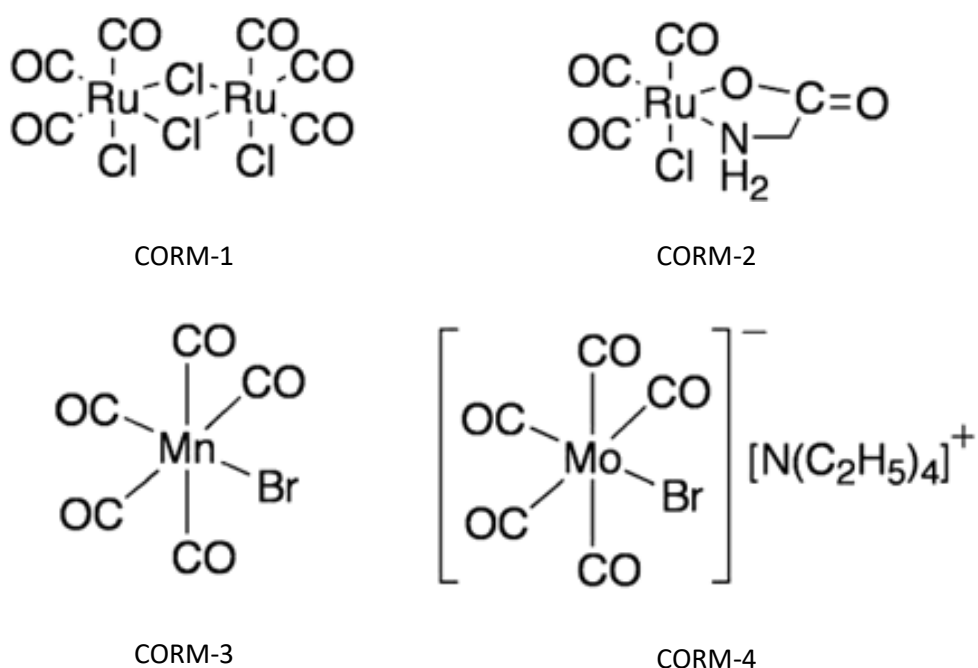


**Figure 3. 1 – CORMs that have shown to exert bactericidal activity against *Escherichia coli* and *Staphylococcus aureus*. Adapted from Nobre *et al.* (2007).**

Specifically, a manganese based CORM (Figure 3. 1, CORM-3) was shown to exert antimicrobial activity against a multi-drug resistant strain of *Escherichia coli* when activated by light (Tinajero-Trejo *et al.*, 2016). Addition of the CORM also potentiated the antibiotic doxycycline (Tinajero-Trejo *et al.*, 2016). CORM activation required 30 minutes of exposure to UV light and its efficacy was shown to be strain specific, whereby concentrations of 500  $\mu\text{M}$  were sufficient to inhibit the growth of a pathogenic strain but

only slightly inhibited a non-pathogenic strain (Tinajero-Trejo *et al.*, 2016). The study also showed that the photo activated CORM was more toxic against *E. coli* than dissolved CO gas and it is suggested that direct CORM delivery into the bacterial cells and subsequently higher local CO concentrations could explain this phenomenon (Tinajero-Trejo *et al.*, 2016). In addition, no accumulation of manganese was found within bacterial cells. This infers that it was in fact the intracellular activity of the CO that inhibited the growth of the strain and not the metal centre itself. Moreover, in this case, the CORM activity was shown to be similar to that of dissolved CO in that the CORM could inhibit respiration through binding to intracellular respiratory oxidases (Tinajero-Trejo *et al.*, 2016).

A ruthenium-based CORM ( $[\text{Ru}(\text{CO})_3\text{Cl}_2]$ , CORM-1 Figure 3.1) has also been shown to inhibit bacterial growth and prevent biofilm maturation in *P. aeruginosa* (Murray *et al.*, 2012). However, as noted in the previous section, with a half-life of 1 minute (Motterlini and Otterbein, 2010), the pharmacokinetics of this ruthenium-based CORM may not be viable in a clinical setting.

#### **2.1.5. Towards a Virulence Factor activated CORM**

Specific CORM activation requirements has limited the use of CORMs in several therapeutic settings. For instance, a CORM that is activated by light may be useful for skin treatment, but would be impractical in the lungs. To address this issue, recently the Lynam Group at the University of York have been developing a CORM that is activated by synthetic pyocyanin.

Pyocyanin is an important pseudomonal virulence factor in both acute and chronic lung infections and is involved in many aspects of pathogenesis including elimination of competing microbiota, mucus hypersecretion, reducing mucociliary clearance from the lungs and maintaining redox balance in the low oxygen environments present in chronic infections (Muller and Merrett, 2014, Miller *et al.*, 2015, Bhargava *et al.*, 2014, Hao *et al.*, 2013, Winstanley and Fothergill, 2009). Pyocyanin can also react with topoisomerases in eukaryotic cells, facilitates bacterial nutrition (Hassani *et al.*, 2012, Muller and Merrett, 2014) and can cause apoptosis of neutrophils which in-turn reduces clearance by the immune system (Usher *et al.*, 2002).

In addition, pyocyanin is a phenazine derived compound with a characteristic blue-green colour (Figure 2. 1) (Cox, 1986). This colour is commonly seen in skin infections (Figure

2. 1) (Muller and Merrett, 2014, Mutluoglu and Uzun, 2011) and in the sputum of CF patients where pyocyanin levels can accumulate to  $\sim 100 \mu\text{M}$  (Lundgren *et al.*, 2013).

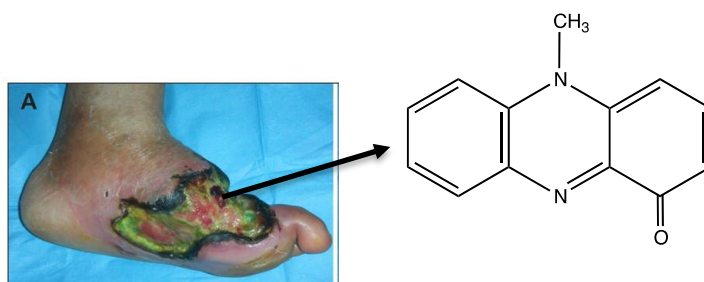


**Figure 2. 1- Chemical structure of pyocyanin (right) and green wound discoloration characteristic of *P. aeruginosa* infection (left). Adapted from Mutluoglu and Uzun (2011).**

#### **2.1.6. Targeting a Bacterial Virulence Factor**

Due to the inevitable development of resistance to classical antibacterial agents, an alternative strategy of specifically targeting bacterial virulence factors is increasingly being investigated. This strategy aims to apply selective pressure to the bacteria in order to cause reduced expression of the virulence factor, thereby making the bacteria less pathogenic and easier to clear by the immune system (Miller *et al.*, 2015). The activation of CORMs by pyocyanin represents a possible application of this idea. As a reduction of bacterial toxicity has been observed in *P. aeruginosa* strains that have reduced expression of pyocyanin (Fuse *et al.*, 2013), it is plausible that development of resistance to 'pyocyanin activated CORM' may effectively attenuate *P. aeruginosa* virulence.

#### **2.1.7. CORM Activation by Synthetic Pyocyanin**

As pyocyanin is redox active and structurally similar to other typically strong metal binding chelate ligands, there is a strong likelihood that it can effectively displace CO from a CORM. To this end, the Lynam Group at the University of York have been working on the development of a CORM that can be activated by synthetic pyocyanin. This CORM, termed 'pyo-CORM', comprises a manganese centre with four carbonyl groups (Figure 2. 2). This structure ( $[\text{Mn}(\text{CO})_4\text{Br}]\text{NEt}_4$ ) is water soluble, and exists in a tetraethylammonium salt.

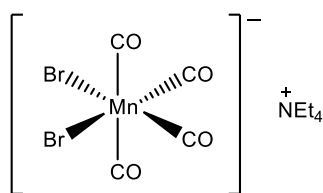


**Figure 2. 2- Structure of pyo-CORM comprises a manganese central transition metal and 4 carbonyl groups in a tetraethylammonium salt.**

The four carbonyl ligands in the pyo-CORM (Figure 2.1) have been verified by infrared (IR) analysis (Figure 2.3).

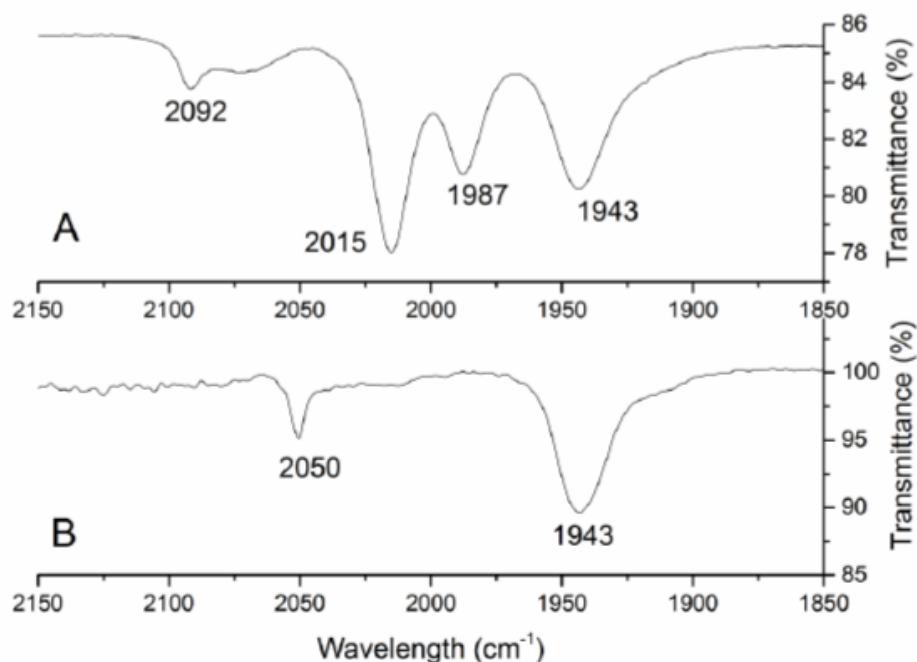


**Figure 2. 3- IR spectra of the reaction of 5 mM of pyo-CORM and 2.5 mM of pyocyanin over 35 mins.**

Figure 2.3 shows the four distinct carbonyl bands observed, at 2092, 2015, 1987 and 1943  $\text{cm}^{-1}$ , when pyo-CORM is dissolved in chloroform (A), and two distinct bands, at 2050 and 1943  $\text{cm}^{-1}$ , when the compound is dissolved in water (B). In order to confirm there was no rapid CO release in the water solution, the pyo-CORM was dissolved in water, immediately dried and redissolved in chloroform. The resulting IR spectrum was identical to pyo-CORM dissolved in chloroform (A), indicating that the change in absorbance frequencies simply reflects a symmetry rearrangement when the compound is dissolved in a different solvent. The water-based spectrum remained stable over short periods of time (<30 min), indicating that dissolution in water did not activate immediate CO release.

The changes in carbonyl bands that result after adding synthetic pyocyanin to an aqueous solution of pyo-CORM were then monitored by infrared spectroscopy (Figure 2.4).

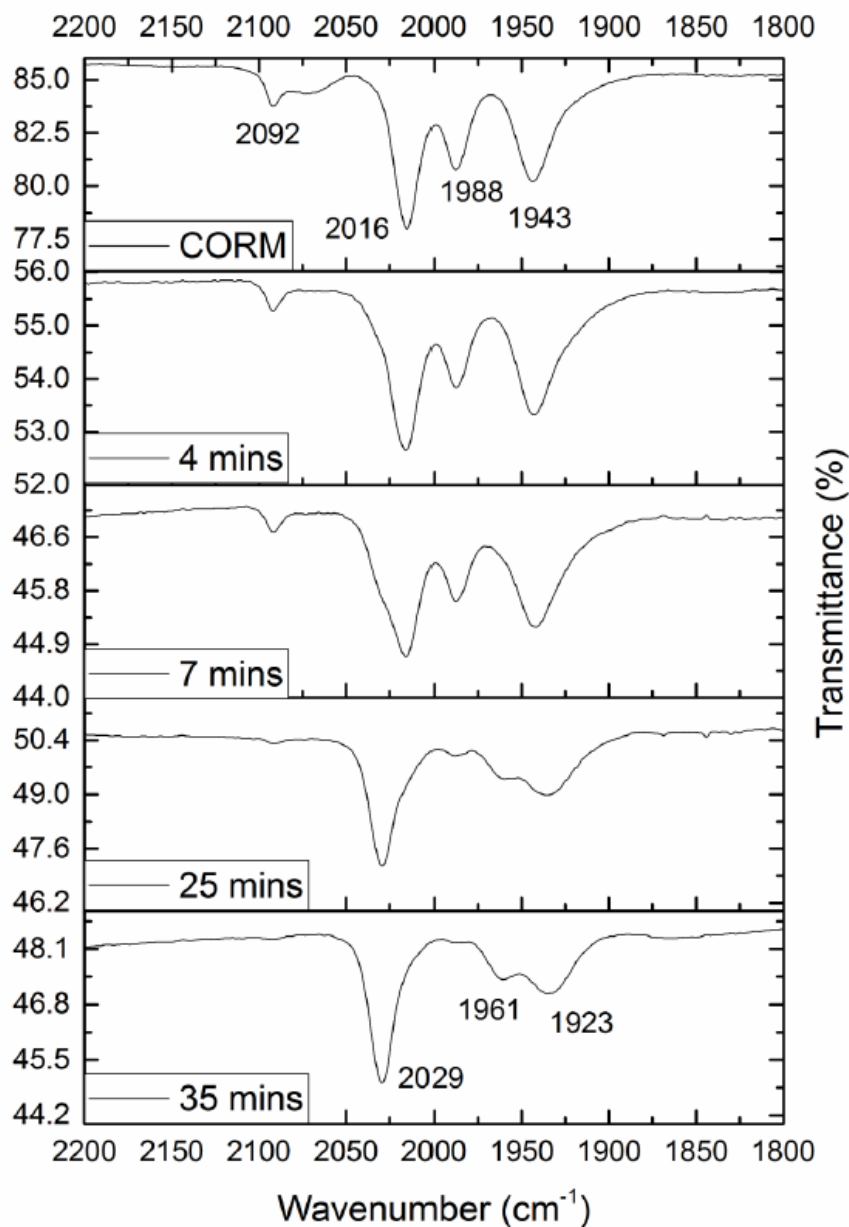


Figure 2. 4- FTIR spectra of the reaction of 5 mM of pyo-CORM and 2.5 mM of pyocyanin over 35 mins.

These spectra (Figure 2.4) show that after just 35 min, addition of pyocyanin to the pyo-CORM has resulted in comprehensive changes in the range 2200-1800 cm<sup>-1</sup>, the characteristic region at which CO stretching frequencies are interrogated (J., 1980). Such changes indicate a ligand rearrangement in the complex, and we interpret this as suggestive of carbon monoxide release, since earlier work by others has shown that pyo-CORM degrades via this mechanism (Zhang *et al.*, 2009). This was shown to be a

pyocyanin-specific activation mechanism because the Lynam group showed pyocyanin analogues do not stimulate changes in the IR bands of pyo-CORM. Further experiments, to conclusively link these solution IR spectral changes to the gaseous release of CO, were also conducted by Rachel Steen and are reported in her Thesis (Steen, 2017).

The specific addition of synthetic pyocyanin to the pyo-CORM is therefore predicted to engender CO release however, to date, the potential inhibitory effects of this pyo-CORM on *P. aeruginosa* growth *in vitro* have not been characterised.

## **2.2. Aims**

The aim of this piece of work was to assess the efficacy of pyo-CORM against *P. aeruginosa* cultures *in vitro* and in terms of growth inhibition and biofilm formation. In addition, in order to investigate the specificity of the pyo-CORM, non-pyocyanin producing *P. aeruginosa* strains and other microbial species will be tested.

## **2.3. Hypothesis**

It is hypothesised that, through CO release, the pyo-CORM will exert effects on bacterial growth and biofilm formation. As pyo-CORM has been shown to be specifically activated in the presence of synthetic pyocyanin, it is also anticipated that pyo-CORM will only be effective against bacteria that express pyocyanin.

## **2.4. Materials and Methods**

### **2.3.1. CORM**

The CORM, pyo-CORM, used throughout experimentation was synthesised by the Lynam Group at the University of York Chemistry Department.

### **2.3.2. Strains**

The *P. aeruginosa* laboratory strain PA01 was used as well as a clinical isolate strain obtained from Liverpool Hospital. The clinical strain was isolated by Siobhan O'Brien from the Brockhurst Group at the University of York Biology Department. The phenazine mutant strain was denoted  $\Delta$  phz. Other strains used were *Staphylococcus aureus* subspecies aureus, DSM-20231, *Stenotrophomonas maltophilia*, DSM-50170 and *Ralstonia solanacearum* G1000.



### **2.3.3. pyo-CORM Toxicity Assays**

A final concentration of either 1500 or 800  $\mu\text{M}$  pyo-CORM was made up in both 10 and 100 vol% LB. Two-fold serial dilutions were then performed in a 96 well plate, down to 188  $\mu\text{M}$  and 200  $\mu\text{M}$  pyo-CORM respectively. CORM-free control wells containing only 10 and 100 vol% LB growth media were also used. Each well condition (dilution) was replicated five times. The 1500  $\mu\text{M}$  pyo-CORM dilution series were used to evaluate the efficacy for PA01 stains while the 800  $\mu\text{M}$  pyo-CORM dilutions were used for testing the phenazine mutant strain and other microbial species. To each well, 5 vol% of a 1:10 diluted bacterial strain was added and the starting point absorbance measured at 600 nm (i.e. time = 0 hours) using plate reader, and associated software, Tecan Infinity 200 plate reader. The plates were incubated for 24 hours at 37°C and the absorbance was again measured at 600 nm. Where  $\Delta\text{OD}$  is reported, this is the difference between the OD<sub>600nm</sub> at 24 hours and 0 hours.

### **2.3.4. pyo-CORM Biofilm Assays**

All biofilm assays were performed by adding crystal violet to wells containing PA01 cultures to give a final concentration of 10 vol%. After 15 minutes, the plates were rinsed in water three times and 210  $\mu\text{L}$  of ethanol was added to each well. The absorbance was then measured at 600 nm.

### **2.3.5. Data Analysis**

For each data point, there were 5 replicates of any tested condition. For plotting, each group of replicates were averaged and the standard deviation calculated for each group. The p values were then obtained by performing 2 tailed t tests and assuming equal variance.

## **2.5. Results and Discussion**

### **2.5.1. pyo-CORM and PA01 Assays**

pyo-CORM was shown to reduce total bacterial growth in a concentration dependent manner (Figure 2. 5). In addition, the growth assays indicate that the effects of pyo-CORM were dependent on the bacterial growth conditions, whereby the tested pyo-CORM concentrations were much more potent in 10 vol% LB than 100 vol% LB (Figure 2. 5).

The corresponding biofilm assays show that pyo-CORM is able to exert a significant reduction in biofilm formation (Figure 2.5). These results are similar to a previous study that trialled a ruthenium based CORM against PA01 in different growth media (Murray *et al.*, 2012). Their work showed that in media containing high concentrations of LB, PA01 growth and biofilm formation were unaffected by the ruthenium based CORM. Our results are therefore promising, in particular as the pyo-CORM exerted a notable effect on the biofilm formation in both nutrient conditions (Figure 2.5).

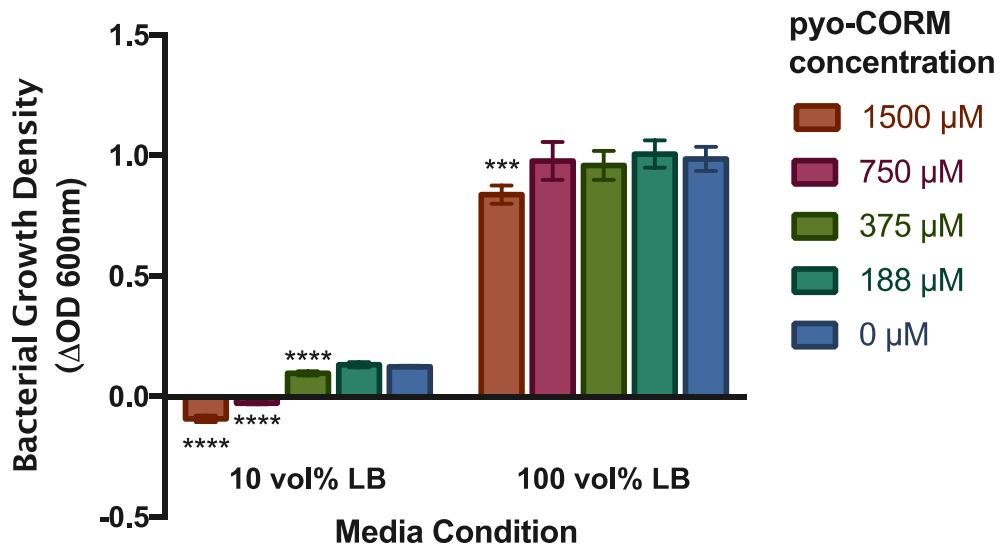


Figure 2. 5- Growth of PA01 for 24 hours at 37°C in either 10 or 100vol% LB. Bacteria were grown in increasing concentrations of pyo-CORM.

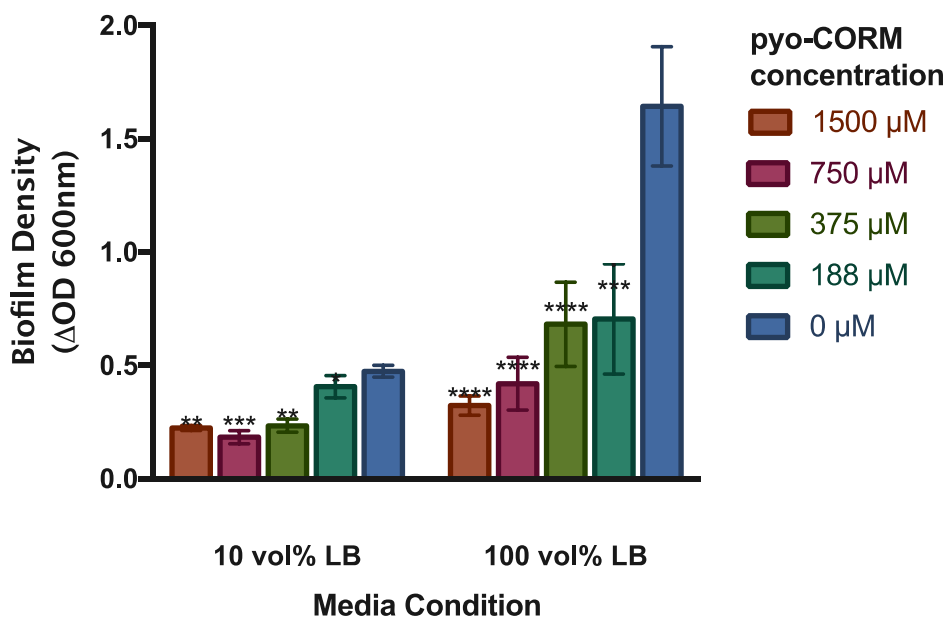


Figure 2. 6- Biofilm assay for PA01 for 24 hours at 37°C in either 10 or 100 vol% LB. Assays shown for bacteria grown in increasing concentrations of pyo-CORM.

### 2.5.2. pyo-CORM Assays for PA01 and Phenazine Mutant

The growth and biofilm density of PA01 and the phenazine mutant ( $\Delta$ phz) in the presence of pyo-CORM under varying concentrations is shown in Figure 2.6 and Figure 2. 8. The total bacterial growth results indicate that pyo-CORM was inhibitory against both PA01 and the phenazine mutant strain. This suggests that pyo-CORM is potent against *P. aeruginosa* regardless of the amount of pyocyanin produced and that pyo-CORM is being activated to release CO by a mechanism other than pyocyanin.

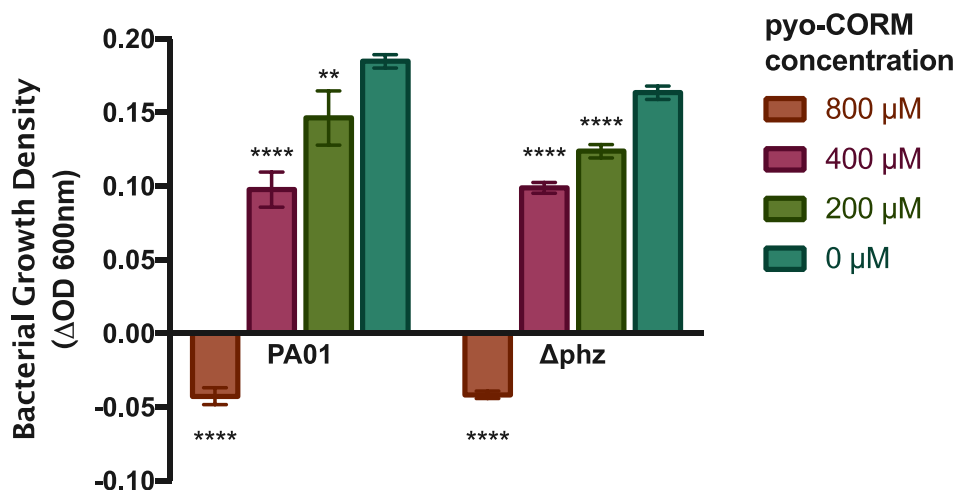


Figure 2. 7- Growth of PA01 and the *P. aeruginosa* phezanine mutant ( $\Delta$ phz) for 24 hours at 37°C. Bacteria were grown in 10 vol% LB in concentrations of pyo-CORM ranging from 0 to 800  $\mu$ M.

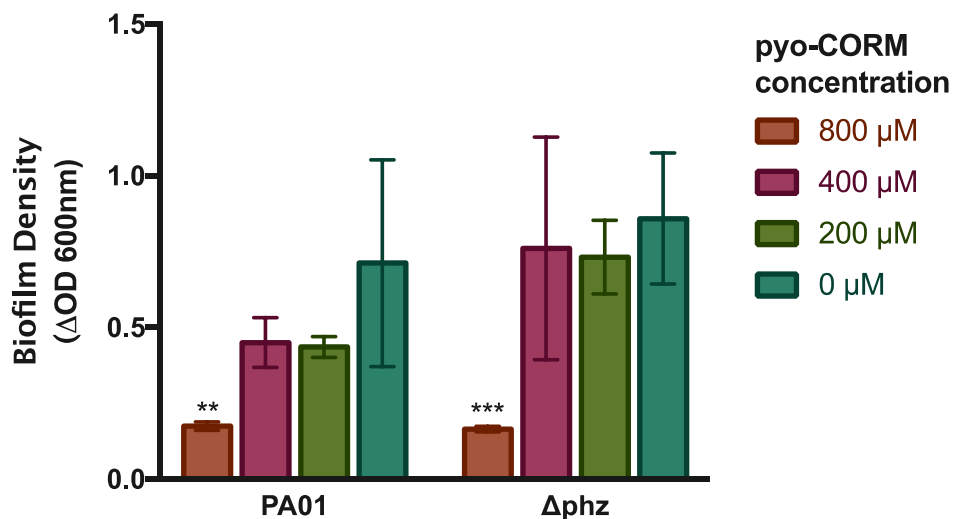


Figure 2. 8- Biofilm assay of PA01 and the *P. aeruginosa* phezanine mutant ( $\Delta$ phz) grown for 24 hours at 37°C. Bacteria were grown in 10 vol% LB in concentrations of pyo-CORM ranging from 0 to 800  $\mu$ M.

### 2.5.3. pyo-CORM Assays for *Ralstonia*, *Staphylococcus* and *Stenotrophomonas* Species

The bacterial growth and biofilm assays for *R. solanacearum*, *S. aureus* and *S. maltophilia* exposed to pyo-CORM (Figure 2. 9 and Figure 2. 10) show that pyo-CORM was able to reduce total growth and biofilm formation for all tested microbial species. A similar trend is observed across all species and shows that as the pyo-CORM concentration increases, the total bacterial growth decreases. This trend is similar across the biofilm assays however there is more variability in samples tested. At pyo-CORM concentration of 800  $\mu\text{M}$ , there is a clear disruption in biofilm formation compared to the control (with all p values < 0.0001). This supports the finding from the phenazine mutant results and indicates that pyocyanin is not required to release CO from the CORM. This further supports a body of evidence that CO is an effective, broad-spectrum antimicrobial, exerting toxic effects across Gram negative and Gram positive organisms.

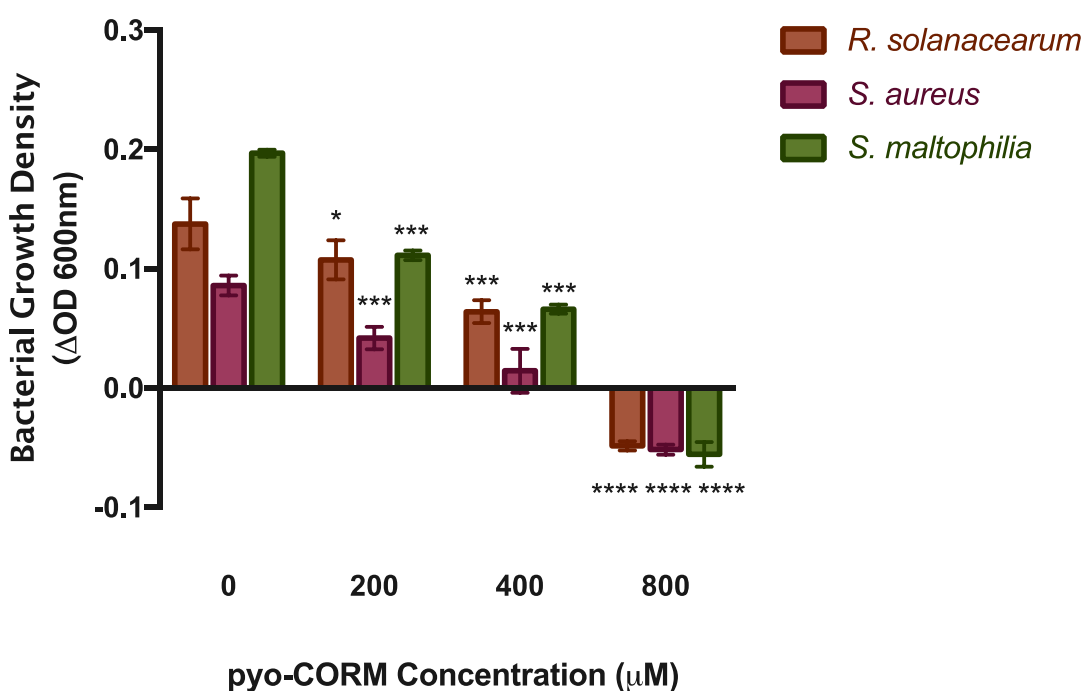


Figure 2. 9 - Growth of microbial species for 24 hours at 37°C in 10 vol% LB. Microbial species were grown in concentrations of pyo-CORM ranging from 0 to 800  $\mu\text{M}$ .

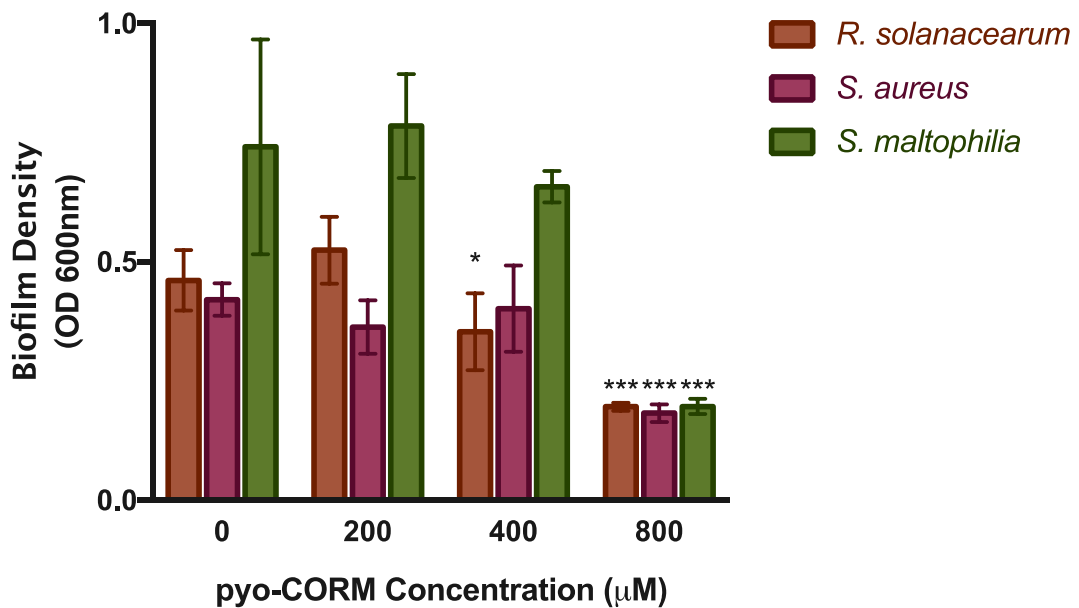


Figure 2. 10- Biofilm assay for of microbial species for 24 hours at 37°C in 10 vol% LB. Microbial species were grown in concentrations of pyo-CORM ranging from 0 to 800 µM.

## 2.6. Conclusions and Future Work

It was found that the pyo-CORM was not specifically active against pyocyanin producing bacteria and was, in fact, toxic against a wide range of bacteria, including the plant pathogen *R. solanacearum* and important CF pathogens *S. aureus* and *S. maltophilia*. At concentrations greater than 400 µM, pyo-CORM was found to decrease both bacterial growth and biofilm formation for all tested bacteria. However, it was noted that the efficacy in growth reduction was dependent on nutrient conditions. In the future, it would be beneficial to test the efficacy of the pyo-CORM on multi-drug resistant bacteria.

Further work needs to be done on evaluating the effects of the transition metals used in CORMs. To date, most studies have analysed the biological properties of metals through metal chlorides (Desmard *et al.*, 2009). For instance, to ensure that the efficacy of the CORM was due to the presence of CO only, in the future, bacterial growth experiments will need to be performed in tandem with a CO scavenger. If the bactericidal activity is reversed in the presence of a CO scavenger we could thus conclude that it is the presence of the CO, and not the metal ligands eliciting activity. Moreover, to ensure pyo-CORM activity is not related to its decomposition products, we will need to test the effects of tetraethyl ammonium bromide on bacterial growth. It will also be important to measure

the presence, if any, of manganese within bacterial cells as this will confirm whether or not the pyo-CORM is able to be shuttled across the bacterial cell membrane.

To ensure the safety of pyo-CORM in future work, toxicity in mammalian cells will need to be established. For instance, the effects of pyo-CORM in a hemolysis assay will be undertaken to ensure safety in pre-clinical evaluation.

Ultimately, the precise activation mechanism of pyo-CORM remains unknown. More chemistry based studies will be required to understand what other ligands or activators are facilitating CO release before biological assays are repeated in the future.

## SECTION 3: TARGETING BIOFILMS IN MODEL CF INFECTIONS

### 3.1. Background

#### 3.1.1. Biofilms

As discussed in Section 1.3.1, biofilm formation is an essential factor in *P. aeruginosa* pathogenesis and drastically reduces the efficacy of the immune system in clearing the pathogen as well as the majority of conventional antibiotics. Therefore, novel treatment options, particularly those that can combat or penetrate biofilms, are required. The mucoid phenotype of *P. aeruginosa*, in particular, is associated with biofilm formation.

#### 3.1.2. The Mucoid Form of *P. aeruginosa*

When *P. aeruginosa* initially infects the lungs, the bacteria express a non-mucoid phenotype (Berry *et al.*, 1989), however, over the course of infection the organism undergoes genetic and phenotypic changes that allow chronic infections to be established (Troxler *et al.*, 2012). In particular, the change of *P. aeruginosa* to the mucoid phenotype is associated with progression of lung disease in CF patients (Bayer *et al.*, 1991). The mucoid phenotype is associated with over production of the polysaccharide alginate which is visually identifiable in culture (Figure 3. 2).

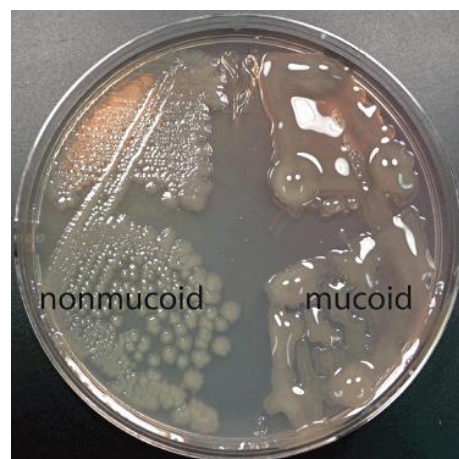


**Figure 3. 2 – Image showing non-mucoid (left) and mucoid (right) variants of *P. aeruginosa* grown on a Petri dish. Mucoid variant shows characteristic production of the viscous substance alginate.**

(Damron and Goldberg, 2012).

This viscous substance contributes to the high mucous environment already established in the lungs of CF patients (Berry *et al.*, 1989). In addition, mucoid variants of *P. aeruginosa* are associated with reduced efficacy in antimicrobial therapy. An experiment monitoring mucoid bacteria showed that when the bacteria reverted back to non-

mucooid forms (e.g. by growing them under aerobic conditions) they became susceptible to both immune cells (phagocytes) and antibiotics (Yoon *et al.*, 2002).

### 3.1.3. The Importance of Alginate in *P. aeruginosa* Pathogenesis

A key characteristic of the mucooid form of *P. aeruginosa* is the secretion of the polysaccharide alginate. Alginate is a naturally occurring linear polysaccharide and consists of mannuronate (M) and guluronate (G) residues (Figure 3. 3).

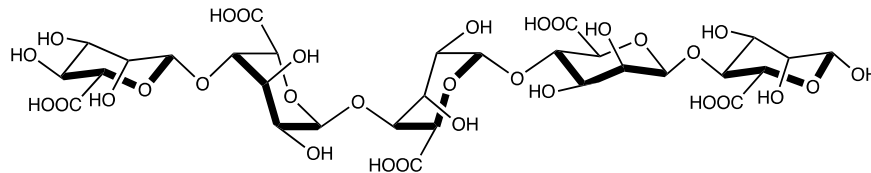


**Figure 3. 3 – Chemical structure of an alginate oligomer comprising mannuronate (M) and guluronate (G) residues joined by  $\beta$ -1-4 glycosidic linkages. Image shows an alginate pentamer with residue sequence MGGMM.**

Alginate has shown to help *P. aeruginosa* avoid phagocytosis by the immune system (Troxler *et al.*, 2012). Further studies on mucooid strains *in vitro* have suggested that antibiotic resistance is proportional to the production of alginate (Schülin, 2002, Shawar *et al.*, 1999). This hypothesis is further supported by Alkawash *et al.* (2006) who showed that an alginate lyase could enhance antibiotic efficacy against mucooid *P. aeruginosa* strains.

The secretion of alginate polysaccharide also helps the bacteria grow in a dense, highly organised biofilm structure (Troxler *et al.*, 2012). By forming a thick biofilm structure, the mucooid form of *P. aeruginosa* can reduce penetration and efficacy of antibiotics whereby for instance, the antibiotic can interact with and adsorb onto the polymer matrix (Lebeaux *et al.*, 2014). Moreover, slow diffusion can expose the bacteria to sub-lethal concentrations of the drug and thereby allow for the bacteria to undergo transcriptional changes and adaptation (Lebeaux *et al.*, 2014). Recently, a study found that alginate production promoted coinfection with *S. aureus* and resulted in poorer health outcomes for CF patients (Limoli *et al.*, 2017).

### 3.1.4. Alginate as a Biofilm Disruptor

Several studies have found that alginate fragments are able to reduce both growth and biofilm integrity in *P. aeruginosa* and bacteria (Edvar Onsoyen, 2008, Roberts *et al.*, 2013, Yan *et al.*, 2011, Powell *et al.*, 2014). The exact mode of action is currently unknown, however, mechanistic studies have shown that alginates can reduce interactions within



the extracellular polymer matrix substances and reduce cross-linking, thereby weakening the overall biofilm structure (Roberts *et al.*, 2013).

### **3.2. Aims**

The aims of this work were to generate and purify alginate fragments and then assess their biofilm disruptive capacity against *P. aeruginosa in vitro*. In addition, in an attempt to increase toxicity against *P. aeruginosa*, this work has investigated the potential of alginate fragments to inhibit growth and ultimately potentiate pyo-CORM efficacy.

### **3.3. Hypothesis**

It is hypothesised that alginate fragments will be effective in reducing the bacterial growth and biofilm integrity in *P. aeruginosa* and that this will potentiate the activity of pyo-CORM.

### **3.4. Materials and Methods**

#### **3.3.1. Alginate Hydrolysis**

Alginate isolated from *Laminaria hyperborea* was obtained from Sigma Aldrich (product 18097) with mannuronate:guluronate ratio of 1:1.56 and an average molecular weight of 155 kDa. To generate fragments, alginate was dissolved in dH<sub>2</sub>O to a final concentration of 1 wt%. The solution was adjusted to a pH of 5 using 1M HCl and then stirred under nitrogen at 95°C for 3 hours. Subsequently, the sample was adjusted to a pH of 3 with 1M HCl and stirred under nitrogen at 95°C for 4 hours. Finally, the sample was neutralised with 1M NaOH, lyophilised and analysed via liquid chromatography mass spectrometry using negative mode ESI.

#### **3.3.2. Alginate Viscosity**

To assess the change in viscosity with hydrolysis, 10 wt% of alginate (18097) was dissolved into dH<sub>2</sub>O. The solution was adjusted to a pH of 3 using 1M HCl and stirred under nitrogen at 95°C. At 2.5, 4.5, 6.5 and 24 hours the samples were tested using a Brookfield low-range viscometer.

### **3.3.3. Separation of Hydrolysed Alginate**

To generate smaller alginate fragments, 340 mg of a lyophilised sample was passed through a Sephadex LH-20 column<sup>§</sup> with size exclusion limit 4000-5000 g/mol. Fractions were analysed using mass spectrometry in negative mode ESI and those containing the desired fragments were pooled and lyophilised.

### **3.3.4. Growth of PA01 in Hydrolysed Alginate**

To assess the effects of hydrolysed alginate on growth and biofilm formation in PA01, wells were prepared containing 10 wt% alginate in either 10 or 50 vol% LB. Two-fold serial dilutions were performed to observe the effects under different alginate concentrations. To each well, 5 vol% of 1:10 diluted PA01 was added and the plates were incubated for 24 hours. To assess the effects of temperature, this was performed at both 28 and 37°C. The absorbance was measured at 600 nm before and after incubation. Biofilm assays were performed post incubation.

### **3.3.5. Biofilm Assays of PA01 in Hydrolysed Alginate**

All biofilm assays were performed by adding crystal violet to wells containing PA01 cultures to give a final concentration of 10 vol%. After 15 minutes, plates were rinsed in water three times and 210 µL of ethanol was added to each well. The absorbance was then measured at 600 nm. To compensate for alginate binding of crystal violet, the absorbance of media containing 0, 5 or 10 wt% alginate at 600 nm was used to normalise data.

### **3.3.6. Dosing of PA01 in Hydrolysed Alginate**

To assess the immediate effects of hydrolysed alginate on biofilms, wells containing 5 vol% of 1:10 diluted PA01 in either 10 or 50 vol% LB were incubated for 24 hours at 37°C. After incubation, all supernatant was collected and 200 µL of either 50 vol% LB or water was pipetted into each well. The plate was then incubated for 1 hour and a biofilm assay performed.

### **3.3.7. Hydrolysed Alginate and Separated Hydrolysed Alginate PA01 Assays**

To assess the functionality of different sized fragments, 10 wt% of either hydrolysed or separated and hydrolysed alginate was dissolved into 50 vol% LB. To each well, 5 vol% of

---

<sup>§</sup> Sephadex LH-20 obtained from GE Healthcare Life Sciences.

1:10 diluted PA01 was added and the starting point absorbance measured at 600 nm. The plates were then incubated for 24 hours at 37°C and the absorbance measured at 600 nm. A biofilm assay was then performed (described in 3.3.5).

### **3.3.8. Synergistic CORM and Alginate Assays**

CORM concentrations of 500 and 1000  $\mu$ M were tested in 50 vol% LB in the presence or absence of 5 wt% hydrolysed alginate. Controls containing 5 wt% alginate or water-only treatments were used. The starting point absorbance was measured at 600 nm and then each well had 5 vol% of 1:10 diluted PA01 added. The plates were incubated for 24 hours at 28°C and the absorbance measured at 600 nm. A biofilm assay was then performed (described in 3.3.5).

### **3.3.9. Long Term Exposure to Hydrolysed Alginate**

To ascertain the effects of long term exposure of hydrolysed alginate on PA01, 5 vol% of a 1:10 dilution of PA01 was added into wells containing 0, 5 and 10 wt% alginate in 50 vol% LB. The absorbance of the plate was then measured at 600 nm before the plate was incubated aerobically at 37°C. Transfers and cryopreservation were then performed every 48 hours. The absorbance was measured at 600 nm and then 20  $\mu$ L of each well was transferred into a plate containing fresh 0, 5 and 10 wt% alginate in 50 vol% LB media. 50  $\mu$ L from each well was cryopreserved and the remainder was used for biofilm assay (described in 3.3.5).

### **3.3.10. Assessing Pyocyanin Levels in Alginate Treated PA01 Cultures**

To assess whether there was a correlation between pigment production and alginate treatment, PA01 cultures were exposed to 0, 2.5, 5 or 10 wt% of hydrolysed alginate. To each well, 5 vol% of 1:10 diluted PA01 was added and the starting point absorbance measured at 600 and 691 nm. The plates were then incubated for 24 hours at 37°C and the absorbance of the plates measured at 600 and 691 nm.

## **3.5. Results and Discussion**

### **3.4.1. Hydrolysed Alginate Analysis**

The mass spectrometry analysis of the hydrolysed alginate indicates that polymer fragmentation was successful (Figure 3. 4)

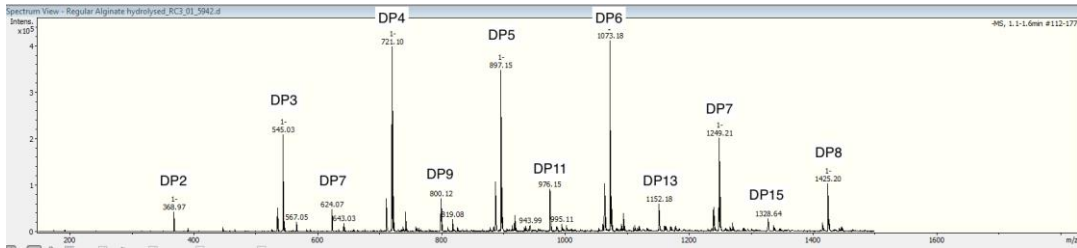


**Figure 3. 4- Mass spectrometry analysis of the non-separated hydrolysed alginate mixture. Results obtained in ESI negative mode.**

The spectrum shows that the hydrolysed alginate mixture contains fragments ranging from degree of polymerisation (DP) 2-18. This is similar to previous characterisation of alginate fragments by negative ion ESI mass spectrometry (Lang *et al.*, 2014). However, as the mass spectrometry detection limit is 3000 g/mol, it is uncertain whether larger, undetectable fragments exist in mixture. The column separation of hydrolysed alginate liberated 47.7% of the applied sample. Based on the separation limit of the Sephadex LH-20, this implies that at least 47.7% of the hydrolysed alginate contains fragments with an average molecular weight ( $M_w$ ) less than 5000 g/mol. The average degrees of polymerisation (DP) for the separated fragments must therefore range between 1-28 and the mass spectrometry results show us that the dominant fragments range from DP4-9, with the dominant peak corresponding to DP4 (721 g/mol) (Figure 3. 5).

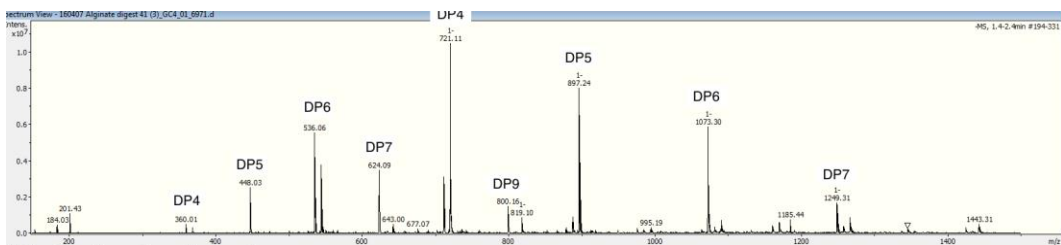


**Figure 3. 5- Mass spectrometry analysis of the separated hydrolysed alginate. Results obtained in ESI negative mode.**

The fragmentation of the alginate polymer mixture was also confirmed by measuring the viscosity of the mixture at different hydrolysis times (Table 3. 1).

**Table 3. 1 – Viscosity of alginate at different hydrolysis times**

<b>Hydrolysis time (hours)</b>	<b>Viscosity 10 wt% alginate in dH<sub>2</sub>O (cP)</b>
0	42
2.5	24
4.5	20
6.5	17
24	10

As shown in Table 3. 1, the viscosity of the alginate-dH<sub>2</sub>O mixture reduces over time, indicating that the average alginate polymer length has decreased with hydrolysis time. This is consistent with similar analyses performed on alginate (Masuelli and Illanes, 2014).

### **3.3.11. Separated and Non-separated Hydrolysed Alginate**

Based on the column exclusion limit and the mass spectra analysis (section 3.4.1), we can definitively state that the separated alginate fragments contained smaller fragments than the hydrolysed mixture. Extending from these findings, the PA01 assays suggest that the separated, smaller alginate fragments exerted greater reduction in PA01 growth than the non-separated hydrolysed alginate (Figure 3. 6).

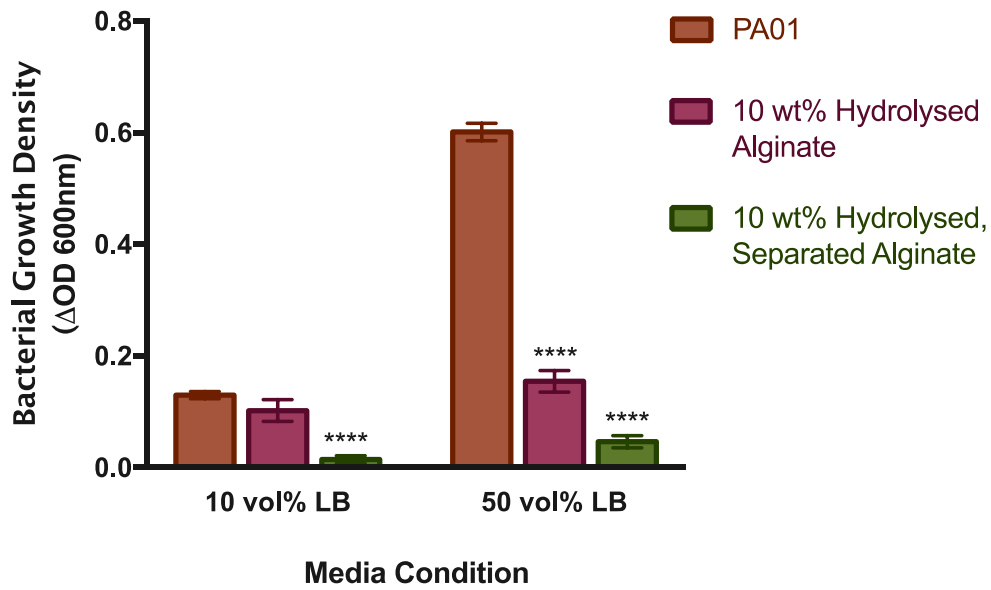


Figure 3. 6- Growth of PA01 for 24 hours at 37°C in 10 and 50 vol% LB. PA01 was exposed to either separated hydrolysed alginate or non-separated hydrolysed alginate.

The corresponding biofilm assay (Figure 3. 7) however, indicates that the non-separated alginate fragments were slightly more effective at reducing biofilm formation than the separated fragments. However, the variability in the biofilm assay replicates suggests that the smaller fragments and hydrolysed mixture exhibited similar reductive effects in this instance.

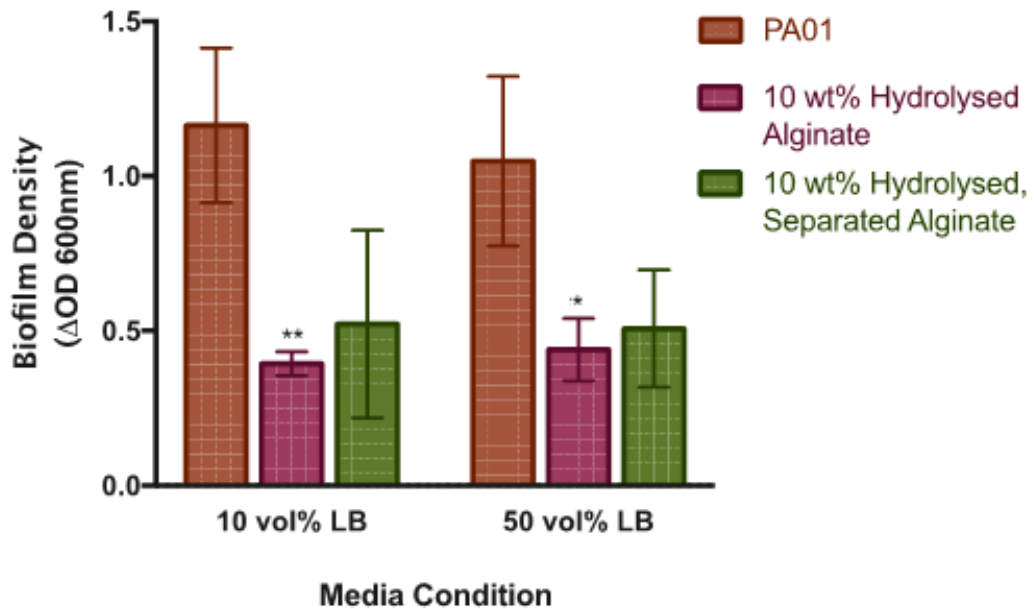


Figure 3. 7- Biofilm assay of PA01 grown for 24 hours at 37°C in 10 and 50 vol% LB. PA01 was exposed to either separated hydrolysed alginate or non-separated hydrolysed alginate.

### 3.3.12. Hydrolysed Alginate Affects Growth and Biofilm Formation

Exposure of PA01 to varying levels of hydrolysed alginate showed that, generally, at concentrations <5 wt% the bacterial density and biofilm formation exceeds the PA01 control (Figure 3. 8). However, at hydrolysed alginate concentrations  $\geq 5$  wt%, the bacterial density and biofilm formation markedly decrease. This trend was consistent regardless of whether high or low LB levels were provided for incubation, and independent of whether incubation temperatures of 28 or 37°C were used. A similar phenomenon has been reported when *Porphyromonas gingivalis* was treated with alginate fragments (containing predominantly guluronic acid) (Roberts *et al.*, 2013). We therefore suggest that alginate fragments exert similar effects regardless of the M:G ratio. Moreover, the treatment of *P. gingivalis* with these G rich fragments showed that 2wt% enhanced growth and biofilm formation while concentrations  $\geq 6$ wt%, reduced growth and biofilm formation, also in-line with our findings (Roberts *et al.*, 2013).

In addition, from antibiotic studies, it is known that sub-inhibitory concentrations of antibiotics can induce expression of stress-activated transcription factors, alter gene expression and influence bacterial virulence. (Linares *et al.*, 2006, Mirani and Jamil, 2011). We propose that such a phenomenon may explain why, in this study and similar studies, low concentrations of alginate cause increased growth and biofilm formation (Linares *et al.*, 2006, Mirani and Jamil, 2011). Together, these results suggest that, at sub-lethal concentrations, hydrolysed alginate can facilitate growth and biofilm formation and that efficacy of treatment is highly dependent on alginate concentration.

Another factor which could contribute to the efficacy of alginate at 10 wt% could be its viscosity; whereby for instance the viscosity of the alginate treatment could influence the overall density in the bacterial culture. Subsequently, if for instance, viscosity was a contributing factor to bacterial growth, this could explain why the 5 wt% alginate is less efficacious than alginate at 10 wt%.

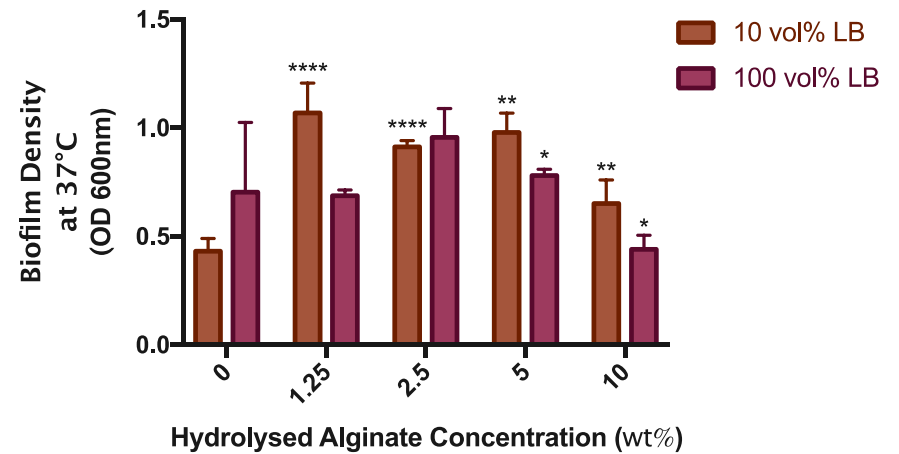
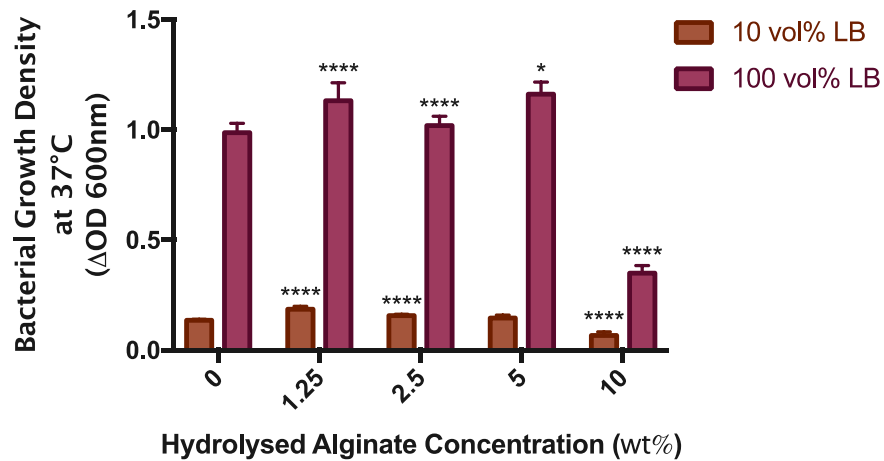
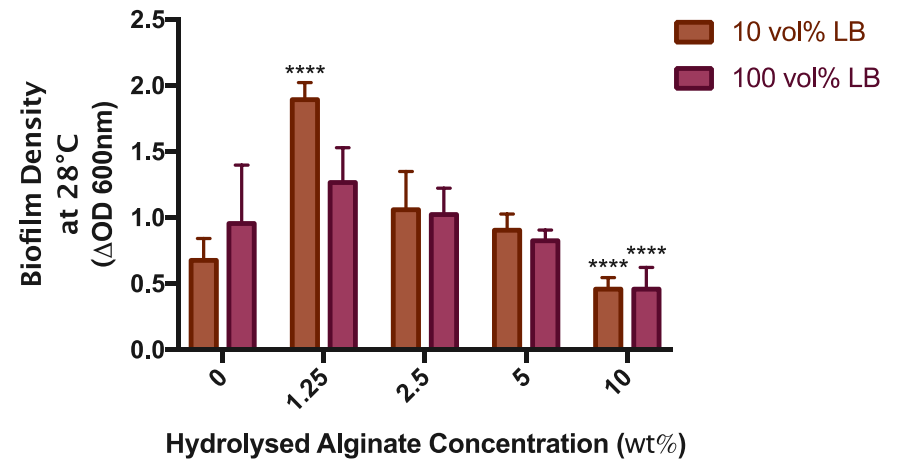
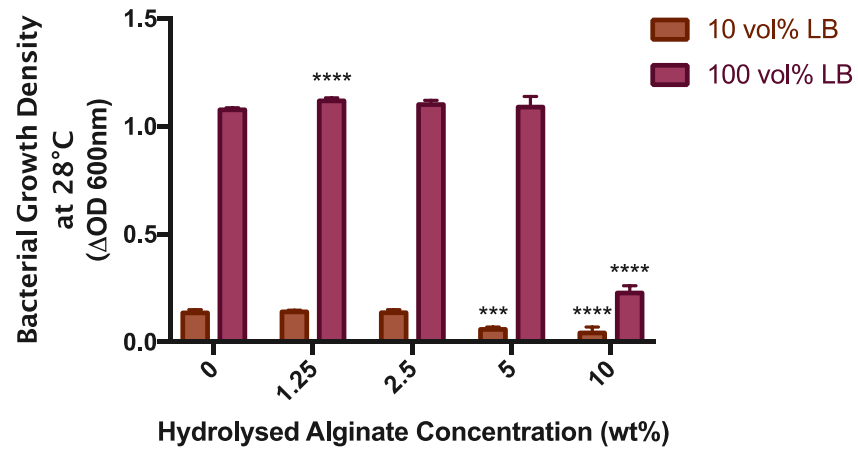


Figure 3. 8- Growth of PA01 in 10 and 100 vol% LB containing varying concentrations of alginate for 24 hours at 28°C. (top left) and for 24 hours at 37°C (top right). Biofilm Assays for PA01 in 10 and 100 vol% LB containing varying concentrations of alginate for 24 hours at 28°C (bottom left) and for 24 hours at 37°C (bottom right).



### 3.3.13. Dosing with Hydrolysed Alginate

The dosing assays indicate that exposure of PA01 biofilms to hydrolysed alginate has an immediate effect on biofilm integrity in 50 vol% LB (Figure 3.9). The effect for cells growing in 10 vol% LB is consistent with previous experiments that showed exposure of PA01 to 10 wt% alginate in 10 vol% LB had a relatively minor impact on reducing biofilm formation (Figure 3.8). These results lend to the hypothesis that, at higher concentrations of hydrolysed alginate, the effects on biofilm disruption can be attributed to the nature of the alginate rather than the viscosity itself. Together, these results suggest that alginate fragments are able to disrupt established biofilms and reduce the formation of biofilms in culture, but their efficacy depends on dosage and media conditions.

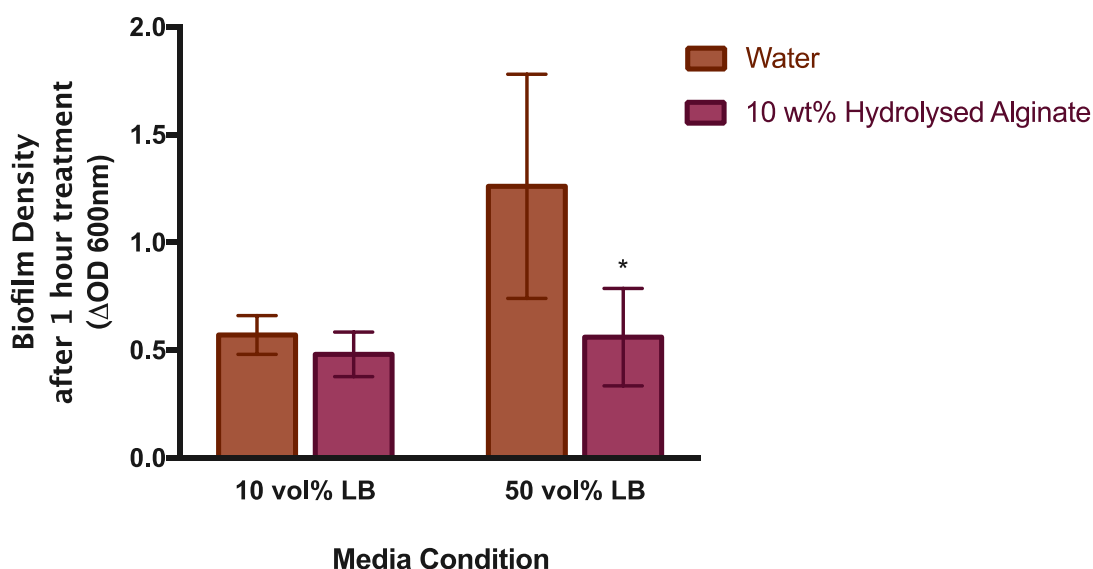


Figure 3.9 – Biofilm Assay for PA01 cultures at 37°C after 1 hour treatment with either water or hydrolysed alginate.

### 3.3.14. Long-term Exposure of PA01 to Hydrolysed Alginate

The long-term exposure of PA01 to hydrolysed alginate showed that again 5 wt% alginate can slightly increase total bacterial growth and this will continue even after 288 hours of exposure (Figure 3.10 and Figure 3.11). Despite having minimal effects on growth, after 24 hours, 5 wt% hydrolysed alginate was still effective at reducing biofilm formation (Figure 3.11). In addition, 10 wt% alginate was shown to be increasingly effective after 288 hours and significantly reduced both bacterial growth and biofilm formation. This suggests that appropriate concentrations of hydrolysed alginate have potential to be an effective long-term treatment for PA01.

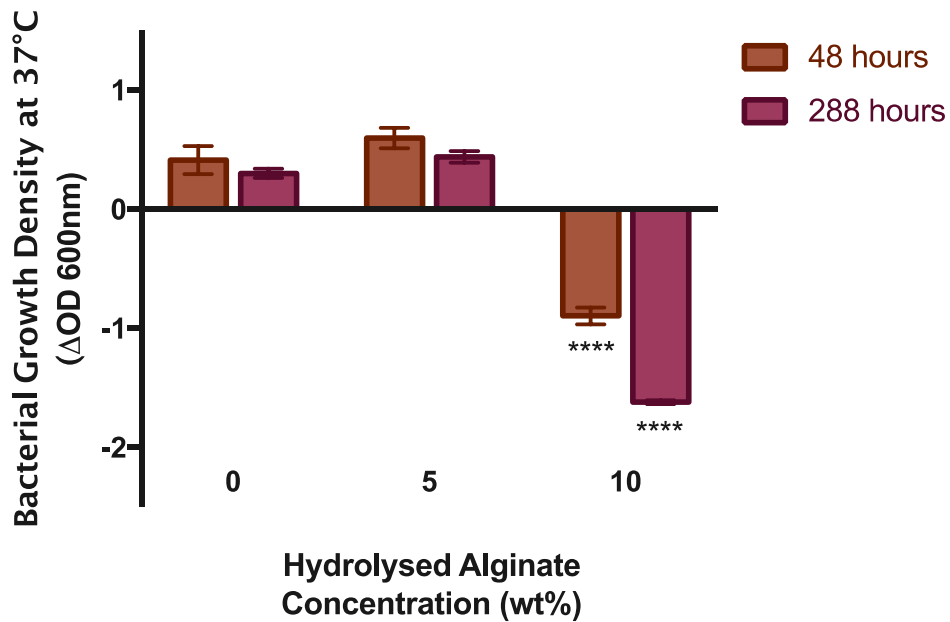


Figure 3. 10 - PA01 growth at 37°C in 50 vol% LB containing either 0, 5 or 10 wt% hydrolysed alginate. Measurements taken at 48 and 288 hours.

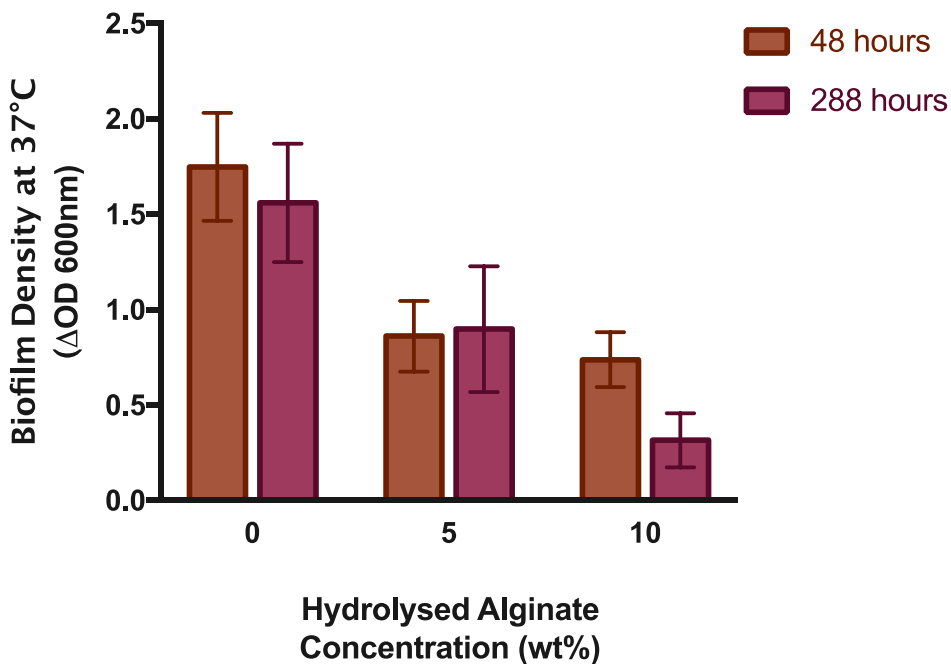


Figure 3. 11 - PA01 biofilm assay after growth at 37°C in 50 vol% LB containing either 0, 5 or 10 wt% hydrolysed alginate. Assays performed at 48 and 288 hours.

### 3.3.15. Synergistic pyo-CORM and Hydrolysed Alginate Assays

Having established the impact of just alginate and CORM on PA01 growth, combination experiments were conducted to see if alginate enhanced the antimicrobial activity of the pyo-CORM. The results from this assay (Figure 3. 12) indicate that the addition of alginate renders CORM less effective in reducing bacterial growth. However, the biofilm

reduction capacity in the tested combinations appears to have a more pronounced effect than CORM alone (Figure 3. 13). The combination of 1000  $\mu\text{M}$  CORM and 5 wt% hydrolysed alginate appears to be the most effective combination, achieving both reduced bacterial growth and biofilm formation. Moreover, as the biofilm density is less in the combined treatment than for either, CORM or alginate alone, this suggests that the treatments may be working synergistically to reduce biofilm integrity. Ultimately, however, as the mode of action and CO release mechanism from pyo-CORM is yet to be determined, it is difficult to predict how the alginate and the pyo-CORM might interact.

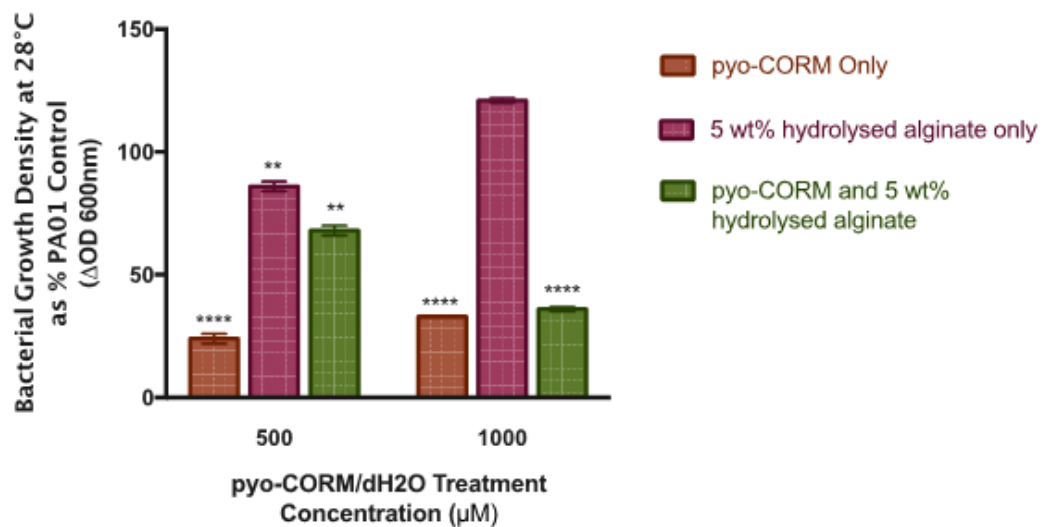


Figure 3. 12 - Growth of PA01 cultures in 10 vol% LB exposed to CORM, hydrolysed alginate (with 500 or 1000  $\mu\text{M}$  water treatment), or both. Assays incubated at 28°C for 24 hours.

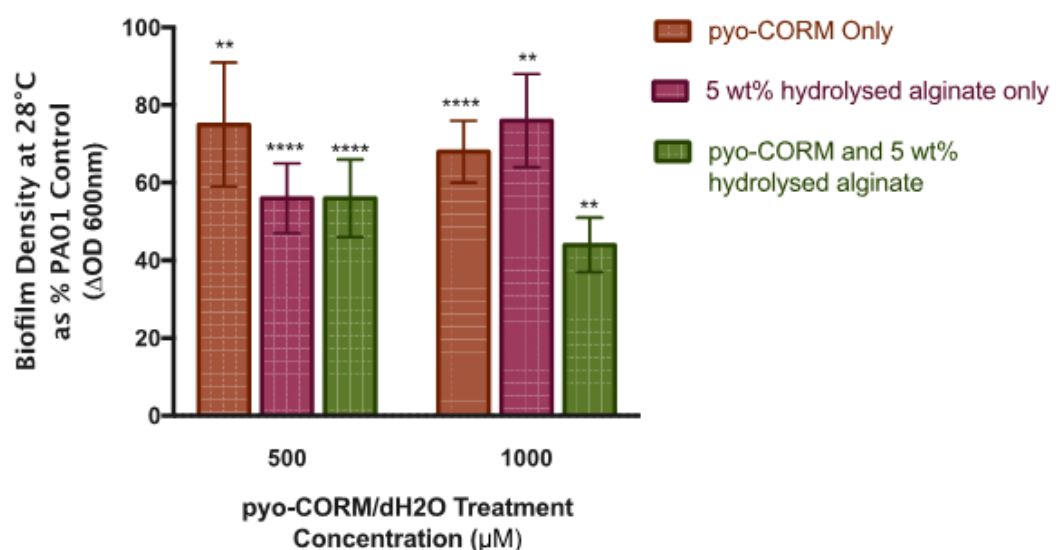


Figure 3. 13 - Biofilm assays for PA01 cultures grown in 10 vol% LB exposed to CORM, hydrolysed alginate (with 500 or 1000  $\mu\text{M}$  water treatment), or both. Assays incubated at 28°C for 24 hours.

This is similar to findings proposed by previous studies whereby, in general, low molecular weight fragments (average  $M_w$  2600 g/mol and DP13) derived from alginate were able to enhance the action of antibiotics against *P. aeruginosa* through biofilm disruption (Powell *et al.*, 2014). However the M:G ratio was shown to have an effect on potentiation of antibiotics and the fragments did not always work synergistically with antibiotics for all tested combinations (Khan *et al.*, 2012). Moreover, as indicated in this study, smaller fragments were shown to be more effective at reducing PA01 growth. Our varied results could therefore be explained by a variety of factors including the high average molecular weight and fragment sizes within our hydrolysed alginate, the M:G ratio or simply, the synergistic combinations tested.

Another possibility is that the viscosity of alginate itself limited the pyo-CORM penetration through to the bacterial cell surface and subsequently reduced the toxicity of pyo-CORM against *P. aeruginosa*.

### 3.3.16. Hydrolysed Alginate Influences Pyocyanin Production

An additional finding of note, was that cultures treated with hydrolysed alginate did not exhibit the characteristic blue-green colour generated in non-treated PA01 cultures (Figure 3. 14).



**Figure 3. 14 - Image of PA01 growth in 100 vol% LB (top row) and PA01 growing in 100%LB with alginate treatment (bottom row).**

As aforementioned, this blue-green colour seen in *P. aeruginosa* cultures is often associated with the presence of the virulence factor pyocyanin (Miller *et al.*, 2015). This phenomenon was also assessed by measuring pyocyanin through spectroscopy recording the absorbance at pyocyanin's maximum absorbance wavelength, 691 nm (Das and Manefield, 2012) (Figure 3. 15).

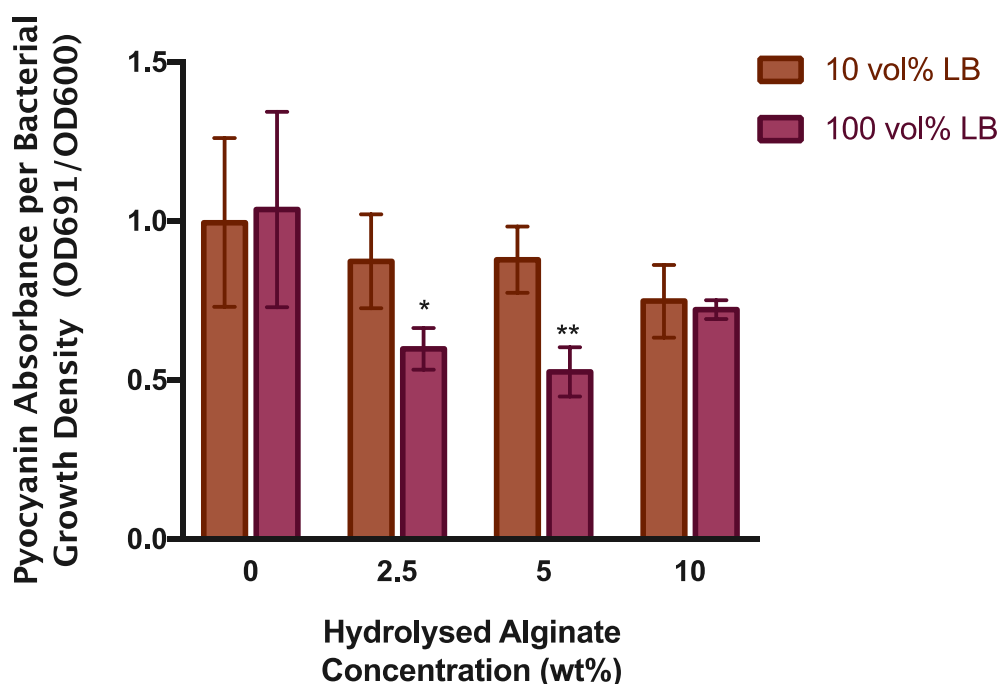


Figure 3. 15 - PA01 pyocyanin production and bacterial growth after growth at 37°C in either 10 or 100 vol% LB and containing either 0, 2.5, 5 or 10 wt% hydrolysed alginate. Pyocyanin levels (assumed proportional to absorbance at 691 nm) generated per total bacterial growth.

This shows that the pyocyanin levels, or state of oxidation, may be impacted by the presence of hydrolysed alginate. This could contribute to the reduced efficacy of pyo-CORM killing bacteria in the presence of alginate however, as it was shown that the action of pyo-CORM was not explicitly activated by pyocyanin (see Section 2), this is unlikely to be the case.

### 3.6. Conclusions and Future Work

At sufficient concentrations (10 wt%), hydrolysed alginate was shown to inhibit both bacterial growth and biofilm formation. Moreover, through dosing experiments, alginate was shown to reduce biofilm integrity in established biofilms. At lower concentrations however, alginate was shown to stimulate biofilm formation and growth. This represents a potential challenge for working towards clinical use of alginate. However, as highlighted in the discussion, this phenomenon has been seen with other antibiotics and thus alginate fragments still have potential to be a therapeutic agent. Moreover, the scope of this project did not perform testing on alternate antibiotic-alginate combinations and therefore this is something that can be explored in the future.

Combination assays showed that alginate and pyo-CORM worked synergistically in reducing bacterial biofilms, yet the combined effect was less clear for total bacterial

growth. In an attempt to further explore synergistic effects between pyo-CORM and alginate, different alginate and pyo-CORM combinations will be trialed. In particular, it is noted that higher levels of alginate for combination experiments need to be tested. The putative reduction in pyocyanin production could play an important role in reducing part of the morbidity associated with lung infections. To confirm that alginate is able to reduce the levels of pyocyanin product, in the future pyocyanin will need to be purified from cultures grown in the presence and absence of alginate. The mass spectrometry analysis and amounts liberated will serve as a definitive method to establish whether alginate is in fact influencing pyocyanin production. Moreover, to explore other specific effects on virulence factors, *P. aeruginosa*, gene expression studies could also be performed.

Future characterisation and purification of the hydrolysed alginate is essential. Although we were able to show that smaller fragments were more effective at reducing bacterial growth than larger fragments, a direct understanding of the exact fraction composition and M:G content will help to inform which fragments are the most successful at reducing bacterial growth and biofilm formation. Another important experiment to inform these studies will be testing the effects of viscosity on bacterial growth. This could be achieved for instance through the use of polyethylene glycol (PEG) and would enable us to confirm the efficacy of hydrolysed alginate at higher concentrations.

Overall these preliminary studies have found that hydrolysed alginate was efficacious in disrupting biofilms against *P. aeruginosa*. There is significant work to be done in this space to ensure appropriate concentrations, drug combinations and application method.

## SECTION 4: OPTIMISING SUGAR PURIFICATION METHODS

### 4.1. Background

#### 4.1.1. Towards Bacterial Vaccines

Many bacterial pathogens that cause chronic lung infections in CF patients have developed resistance to multiple conventional therapies. Multi-drug resistant pathogens such as *P. aeruginosa*, *S. aureus* and *B. cepacia* can cause fatal infections (Moigne *et al.*, 2016, Heijerman *et al.*, 2009a). As mentioned in the introduction, there is an ongoing discussion on the use of vaccines to prevent these bacterial infections in CF patients. This approach is additionally viable, as it would minimise the impact on protective microflora in the lungs.

A common approach to vaccine development is through targeting a specific pathogen characteristic or a virulence factor. Moreover, carbohydrate based vaccines have proven effective preventative strategies for preventing bacterial infections. For instance, the *S. pneumoniae* vaccine is comprised of a polysaccharide that mimics the capsule expressed on the bacterium's surface (Jennings, 1990). There are currently no vaccines available for *P. aeruginosa*, *S. aureus* or *B. cepacia* however several studies are underway and seeking to exploit specific characteristics of these pathogens.

Prominent vaccine targets for *P. aeruginosa* include lipopolysaccharide (LPS), flagella and secreted substances. A recent pre-clinical study has evaluated the use of a vaccine comprising Pseudomonas alginate conjugated to carrier protein. The vaccine (Farjah *et al.*, 2015) vaccine was shown to offer protective immunity and eliminate *P. aeruginosa* in subsequently infected mice.

Another promising vaccine target is the polysaccharide Poly-N-Acetylglucosamine (PNAG). PNAG is expressed by many important CF pathogens, including *S. aureus* and *B. cepacia*, and plays key roles in colonisation, biofilm formation, antibiotic resistance and immune evasion (Lin *et al.*, 2015, Izano *et al.*, 2008, Chen *et al.*, 2014, Yakandawala *et al.*, 2011, Gening *et al.*, 2010).

Recently, it was demonstrated that when mice were exposed to PNAG fragments conjugated to carrier proteins, the mice produced PNAG-specific antibodies that mediated protection to *S. aureus* (Gening *et al.*, 2010). The authors did however note

that, in order to maximise antibody production in the future, the specific number of *N*-acetylglucosamine (NAG) monomers would need to be standardised and optimised.

#### **4.1.2. Making Sugars for Vaccines**

The manufacturing of well-defined sugars in sufficient quantities is essential for the successful design of sugar-based vaccines. Despite their abundance in the environment, the purification of carbohydrates from natural sources is often difficult as they exist in low concentrations or are structurally variable (Plante *et al.*, 2001). Moreover, the complex nature of long chains of oligosaccharides makes synthesis and isolation of such compounds extremely difficult (Calin *et al.*, 2013a, Gad, 2007, Seeberger and Haase, 2000). In addition, the purification of specific sugars from bacterial cultures requires huge amounts of culture and many purification steps. For instance, in the alginate vaccine study, alginate purification from *P. aeruginosa* required 4 litres of bacterial culture, more than 120 hours of growth and significant purification and obtained less than 20 g of product (Theilacker *et al.*, 2003).

Therefore, in order to obtain sufficient and well-defined quantities, access to oligosaccharides typically relies heavily on chemical or enzymatic synthesis (Gad, 2007, Nilsson, 1988). However, as biological synthesis requires specific enzyme isolation and characterisation and often necessitates specific co-factors (Seeberger *et al.*, 2009) chemical synthesis of sugars are generally favoured.

#### **4.1.3. Solid Phase Oligosaccharide Synthesis**

Chemical synthesis of oligosaccharides is currently achieved by linking a sugar monomer to a solid support, or resin (Seeberger and Haase, 2000). Two types of support can be used to facilitate glycosylation. These are classified as solid phase, if the support is insoluble, or soluble phase, if the support is soluble (Fraser-Reid *et al.*, 2012).

Due to solubility and molecular motion, in soluble phase support, the diffusivity of the resin throughout a mixture exceeds that of solid phase (Fraser-Reid *et al.*, 2012). Although this diffusion enhances reactivity, the soluble phase method requires precipitation of the resin after each glycosylation step and this can result in a significant loss of yield (Fraser-Reid *et al.*, 2012, Seeberger and Haase, 2000). Conversely, solid phase synthesis allows for the use of excess reagents that can be efficiently removed by filtration after each glycosylation step (Collot *et al.*, 2013, Plante *et al.*, 2001). Upon completion of the synthesis, the full-length oligosaccharide chain is recovered by



cleavage from the support. The other, distinct advantage of solid support synthesis is that the entire process can be automated (Fraser-Reid *et al.*, 2012).

To achieve a glycosidic linkage, or perform a glycosylation, an excess of a reactive glycosyl donor is added to a resin-bound monomer, the glycosyl acceptor (Figure 4. 1).

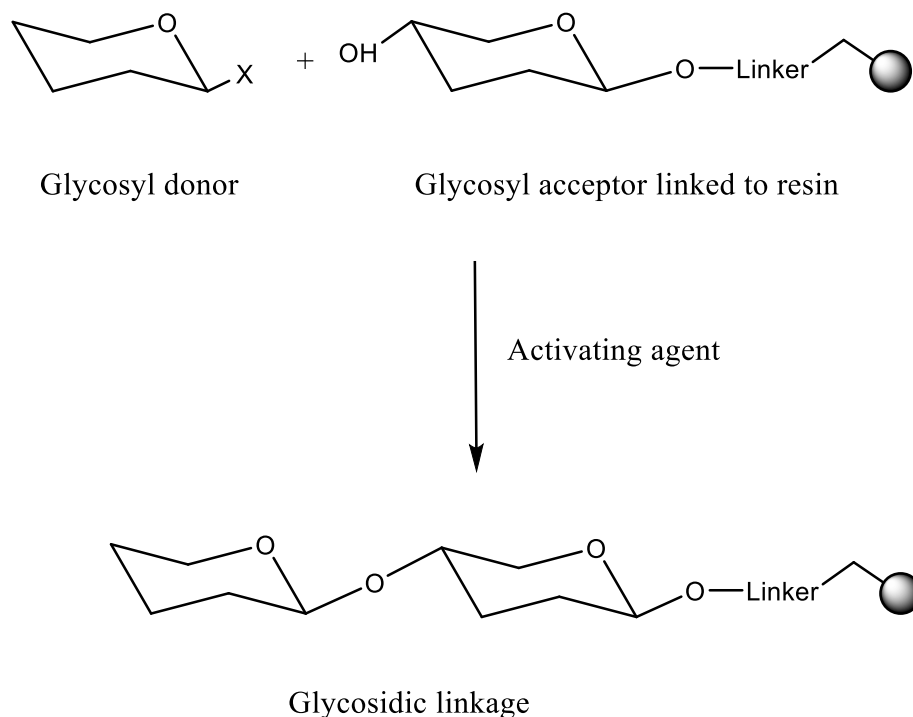


**Figure 4. 1 - Upon activation of X, A  $\beta$ -1-4 Glycosidic linkage is formed between the anomeric centre of the glycosyl donor and the hydroxyl group of the glycosyl acceptor anchored to the resin. 'X' refers to a good leaving group (e.g. I, NHCTA). Adapted from (Davis and Fairbanks, 2002).**

Contrary to the simplification depicted in Figure 4. 1, a monosaccharide contains many reactive functional groups that are capable of forming glycosidic linkages or other undesired side products. Monosaccharides can also exist in different orientations whereby the C1 functional group can point in an equatorial orientation, a beta conformation, or axially, an alpha conformation (Figure 4. 2) (Davis and Fairbanks, 2002). The conformer that is formed in a glycosylation is controlled invariably by a combination of steric and electronegative effects, including the often dominant anomeric effect (Davis and Fairbanks, 2002).

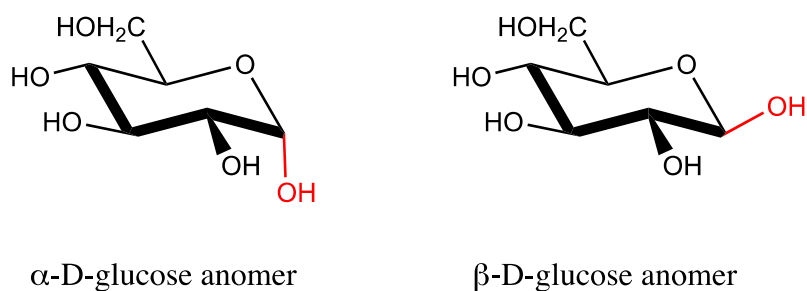


Figure 4. 2 - an  $\alpha$ -form and  $\beta$ -form of a glucose Monosaccharide. Adapted from (Davis and Fairbanks, 2002).

Therefore, in order to form the desired linkage (regioselectivity) and orientation (stereoselectivity), appropriate protecting groups must be used and removed orthogonally throughout synthesis and purification (Guo and Ye, 2010). This complexity therefore commends the use of solid phase synthesis and highlights the significance of automation.

#### 4.1.4. Automated Solid Phase Oligosaccharide Synthesis

Despite the advancement in solid phase synthesis, obtaining the desired regioselectivity and stereochemistry of functional groups in glycosylations requires many complex and time-consuming manipulations (Seeberger and Haase, 2000, Plante *et al.*, 2001). The synthesis of long polysaccharides is further complicated by their changing solubility and the uncontrolled generation of unreacted short-chain sugars (Weaver *et al.*, 2013). These factors dramatically complicate purification and subsequently it can take many months to generate small amounts of oligosaccharides. For instance, a recently synthesised pentasaccharide obtained in 25% yield over 7 steps was commended in the field (Weaver *et al.*, 2013). The complexity of synthesis is compounded by the fact that, until recently, synthesis of sugars exceeding 20mers was extremely rare (Seeberger, 2004).

To facilitate access to such long sugars, Seeberger and colleagues enhanced the process of solid phase synthesis by developing a fully automated oligosaccharide synthesiser—the Glyconeer™ (Plante *et al.*, 2001). The Glyconeer™ has already revolutionised the field of glycobiology by facilitating the synthesis of complex sugars with difficult glycosidic linkages and, most notably, by synthesising a 30mer polysaccharide chain—the longest chemically synthesised oligosaccharide to date (Calin *et al.*, 2013b, Eller *et al.*, 2013).

Moreover, the automated synthesis process has drastically reduced the time required to perform standard glycosylations and purify products, for instance, synthesis of a

hexasaccharide is now achievable within 16 hours (Kandasamy *et al.*, 2013). The Glyconeer™ therefore provides the platform for synthesis of a vast array of biologically relevant polysaccharides.

#### 4.1.5. Towards Automated Synthesis of Poly-*N*-acetylglucosamine

The ability to quickly synthesise pure and well-defined structures of PNAG will be an important tool for vaccine development against *S. aureus* and *B. cepacia*. As there are few methods currently available for efficient synthesis of PNAG (Weaver *et al.*, 2013), the Glyconeer™ is expected to be an effective tool for PNAG production. The Glyconeer™ will therefore initially be programmed and optimised with NAG as a reference point.

#### 4.1.6. Building Block and Protection Strategies

In order to synthesise PNAG using the Glyconeer™, a NAG building block will be created from an NAG monosaccharide (Figure 4. 3).

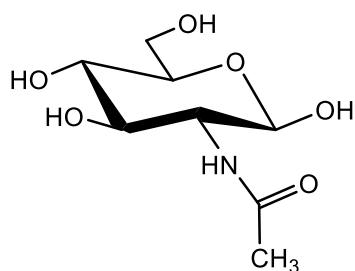


Figure 4. 3 - Monomer of *N*-acetylglucosamine (NAG).

PNAG formed in *S. aureus* bacterial biofilms contain  $\beta$ -1-6-NAG glycosidic linkages (Kröck *et al.*, 2012). Therefore, in order to generate the correct glycosidic linkages during synthesis, the functional groups will need to be protected by 'permanent' and 'temporary' protecting groups (Figure 4. 4).

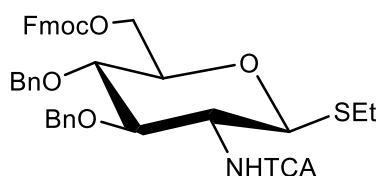
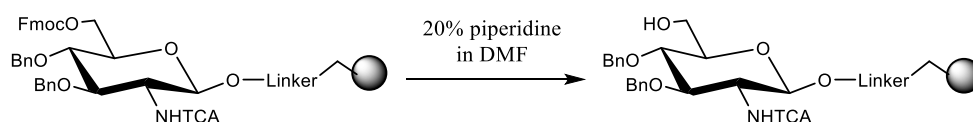


Figure 4. 4 - The *N*-acetylglucosamine (NAG) building block; NAG with protecting groups.

The C3 and C4 groups are protected with permanent benzyl (Bn) protecting groups that are only removed after completion of the full synthesis. The Bn groups are resistant to the acidic and basic conditions used throughout synthesis and are removed using

hydrogenolysis (Plante *et al.*, 2000). In order to incorporate building blocks correctly, a 'temporary' protecting group is used at the C6 position. The temporary group, fluorenylmethyloxycarbonyl chloride (Fmoc) group is readily cleaved under basic conditions and thus allows for selective deprotection of the glycosyl acceptor prior to glycosylation (Figure 4. 5).



**Figure 4. 5 - Selective Deprotection of Glycosyl acceptor with piperidine.**

To facilitate glycosylation at the C1 position, a sulphur ethyl group (SEt) is incorporated. The SEt thioglycoside can be selectively activated by N-iodosuccinimide/ trimethylsilyl trifluoromethanesulfonate (NIS/TMSOTf), with assistance from the trichloroacetimidate (NHTCA), to generate a reactive acyloxonium ion (Figure 4. 6). Through steric interaction, NHTCA additionally promotes the formation of  $\beta$ -linkage in the growing oligosaccharide chain (Zhu and Schmidt, 2009, Guo and Ye, 2010).

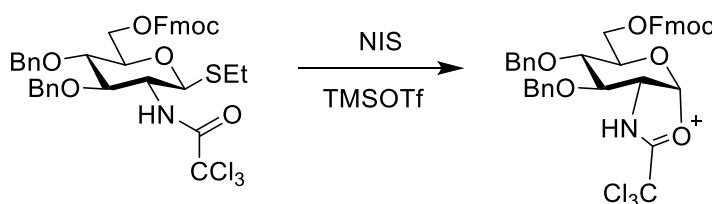


**Figure 4. 6 - Activation of Sulphur ether group on glycosyl donor using NIS/TMSOTf. Reactive acyloxonium ion only susceptible to  $\beta$  attack.**

Upon completion of synthesis, the NHTCA can be removed by hydrogenolysis. This strategy of acceptor deprotection and donor activation thereby allows for selective addition of the building block to the growing oligosaccharide chain (Kröck *et al.*, 2012).

#### 4.1.7. Post Synthesis Cleavage and Purification Strategies

Upon completion of the synthesis, the full-length oligosaccharide chain is recovered from non-desired side products and cleaved from the resin. The protecting groups are then removed to liberate the complete sugar. In an attempt to maximise yield and purity of the products generated in solid phase synthesis, various strategies for sequestration and purification have been used. The design of optimised cleavage and purification strategies will be essential in establishing the Glyconeer™ as a functional tool in glycobiology. Placing an emphasis on yield, ease of purification and efficiency, we have

opted for a continuous flow UV reactor for photocleavage of the resin and a capture-and-release strategy to separate the desired full-length product from deletion sequences. These strategies will be discussed in detail in the following sections.

#### 4.1.8. Choice of Linker

Upon completion The choice of linker joining the first building block to the resin is highly important in synthesis (Seeberger and Haase, 2000). As the linker serves as a protecting group and facilitates correct coupling, it needs to be stable enough to withstand all of the reaction conditions throughout synthesis (Seeberger and Haase, 2000). In previous synthetic strategies, an ester linkage has been used to join the linker to the solid phase resin. Following synthesis, the linker must be cleaved to liberate the sugar. This can be achieved with NaOH or NaOMe/MeOH. However, the stability of the ester linkage during glycosylation reactions is problematic, often leading to reduced yields and over-long reaction times. Therefore, to overcome this issue, in this project, a photocleavable linker will be explored. This will allow for linker cleavage without the need for any reagents or catalysts and prevent inadvertent cleavage during synthesis (Hook *et al.*, 2005). The photocleavable linker (Figure 4. 7) we will use is an *O*-nitrobenzyl type linker modified from Merrifield resin.\*

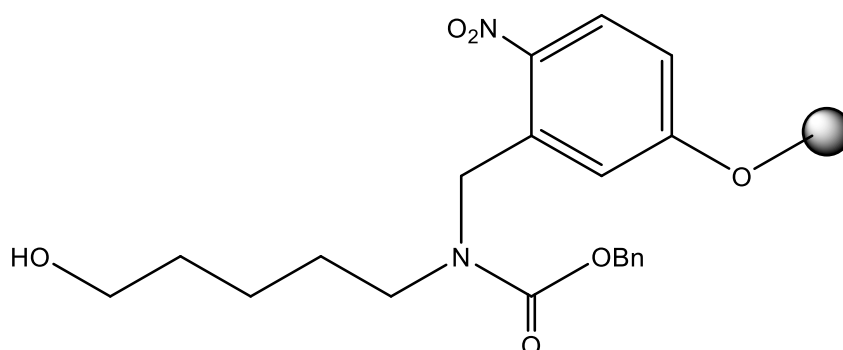
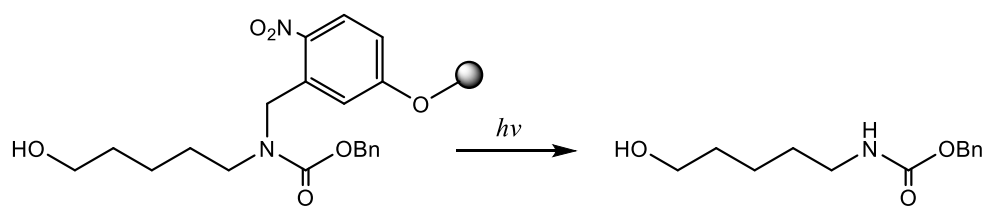


Figure 4. 7 - Photocleavable *O*-benzyl Linker attached to Merrifield Resin (Grey Circle). Adapted from (Calin *et al.*, 2013a).

The benzyl amine bond in this linker is very susceptible to photocleavage and therefore cleavage will generate a CBz protected amine which can be directly used for further glycan array studies, or similar (Eller *et al.*, 2013) (Figure 4. 8).

---

\* Synthesised at the Fascione Group within the University of York Chemistry Department with adaption from Callin *et al.* (2013)



**Figure 4. 8 - Photocleavage of the Linker liberates the resin and leaves a functional CBz protected amine group attached to the sugar.**

Therefore, by simply exposing the product to UV light, the final product can be liberated from the resin. The development of an efficient photocleavage process is therefore essential in purifying the Glyconeer™ product.

#### **4.1.9. Photocleavage in a continuous flow UV reactor**

In photochemical processes, the majority of the photocleavage tends to occur within a short distance from the UV lamp. Therefore, in the past, batch scale photochemical reactions have been limited by lamp size (Hook *et al.*, 2005). Moreover, batch scale reactions can give less sufficient photocleavage due to light scattering and reduced sample penetration; i.e. the light may not efficiently penetrate the resin in the centre of the container (Eller *et al.*, 2013). Therefore, in order to obtain an effective single-pass treatment, permit controlled irradiation times and obtain a high surface area per unit volume of UV light exposure, a continuous UV flow reactor set-up will be developed (Hook *et al.*, 2005). This will allow for irradiation time to be controlled by flow rate and enable efficient treatment of the variable volumes generated in the Glyconeer™ product.

#### **4.1.10. Purification by Tagging and Capture**

After resin cleavage, the purification of the desired polysaccharide product can be a challenging process. This additionally needs to be a selective process, as, upon addition of our building block to the resin-conjugated sugar (Figure 4. 9), there are two outcomes: the building block can completely react with the hydroxyl group to form a glycosidic linkage (Figure 4. 9a) or the glycosyl acceptor does not completely react affording a mixture of monosaccharide and disaccharide (Figure 4. 9b).

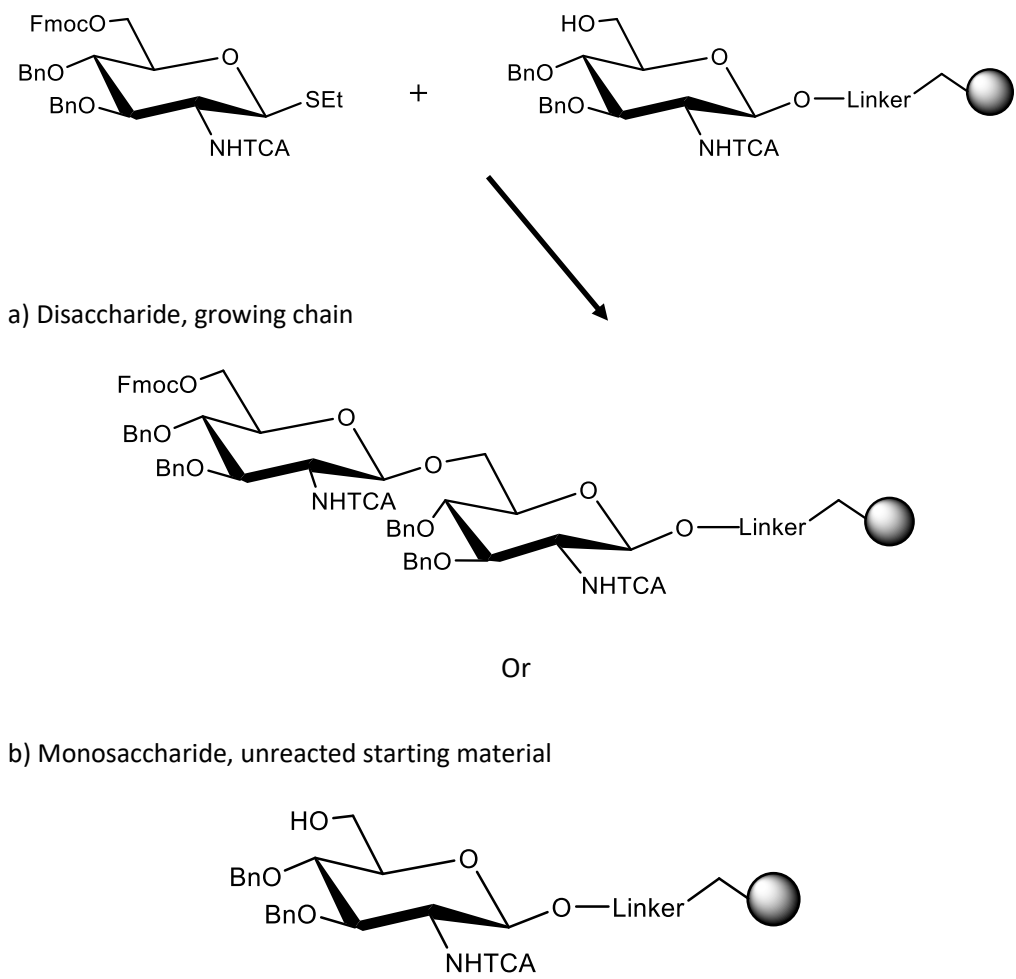


**Figure 4. 9 - In the synthesis of oligosaccharide chains, the addition of the building block to Glycosyl accepto will result in a) desired glycosylation and sugar extension or b) unreacted 'deletion sequences'.** Therefore to ensure that only the full-length sugar is collected at the end of the synthesis, following each coupling step, unreacted hydroxyl groups are 'capped' through acetylation to form stable esters (Davis and Fairbanks, 2002). Acetylation of the free hydroxyl groups occurs through addition of acetic anhydride and a base, such as pyridine (Davis and Fairbanks, 2002) (Figure 4. 10).

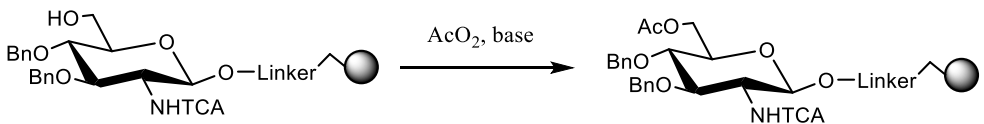


**Figure 4. 10 - Acetylation of free hydroxyl groups in NAG by acetic anhydride (AcO<sub>2</sub>) and a base yields an acetate group at the C6 position, thereby preventing subsequent glycosylation.**

As a result of the multiple glycosylation and acetylation steps involved in long chain oligosaccharide synthesis, at the end of the run, several non-reacted and acetylated by-products may remain.

Previous purification and selection of the 30mer over undesired by-products, has been achieved via a 'catch-and-release' strategy (Calin *et al.*, 2013b). This strategy involved tagging their final monomer building block with 6-aminocaproic acid (Figure 4. 11) so that it could be selectively immobilised (Calin *et al.*, 2013a).

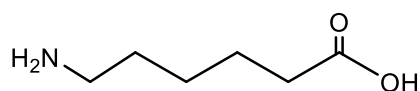


Figure 4. 11 - Aminocaproic acid used as a Tag in catch-and-release strategy.

The tagged building block was used for the final glycosylation step; ensuring that only wholly reacted full-length sugars were tagged. The amine group on the 6-aminocaproic acid tag was then captured on carboxylated magnetic beads by forming an amide linkage. As the deletion sequences have all been capped, this ensures that only the full-length tagged oligosaccharide were recovered, or 'caught' on the beads (Kröck *et al.*, 2012). After removing the deletion-sequences by magnet-assisted decanting, the full-length sugar was 'released' from the beads (Calin *et al.*, 2013b).

In order to employ a similar catch-and-release strategy in our purification, the final glycosyl donor (a NAG building block) will be tagged with Fmoc protected 6-aminocaproic acid (Figure 4. 12).

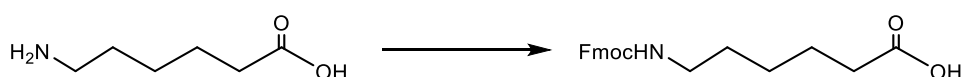


Figure 4. 12 - The tag (Fmoc protected aminocaproic acid) is generated from 6-aminocaproic acid (adapted from Kröck *et al.* (2012)).

This tag will then be selectively recovered through the use of beads that are capable of selectively binding to 6-aminocaproic acid. However, given the expense and volumes of magnetic beads required for sufficient capture, a functionalised and filterable resin will be trialled instead (Kaldor *et al.*, 1996).

## 4.2. Aims

This work will aim to optimise the post synthetic operations involved in the automated synthesis of sugars, utilising PNAG as an example. Within this context, the objectives are: to construct and validate the use of a continuous UV flow reactor for resin photocleavage; to generate an Fmoc tagged building block and; to utilise a functionalised and filterable resin to capture this tagged sugar.



### 4.3. Hypothesis

It is hypothesised that, if successfully constructed, the UV flow reactor will allow for successful, and continuous, cleavage of sugars from the support resin. It is also hypothesised that, post cleavage, the full length sugar will be able to be recovered using the benzoyl chloride beads.

### 4.4. Materials and Methods

#### 4.4.1. Synthesis of Fmoc Protected 6-aminocaproic acid

To synthesise the Fmoc protected aminocaproic acid, 7.7 mmol of 6-aminocaproic acid, 7.7 mmol of FmocOsuc and 10.7mmol of NaHCO<sub>3</sub> were added to a round-bottomed flask. 50 mL of a 1:1 v/v water: acetone mixture was then added and the solution was mixed with a stirrer bead for 6 hours at room temperature. The extent of reaction was monitored by using TLC in 1:1 hexane: ethyl acetate. The mixture was then left to stir overnight. The mixture was then cooled to 0°C using dry ice before being quenched with 1 M HCl. The Fmoc protected aminocaproic acid was then extracted using three washes of ethyl acetate. The organic layer was collected, dried over NaSO<sub>4</sub>, filtered and concentrated *in vacuo* to give the final product.

#### 4.4.2. Removal of Fmoc Protecting Group from NAG Building Block

In a 50 mL round-bottomed flask, 3.3 mmol of the NAG building block was dissolved in 10 mL of 20% (v/v) piperidine in DMF. Approximately 2 mL of DCM was then added to facilitate solubilisation. This reaction was monitored with TLC (1:1 hexane: ethyl acetate) until deemed completed. The reaction was quenched at 0°C with 1 M HCl. The mixture was then transferred to a separating funnel and was extracted with ethyl acetate. The organic layer was collected, dried over NaSO<sub>4</sub> and then concentrated *in vacuo*. The residue was then dissolved in ethanol and refrigerated overnight to facilitate crystallisation.

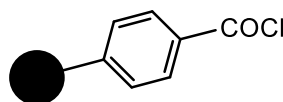
The crystallised product and ethanol mixture was then filtered and deemed to be still impure. The dissolved product was therefore purified by flash silica column chromatography using gradient eluates of 5:1 to 3:2 hexane: ethyl acetate. Fraction pooling and concentration *in vacuo* then afforded the white solid product.

#### 4.4.3. Tagging the NAG Building Block

To couple the 6-aminocaproic acid tag on to our NAG building block, the Steglich reaction was used (Neises and Steglich, 1978). In this reaction, the carboxylic acid on the tag will react with the C6 hydroxyl group of the Fmoc deprotected NAG building block to form an ester. In a round-bottomed flask, 2.4 mmol of deprotected NAG was dissolved in 15 mL of DCM. To the dissolved sugar, 7.1 mmol of the tag, 10mL of pyridine and 0.71 mmol of 4-dimethylaminopyridine were then added and mixed. The round-bottomed flask was then sealed and purged with nitrogen. The mixture was then cooled to 0°C and 7.1 mmol of DCC, diluted in anhydrous DCM, was syringed into the mixture. The mixture was then brought to room temperature and allowed to react overnight. The reaction was then diluted with DCM and quenched with 1 M HCl. The mixture was then extracted using DCM and sodium carbonate dissolved in water. The organic layer was then dried over magnesium sulphate and concentrated *in vacuo*. The product was then tested by ESI mass spectrometry.

#### 4.4.4. Functionalised Bead Recovery of the NAG Tagged Building Block

To capture the tagged, full-length sugar, polymer bound benzoyl chloride beads were used<sup>†</sup> (Figure 4. 13).



4-Chlorocarbonylpolystyrene

Figure 4. 13 - Polymer bound benzoyl chloride beads used for capturing tag.

These beads were chosen as they exhibit a high chemical functionality (1.5 mmol/g) and have previously been successful in amine scavenging (Kaldor *et al.*, 1996). In addition, as the chlorocarbonyl beads have a diameter range of 44- 149  $\mu\text{m}$ , they can be retained in 20  $\mu\text{m}$  polyethylene frits.<sup>‡</sup> This therefore enables separation of non-full length sugars by simple filtration. The chlorocarbonyl resin are also significantly cheaper than magnetic beads and require no further activation steps.

---

<sup>†</sup> Beads supplied by Sigma Aldrich, United Kingdom.

<sup>‡</sup> Extract Clean™ Columns and frits supplied by Grace, Carnforth, United Kingdom

To prepare the resin, two 100mg aliquots of the chlorocarbonyl polystyrene resin were weighed into two frit-containing cartridges (cartridge A and cartridge B). To swell the resin,

3 mL of DCM was pipetted into each cartridge (valve closed). The resin was then mixed with the DCM on the rotator for 1 hour. After swelling, the DCM was drained from the cartridge. The 6-aminocaproic acid tagged sugar to be captured was then dissolved in DMF.

After reaction completion, 53  $\mu$ L of DIPEA (2 mmol equivalents to resin) and 18.4 mg of DMAP (1 mmol equivalent to resin) were added and mixed into the dissolved sugar mixture. Once all mixed and dissolved, the DMF mixture containing sugar, DMAP and DIPEA, was pipetted into cartridge A. Cartridge A was then placed onto the rotator to mix. After 2 hours of mixing, the mixture from cartridge A was drained in to the cartridge B (containing another 100 mg swelled resin). Cartridge B was then placed onto the rotator to mix for 2 hours.

After both incubation steps, the resin in each cartridge was washed to remove DMF traces. The resins were washed 3 times with DCM, 3 times with methanol and 3 times with hexane successively. Each wash step involved addition of solvent, mixing on the rotator for 2 minutes and draining to the manifold. The cartridges were then capped and dried under vacuum overnight.

This process of capturing the sugar is shown in Figure 4. 14 whereby the amine group, present only on full-length tagged sugars, reacts with the acyl chloride on the functionalised beads. This results in the production of hydrochloric acid (HCl) and anchors the full-length sugar to the beads.

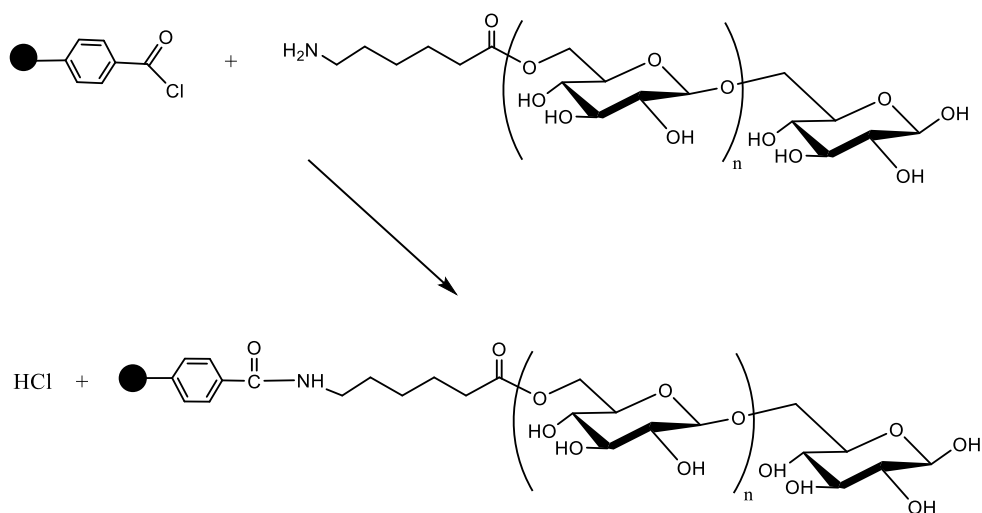


**Figure 4. 14 – The functionalised benzoyl chloride beads will react with the amine group present on the full-length sugars. This reaction generates hydrochloric acid and anchors the full-length sugar to the beads.**

After the cartridges were and dried overnight, the resin in each cartridge was swollen in 0.9mL DCM and 3.2 mL of sodium methoxide in methanol (0.50 M stock  $\text{CH}_3\text{ONa}$  in MeOH) was added. This step allows for the cleavage of the tagged full-length sugar from the functionalised beads. The mechanism of cleavage of the product from the beads is depicted in Figure 4. 15.

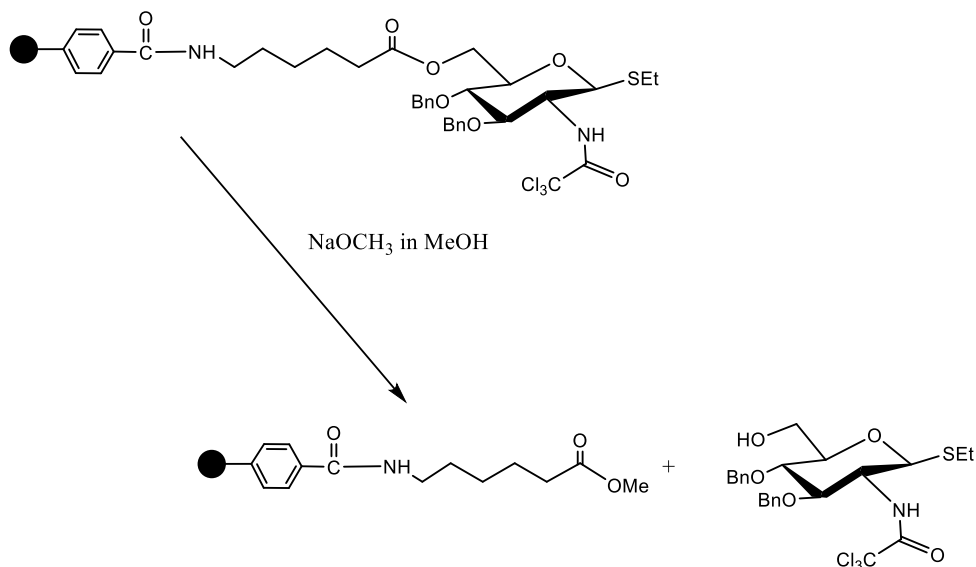


**Figure 4. 15 – Recovery of NAG Building Block from functionalised beads by sodium methoxide/methanol mediated cleavage of 6-aminocaproic acid tag.**

The cartridges were then placed on the rotator and allowed to incubate for a minimum of 6 hours. Amberlite IR H resin was then added to neutralise the mixtures before the

mixtures were filtered into separate round-bottomed flasks. The filtrates were then dried *in vacuo* and the recovered precipitates were tested using mass spectrometry.

#### 4.4.5. Construction of a UV Flow Reactor for Photocleavage

The continuous UV flow reactor was initially designed to comprise five parts; a 400 W mercury UV lamp surrounded by a cooling jacket, tubing wound around the cooling jacket, a pump to push the Glyconeer™ product through the tubing, a resin injection point and a cartridge fitted with a frit to filter the cleaved resin. A diagram of this set-up is depicted in Figure 4.16 below.

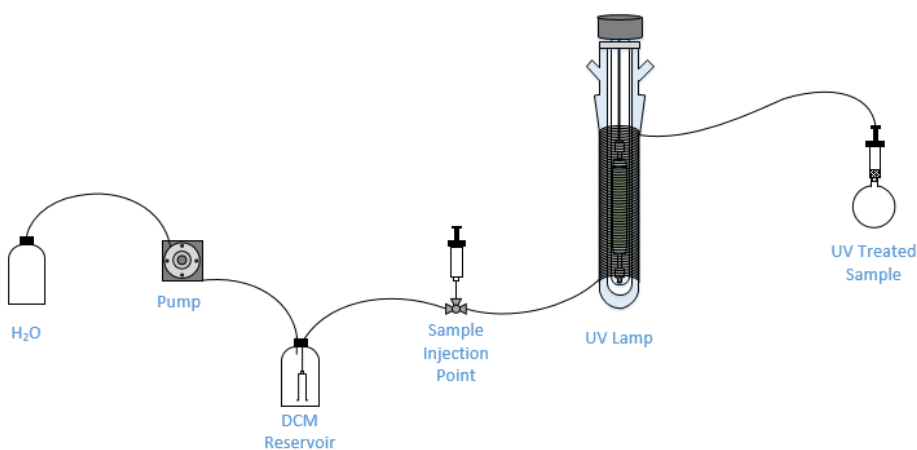
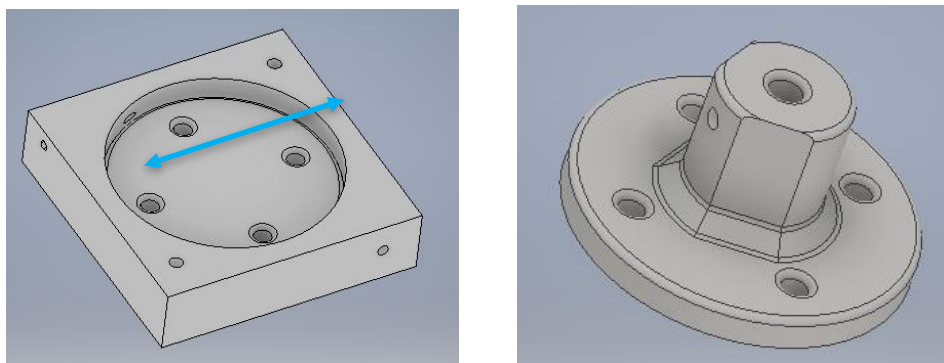


Figure 4. 16 – Set-up for Continuous Flow UV reactor.

In order to ensure safe operation of the flow reactor, solvent and UV resistant fluorinated ethylene propylene (FEP) tubing was obtained (0.75 mm ID, 1.59 mm OD). The FEP tubing was wrapped around the cooling jacket 118 times giving a total surface area per unit volume of 11,289 m<sup>2</sup>/m<sup>3</sup> for UV exposure. To prevent UV exposure to operators, a metal box with safety lock inter-switches was constructed to encase the UV lamp.

Initially, a syringe pump design was proposed, however, due to cost benefits and the desire to have controlled and steady flow, a continuous peristaltic pump design was favoured. The pump was designed using Autodesk Inventor software (Figure 4. 17) and printed with acrylonitrile butadiene styrene (ABS) using a 3D printer. The ability to 3D print the pump in this way was of great economic benefit.



**Figure 4. 17 – Autodesk Inventor Sketches for 3D Printed Peristaltic Pump (Diameter Arrow 4.7 cm).**

Upon printing the components, they were stacked onto each other and screwed in place. The pump was then incorporated into a closed system with an in-built stepper motor, cooling fans and outer speed and flow-direction controls. To connect the pump to the water reservoir, 70 cm of flexible Tygon<sup>§</sup> tubing was fed through the pump and clipped at either side to prevent tube displacement. The final peristaltic pump system is depicted in Figure 4. 18 below.

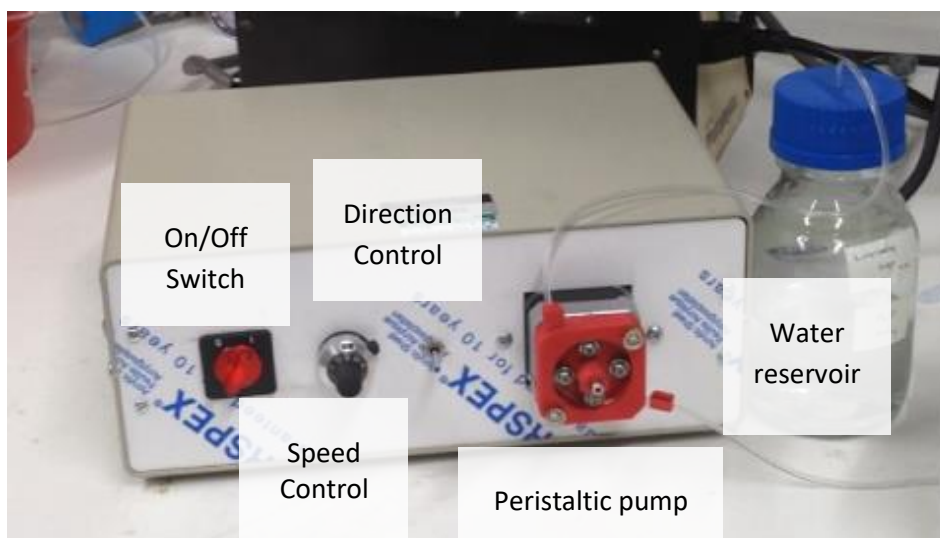


**Figure 4. 18 – Peristaltic Pump and manual control system. Tygon Tubing is Fed into the pump from a water reservoir and held in place with two red clips.**

As Tygon tubing is not resistant to solvent, the peristaltic pump was set up to draw fluid from a water reservoir through to an intermediate container containing solvent. As the pressure builds up within the intermediate container, the solvent is drawn up through a needle and pushed into a three-way connection. Initially, this connection selected was a

---

<sup>§</sup> Tygon tubing was acquired from Saint-Gobain Performance Plastics, Site du Charny, France.

DCM resistant polyvinylidene fluoride (PVDF) tee connector with a 1.6 mm OD. The preliminary design showing the original connector is depicted below in Figure 4. 19.

This connection provided an injection point for the resin, which could then be pushed through by the pump flow into the FEP tubing. Upon injection of the resin, it was found that a significant proportion of resin was pushed back through to the intermediate solvent container. Therefore, to prevent loss of resin during injection, a filter was fitted into the end of the solvent dispenser. This ensures that if any resin does back-flow into the reservoir, it will ultimately be forced through into the FEP upon pressure re-equilibration.

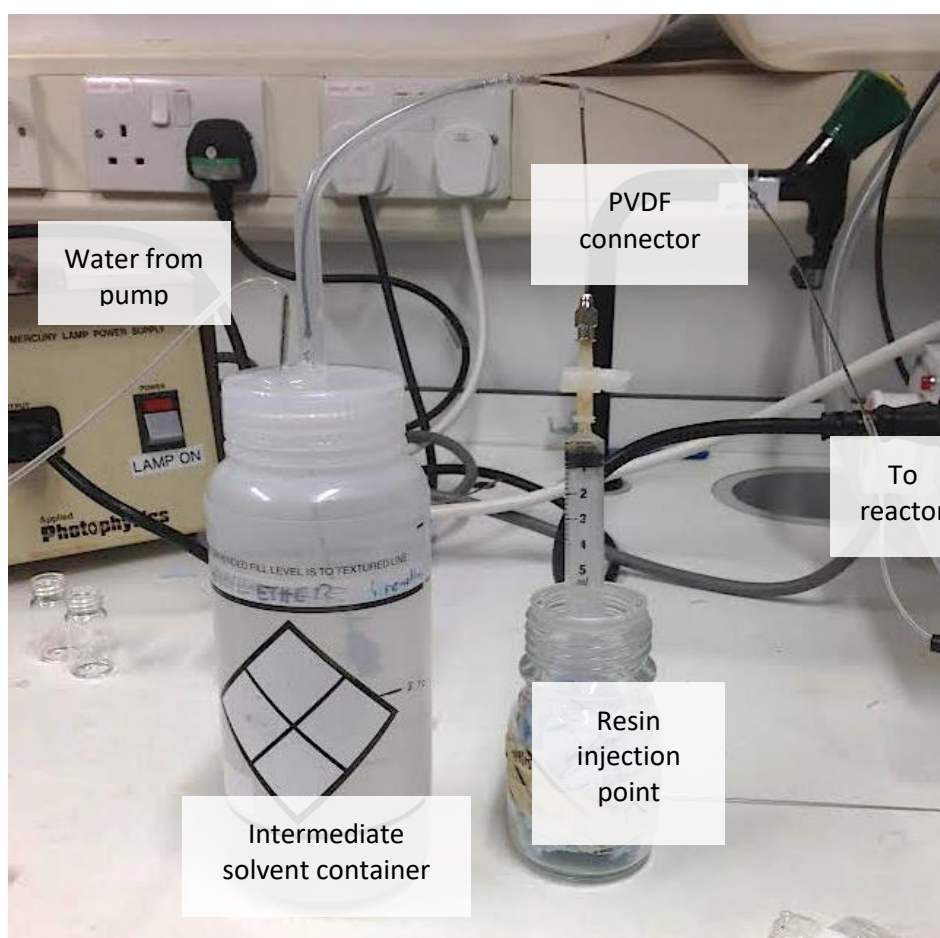


**Figure 4. 19 – Preliminary Set-up with three way PVDF Connection integrated in to FEP tubing with Needles.**

To improve the three-way connector fitting, an unused Äkta mixing chamber was re-purposed (Figure 4. 20). This fitting allowed for threaded connection of the FEP tubing, a superior seal and a more suitable and safe syringe fitted injection point.

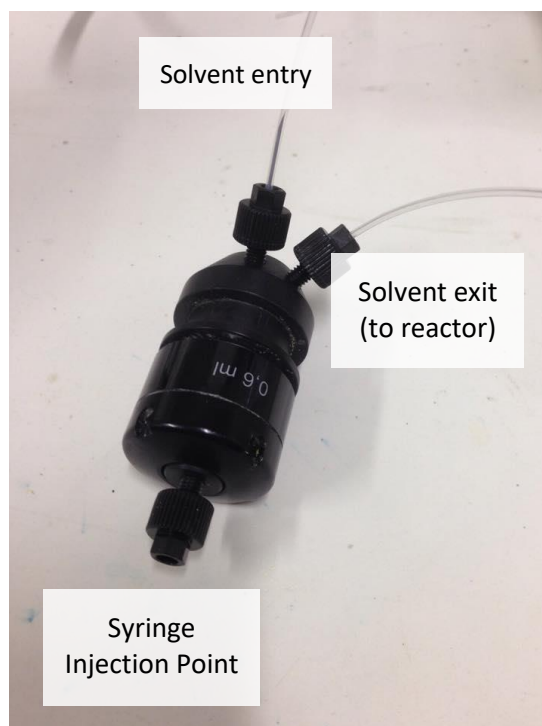


**Figure 4. 20 – Re-purposed Äkta mixing chamber used as FEP tubing and Syringe connector point. Threaded screw fittings allow for tighter, more secure seal. Note small needle insertion at solvent entry point.**

This new fitting additionally allowed for the insertion of a small needle within the FEP tubing at the solvent entry point. Previous work with the resin and fittings had shown that resin was unable to pass through orifices much less than the inner diameter of the FEP tubing (0.75 mm). Therefore, by inserting a smaller diameter needle within the FEP tubing at the entry point, the back-flow of resin into the intermediate container has been minimised.

Upon resin exposure to UV, the desired oligosaccharide should be cleaved from the resin and free in the solvent. Therefore, at the reactor exit point, the FEP tubing is directed into a frit-containing cartridge sitting in a round-bottomed flask. This enables immediate filtration and collection of the cleaved Glycoener™ product in to the flask. The round-bottomed flask can then be easily attached to a vacuum concentrator for precipitation.

#### **4.4.6. Calibration of Pump Flow Rates**

To establish the pump flow rates, the time taken for flowing DCM to fill 1mL of volume was recorded at pump settings 7, 8, 9 and 10. Time measurements were repeated ten times and the average flow rate established for each speed setting. Operability at lower speeds was deemed inappropriate due to bubble formation.



#### 4.4.7. Resin Only Photocleavage Test in Established Reactor Set-up

After turning on the UV lamp and equilibrating the tubing with DCM, 8 mg of functionalised Merrifield resin was injected into the flow reactor and pushed through with DCM at a speed of 850  $\mu\text{L}/\text{min}$ . Approximately 10 mL of DCM was pushed through at this flow rate, affording a minimum irradiation time of 11.30 minutes per pass. To ensure all of the resin was pushed through, another 10 mL of DCM was passed through, followed by 15 mL of methanol that was syringe-pumped through the reactor. The reactor outlet was directed into a filter and the product collected in a round-bottomed flask. The product was then evaporated *in vacuo* and tested for ESI mass spectrometry.

### 4.5. Results and Discussion

#### 4.5.1. Building Blocks

The mass spectra for Fmoc protection of the 6-aminocaproic acid (Figure 4. 21), the Fmoc removal of the NAG building block (Figure 4. 22) and the tag coupling to the NAG building block (Figure 4. 23) indicate that our desired products were formed.

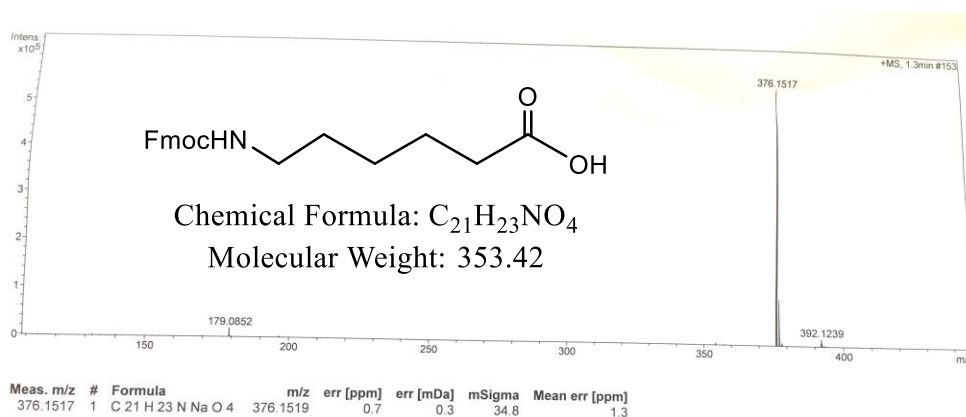


**Figure 4. 21-** Mass Spectra for Fmoc Protected 6-aminocaproic acid tag containing a sodium ion adduct (See Appendix for more detail).

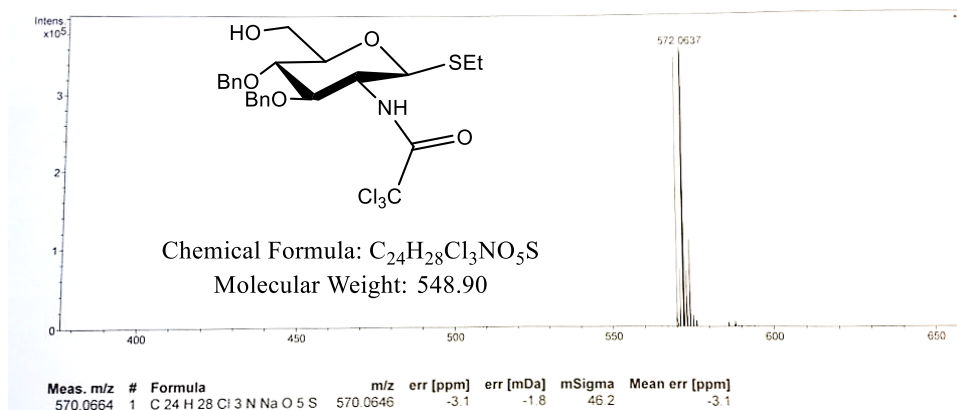


Figure 4. 22- MS results after silica column purification of Fmoc removed NAG building block containing a sodium ion adduct (See Appendix for more detail).

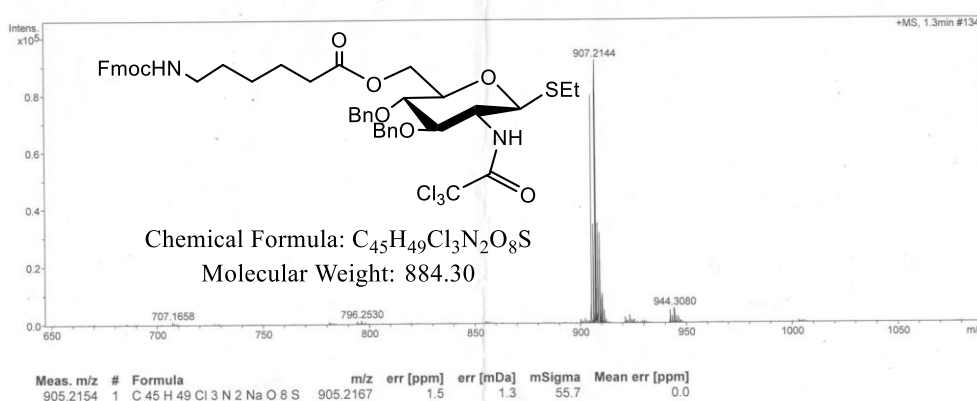


Figure 4. 23- Fmoc protected 6-aminocaproic acid Tagged NAG building block containing a sodium ion adduct (See Appendix for more detail).

#### 4.5.2. Bead Recovery of the Tagged Building Block

The mass spectrometry results of the product recovered from the chlorocarbonyl beads in cartridge A and cartridge B are shown in Figure 4. 24 and Figure 4. 25 respectively.

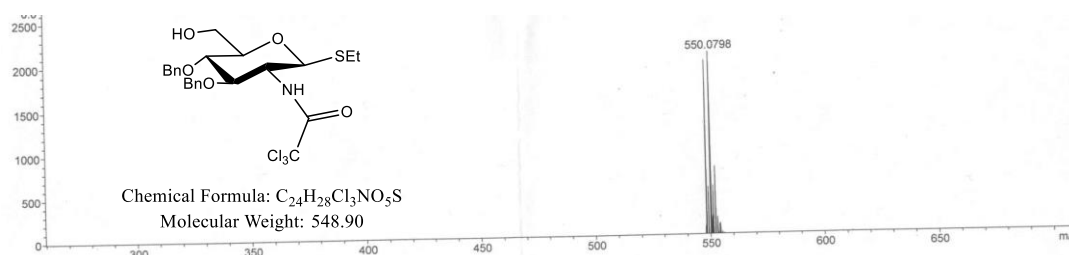
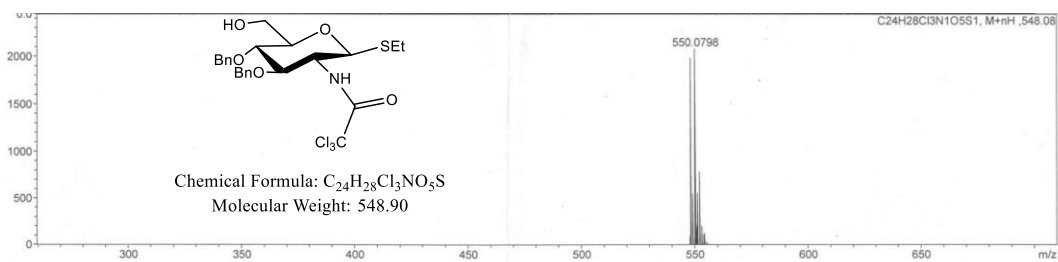


Figure 4. 24- Mass spectrometry results from Sugar recovered from Carboxylated polystyrene beads in Cartridge A (See Appendix for more detail).



**Figure 4. 25- Mass spectrometry results from Sugar recovered from Carboxylated polystyrene beads in Cartridge B (See Appendix more detail).**

In the mass spectra obtained from cartridge A, the measured M/Z ratio was found to be 570.06 with the corresponding chemical formula  $C_{24}H_{28}Cl_3NNaO_5S$ . This confirms that our desired product,  $C_{24}H_{28}Cl_3NO_5S$ , is present and contains a sodium ion adduct. In the mass spectra obtained from cartridge B (Figure 4. 25), the measured M/Z ratio was found to be 548.08 with the corresponding chemical formula  $C_{24}H_{28}Cl_3NO_5S$ . This, again, confirms recovery of our desired product. This suggests that the tagged sugar was indeed recovered by the chlorocarbonyl beads. In total, 13.3 and 7 mg of product was recovered from the cartridge A and cartridge B filtrates respectively. This gives a total yield of 51% and suggests that some of the sugar was lost throughout the process. Moreover, as some of the sugar was recovered in cartridge B, it suggests that further optimisation of the capturing process is required. This can be achieved by increasing the amount of functionalised resin or DMAP in future experiments.

#### 4.5.3. UV Flow Reactor

The final set-up of the continuous UV flow reactor is depicted in Figure 4. 26 below.

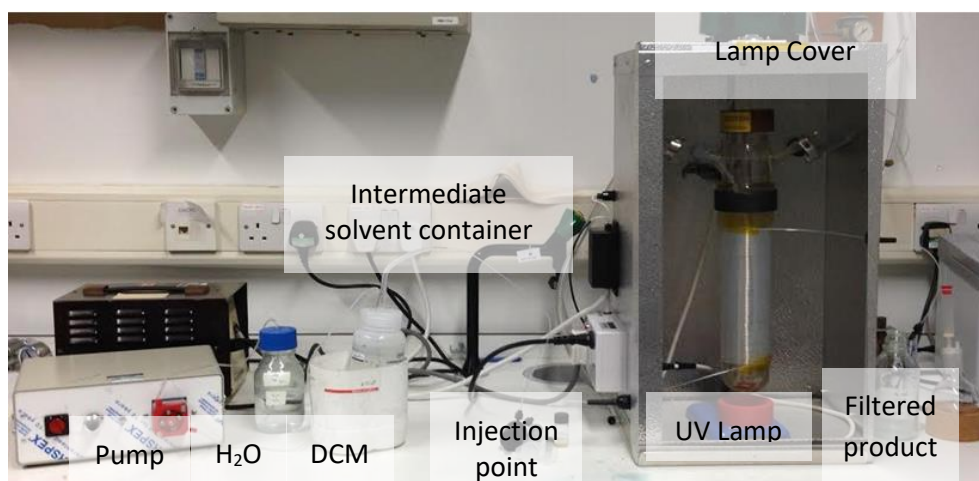


**Figure 4. 26- Final UV Flow Reactor set-up. Pump Draws water from reservoir and pumps into Intermediate Solvent container. DCM is then withdrawn and pushed through into FEP Tubing. Resin is injected as the Injection point and pushed through Reactor by Pump Pressure. FEP tubing at Reactor exit is directed into a frit-containing cartridge for immediate filtration and separation of cleaved product.**

The intermediate reservoir system relies on the density differences between water and DCM, whereby the heavier DCM sinks below the aqueous water layer (Figure 4. 27).

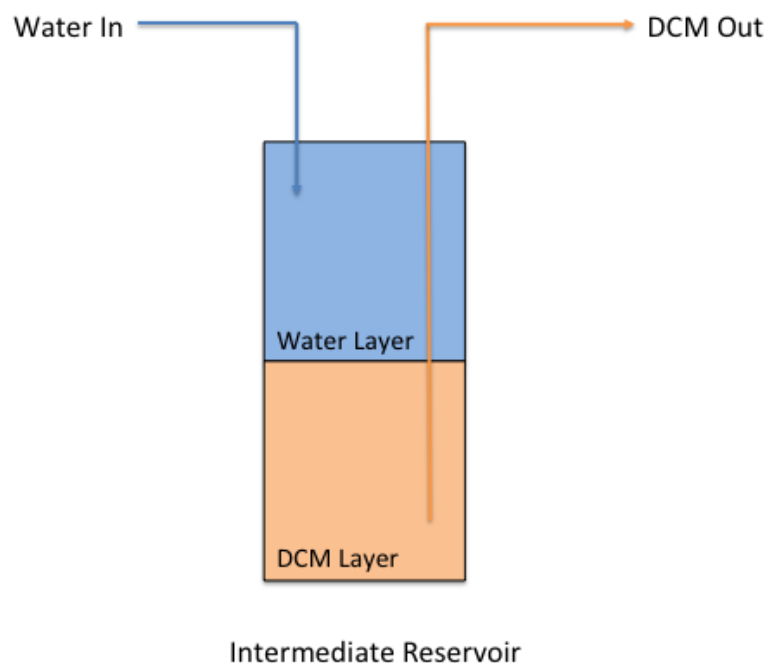


**Figure 4. 27- Schematic of Intermediate Reservoir container showing biphasic conditions that allow for solvent uptake into FEP tubing.**

This set-up is therefore only applicable to solvents with densities higher than water. To use solvents with densities lower than water, the intermediate reservoir could be easily modified by re-positioning the water inlet to the bottom and the solvent outlet to the top layer.

However, given that the solvent uptake point is a syringe connector fitting (Figure 4. 26) this system allows for the efficient injection of any desired solvent via syringe. Although this does not permit user flow control, this modification is particularly useful for post-irradiation clean-up and ensures that all of the resin has been pushed through the tubing.

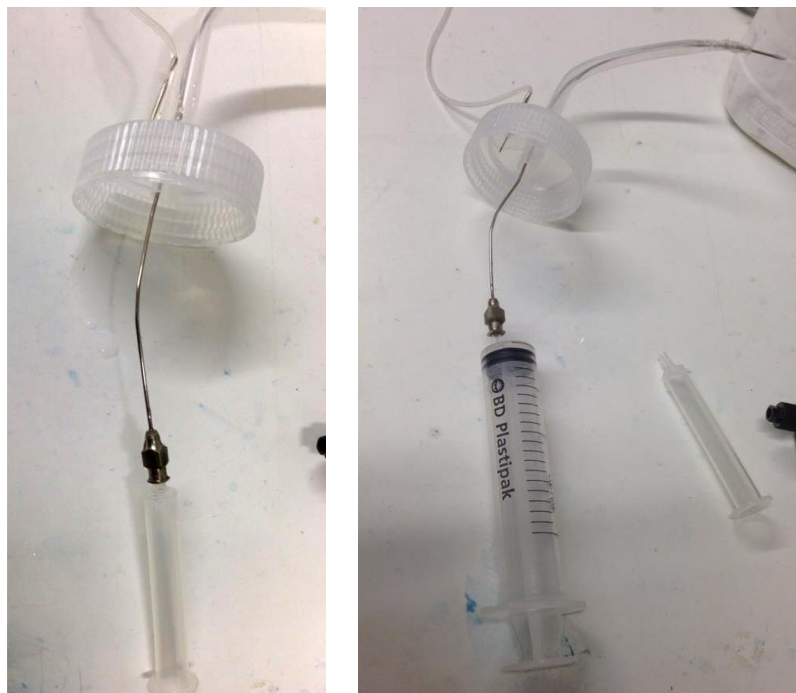


**Figure 4. 28- Intermediate Container Lid showing Syringe Fitting connected to filter-containing cartridge (Left) or Syringe at the solvent uptake point.**

The final specifications for the UV flow reactor set-up are outlined in Table 4. 1.

**Table 4. 1 - UV Flow Reactor Specifications obtained for final set-up.**

<b>UV Flow Reactor Component</b>	<b>Length</b>
Tygon Tubing ID (mm)	0.80
Tygon Tubing OD (mm)	1.00
FEP tubing ID (mm)	0.75
FEP tubing OD (mm)	1.59
Surface Area UV exposure (m <sup>2</sup> )	0.11
Surface Area/Volume UV Exposure (m <sup>2</sup> /m <sup>3</sup> )	11,289
Number coils FEP exposed to UV	118
Total length coils exposed to UV (m)	21.78
Total flow length (m)	22.53
Volume UV exposed coils (mL)	9.62
Volume flow total (mL)	9.95

The irradiation time as a function of flow rate for the reactor can be described by the expression:

$$t_i = \frac{V_{c,hv}}{\dot{V}} \quad \text{Eq. 4.1}$$

where:

$t_i$  is the irradiation time in minutes,

$V_{c,hv}$  is the volume of the FEP coils exposed to UV in mL,

$\dot{V}$  is the flow rate in mL/min.

Given the established set-up for the UV reactor (Table 4.1), this Equation 4.1 can be simplified to:

$$t_i = \frac{9.62}{\dot{V}} \quad \text{Eq. 4.2}$$

The calibrated flow rate results from the peristaltic pump are shown in Figure 4. 29.

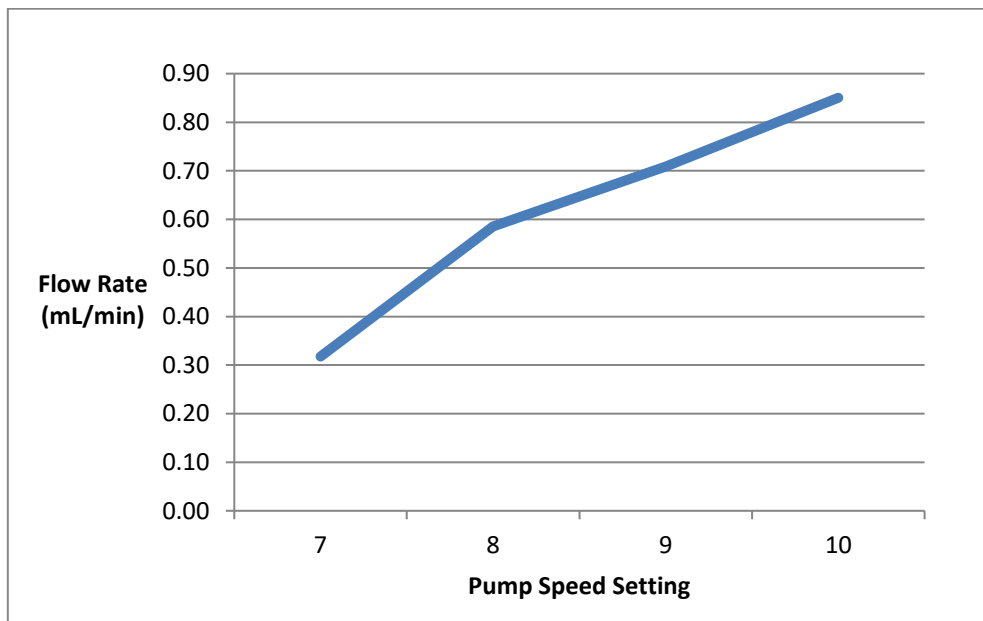
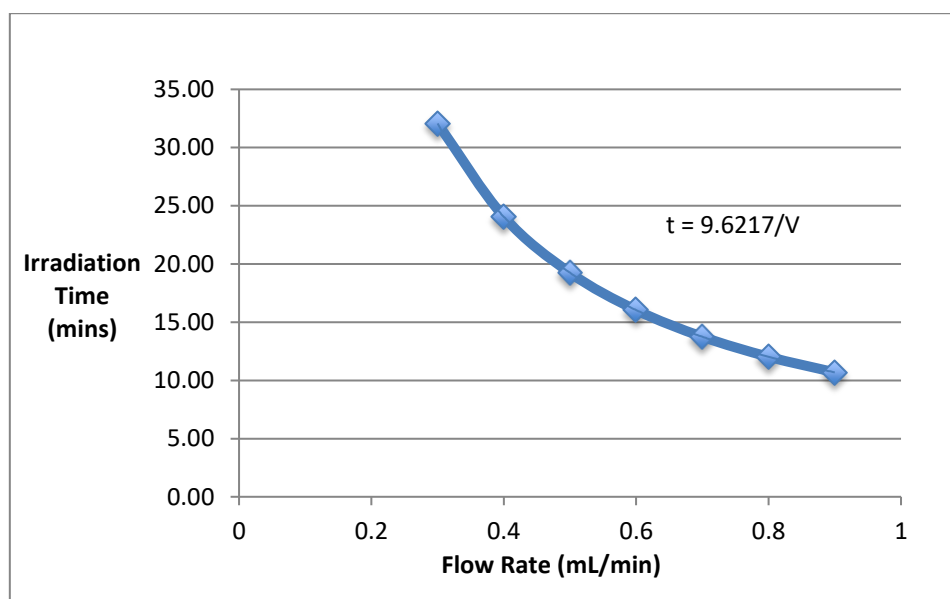


Figure 4. 29- Flow Rates for Peristaltic Pump settings obtained with DCM.

This specifies that the usable \*\* pump speed settings will provide flow rates between 0.30 to 0.90 mL/min. A graphical representation of the possible single-pass irradiation times for the given flow rates is shown below in Figure 4. 30.



**Figure 4. 30- Graphical representation of the Single-pass Irradiation time ranges that can be achieved in a single pass within the achievable pump flow rates.**

This system therefore allows for the user to control single-pass irradiation time between 10 to 20 minutes. In addition, the system is safe, user-friendly and provides a high surface area of exposure per sample volume (>11,000 m<sup>2</sup>/m<sup>3</sup>).

#### **4.5.4. Resin Photocleavage**

The mass spectrometry results from the resin-only photocleavage are shown in Figure 4. 31.

---

\*\* At pump speeds less than 7, significant bubbling occurred. Settings at 7 and above are therefore recommended to ensure steady, continuous flow.

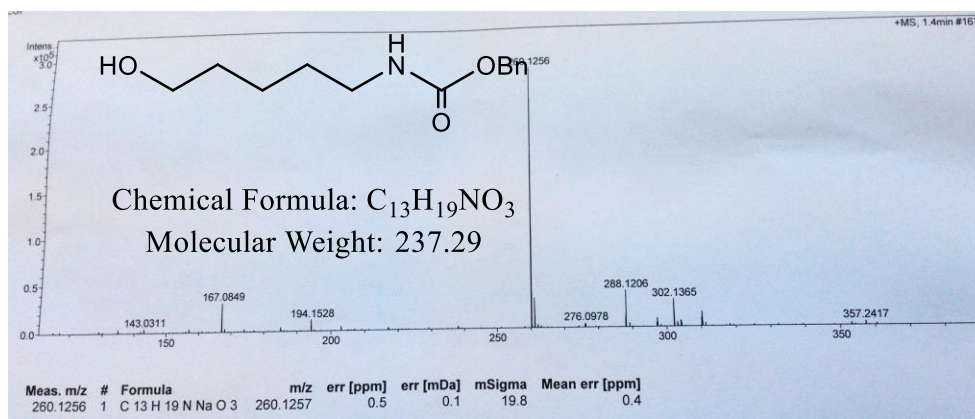


**Figure 4. 31- Mass spectra of Product obtained from Resin-only photocleavage showing product present with a sodium ion adduct (See Appendix for more detail)**

The measured M/Z ratio was found to be 260.13 with the corresponding chemical formula C<sub>13</sub>H<sub>19</sub>NNaO<sub>3</sub>. This confirms that our desired product, C<sub>13</sub>H<sub>19</sub>NO<sub>3</sub>, is present and contains a sodium ion adduct in the spectra. This suggests that the photocleavage of the resin was successful and validates the current set-up of the UV flow reactor.

However, as the loading of the resin is yet to be determined, the efficiency of photocleavage was not yet quantifiable. In an optimised system, the moles of sugar liberated from the resin should be equivalent to the moles initially anchored to the resin. Therefore the efficiency of photocleavage can be determined from the following expression:

$$\eta = \frac{n_{product}}{n_{resin}} \times 100$$

where:

$\eta$  is the % efficiency of photocleavage,

$n_{product}$  is the moles of sugar recovered in mmol,

$n_{resin}$  is the moles of sugar on resin pushed through the UV reactor in mmol.

As, the moles of sugar initially anchored to the resin is dependent on the resin loading, the efficiency of photocleavage can be expressed as:

$$\eta = \frac{n_{product}}{l_{resin} \times m_{r,hv}} \times 100$$

where:

$l_{resin}$  is the loading of the resin in mmol/mg,

$m_{r,hv}$  is the mass of resin pushed through the UV reactor in mg.



As the efficiency is representative of the amount of resin cleaved in a single-pass, in the future, the optimisation of single-pass irradiation time can be readily achieved. The number of passes required for optimum photocleavage will also need to be determined to ensure efficient purification of the Glyconeer™ product.

#### **4.6. Conclusions and Future Work**

Using PNAG as a reference point, a NAG building block was successfully tagged with 6-aminocaproic acid. The tagged sugar was then shown to be recoverable using chlorocarbonyl functionalised polystyrene beads, giving a total yield of 51%. This suggests that capture of a full-length polysaccharide should be a viable purification strategy. Furthermore, through several iterations and adjustments, a practical continuous UV flow reactor has been established. The reactor allows for user controlled irradiation times between 10 to 20 minutes for a single-pass and an integrated filter to allow immediate separation of resin from product. Moreover, based upon the successful resin-only cleavage performed in final set-up, the UV flow reactor can be commended as an effective cleavage process. Future optimisation studies will be required in each of these strategies. For instance, to improve yield in tagged sugar recovery, an excess of functionalised beads and reagents can be trialled. The UV flow reactor system will also need adjustments to determine the optimum irradiation time and number of passes required for a given Glyconeer™ product. Although these purification strategies require further optimisation, these preliminary findings have validated the use of both a UV flow reactor for resin photocleavage and functionalised polystyrene beads for full-length sugar recovery. The purification strategies are subsequently recommended for integration with the Glyconeer™ process and are expected to improve the yield and quality of synthesised sugars hereafter.

## SECTION 5: PROJECT SUMMARY AND FUTURE WORK

This project has investigated aspects within three novel approaches to combatting pathogens in CF patients; CORMs, alginate fragments and optimising sugar purification methods.

CORMs represent a novel approach to antibiotic drug design and shows great promise for treating CF as they are both anti-inflammatory and toxic against *P. aeruginosa*. The pyo-CORM's ability to disrupt Pseudomonal biofilms in particular supports its efficacy as a potential therapeutic agent. However, for CF patients, the ongoing challenge will be to develop CORMs that are specifically activated in the presence of *P. aeruginosa*. Moreover, the specific mode of action for CORMs will be vital, particularly for bacterial-specific targeting. Thorough characterisation of the material will help to inform the mode of action, and, for instance, future studies could include microanalysis of CORMs to establish specific content, purity and stability of the material to be used in biological assays.

In general, at high concentrations, alginate fragments were able to perturb the growth and biofilm formation of *P. aeruginosa*, and smaller fragments were more effective at biofilm disruption than larger fragments. The variation within the mixture of alginate fragments highlights the importance of utilising well established mechanisms to achieve consistently defined fragments – i.e. fragments with defined chain lengths, stereochemistry and M:G content. The ability to combat biofilms, in an optimised way, will continue to be an important therapeutic strategy to pursue in terms of potentiating antibiotics and preventing chronic infections. Future work will therefore investigate the use of automated sugar synthesisers to define the most optimal compositions and lengths for alginate fragments in combatting biofilms.

New post synthetic purification methods were designed and built for automated synthesis of sugar fragments. This was established through building block design, UV flow reactor construction and selective bead recovery. Future work will involve applying these methods to larger polysaccharides within heterogeneous mixtures. The optimisation of these post-synthetic purification strategies will enable provide access to well-defined sugars and support the development of sugar-based vaccines as well as other sugar-based therapeutics, such as alginate fragments.

As antibiotic resistance increases, so does the need for novel therapeutic approaches. Ultimately, it is likely that a combination of these approaches, and treatment methods will be key in combatting CF pathogens and delivering the best possible outcomes for CF patients in the future.

## APPENDIX

### A1. Details of Referenced Compounds

Table A.1 below shows the hypothesis tests used to determine statistical significance of the results obtained throughout the research project.

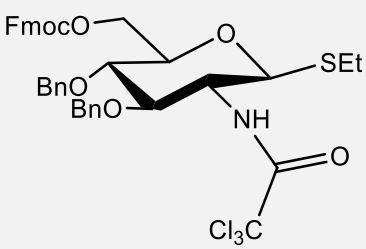
Table A. 1- Symbols used throughout project and associated p values

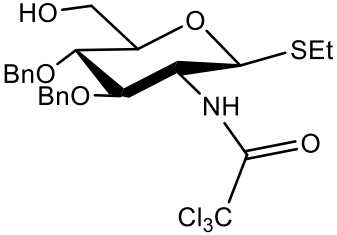
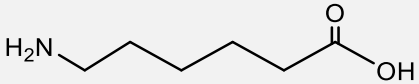
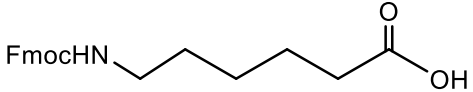
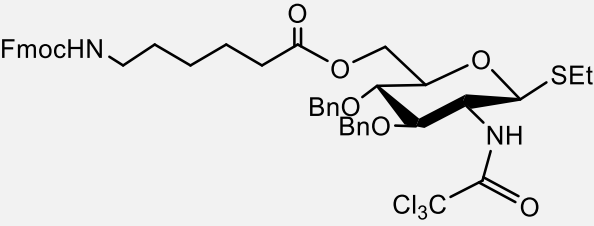
Symbol	P value	Meaning
ns	$P > 0.05$	No evidence against the null hypothesis.
*	$P \leq 0.05$	Weak evidence against the null hypothesis.
**	$P \leq 0.01$	Moderate evidence against the null hypothesis.
***	$P \leq 0.001$	Strong evidence against the null hypothesis.
****	$P \leq 0.0001$	Very strong evidence against the null hypothesis.

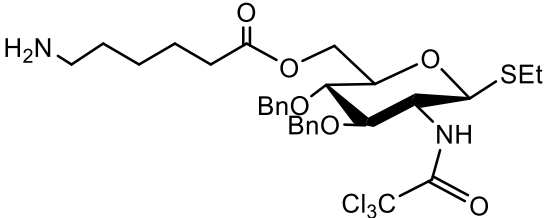
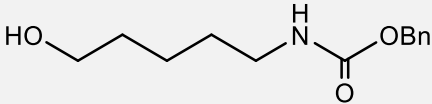
### A2. Details of Referenced Compounds

Table A.2 lists the structures, molecular weights and chemical formulas for the compounds used and synthesised throughout the project.

Table A. 2- The molecular weights and Chemical Formulas for Compounds used and synthesised throughout the project.

Description and Structure	Chemical Formula	Molecular Weight
<b>Fmoc protected NAG BB</b> 	$C_{39}H_{38}Cl_3NO_7S$	771.15

Description and Structure	Chemical Formula	Molecular Weight
<p data-bbox="459 353 785 385"><b>Fmoc deprotected NAG BB</b></p> 	<p data-bbox="975 353 1149 385"><math>C_{24}H_{28}Cl_3NO_5S</math></p>	<p data-bbox="1246 353 1331 385">548.91</p>
<p data-bbox="464 824 780 855"><b>6-aminocaproic acid (tag)</b></p> 	<p data-bbox="1002 824 1121 855"><math>C_6H_{13}NO_2</math></p>	<p data-bbox="1246 824 1331 855">131.17</p>
<p data-bbox="395 1196 847 1227"><b>Fmoc protected 6-aminocaproic acid</b></p> 	<p data-bbox="995 1144 1128 1176"><math>C_{21}H_{23}NO_4</math></p>	<p data-bbox="1246 1144 1331 1176">353.41</p>
<p data-bbox="491 1541 751 1572"><b>Fmoc tagged NAG BB</b></p> 	<p data-bbox="970 1541 1150 1572"><math>C_{45}H_{49}Cl_3N_2O_8S</math></p>	<p data-bbox="1246 1541 1331 1572">884.30</p>

Description and Structure	Chemical Formula	Molecular Weight
<p data-bbox="411 353 831 383"><b>Fmoc deprotected tagged NAG BB</b></p> 	C <sub>30</sub> H <sub>39</sub> Cl <sub>3</sub> N <sub>2</sub> O <sub>6</sub> S	662.06
<p data-bbox="336 757 906 842"><b>Photocleaved functional OBz protected amine group</b></p> 	C <sub>13</sub> H <sub>19</sub> NO <sub>3</sub>	237.29

### A3. Sample Calculations

#### A3.1 Sample calculation for UV flow reactor flow rate at speed 10.0

The time to fill defined volumes at speed 10.0 is shown in Table A.3.

**Table A. 3- Time required for DCM to Fill defined Volumes in a measuring cylinder. Measured at FEP Tubing Outlet of UV Flow Reactor.**

V (mL)	t (s)
1	71.91
1	67.94
1	65.38
1	67.96
3	184.65
1	73.93
1	70.76
1	80.76
1	79.13

Based upon the values obtained in Table A.1, the average flow rate was calculated by:

$$\dot{V}_{av} = \frac{1}{n} \sum_{i=1}^n \frac{V}{t}$$

where:

$\dot{V}_{av}$  is the average flow rate in mL/min,

$V$  is a specified volume in mL,

$t$  is the time taken to fill a specified volume, in minutes

$n$  is the number of measurements taken

The average flow rate obtained at speed 10.0 is therefore:

$$\begin{aligned} \dot{V}_{av} &= \frac{1}{9} \times \left( \frac{1\text{mL}}{71.91\text{s}} + \frac{1\text{mL}}{67.94\text{s}} + \frac{1\text{mL}}{65.38} + \frac{1\text{mL}}{67.96\text{s}} + \frac{3\text{mL}}{184.65\text{s}} + \frac{1\text{mL}}{73.93\text{s}} + \frac{1\text{mL}}{70.76\text{s}} \right. \\ &\quad \left. + \frac{1\text{mL}}{80.76\text{s}} + \frac{1\text{mL}}{79.13\text{s}} \right) \times \frac{60\text{s}}{1\text{min}} \\ &= 0.84\text{mL}/\text{min} \end{aligned}$$

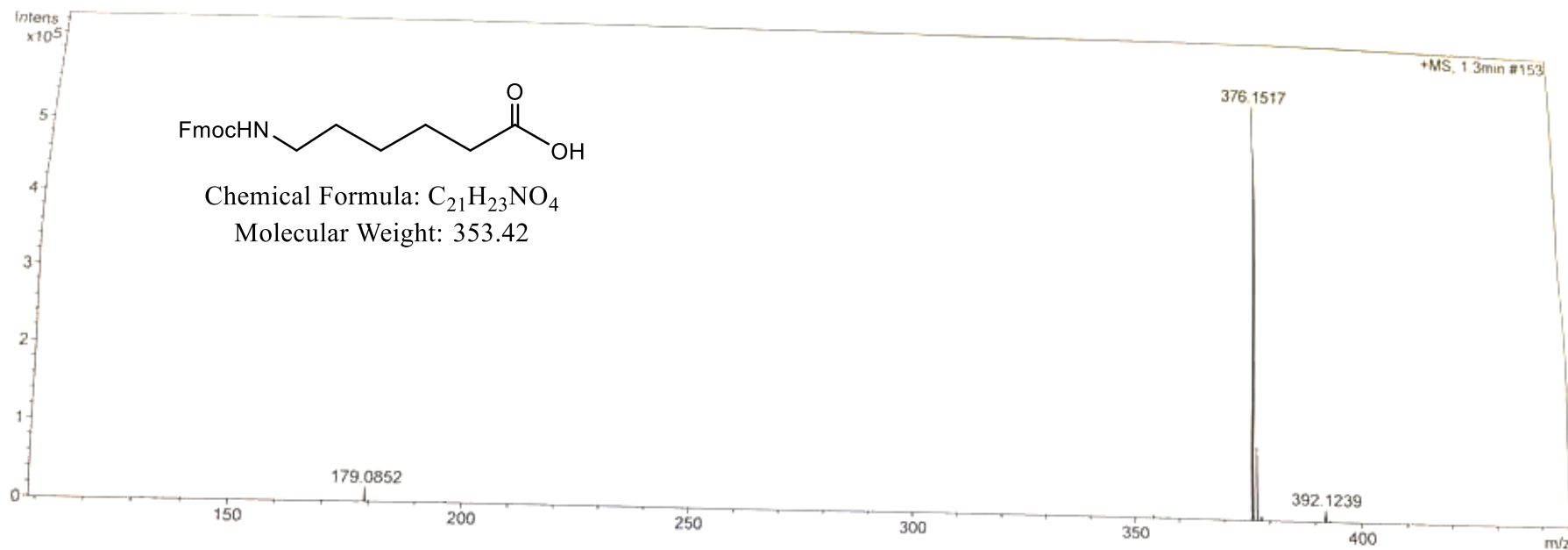
#### **A4. Enlarged Mass Spectrometry Results**

The following pages display enlarged mass spectra of compounds discussed in Results section.



Analysis Filename maf56814k\_P1-F-9\_01\_63535.d  
Method 400p\_meoh1260\_2c1s.m  
Submission Name maf56814k  
Instrument micrOTOF  
ESI Positive

Acquisition Date 26/01/2016 14:21:44



Meas. m/z	#	Formula	m/z	err [ppm]	err [mDa]	mSigma	Mean err [ppm]
376.1517	1	C 21 H 23 N Na O 4	376.1519	0.7	0.3	34.8	1.3

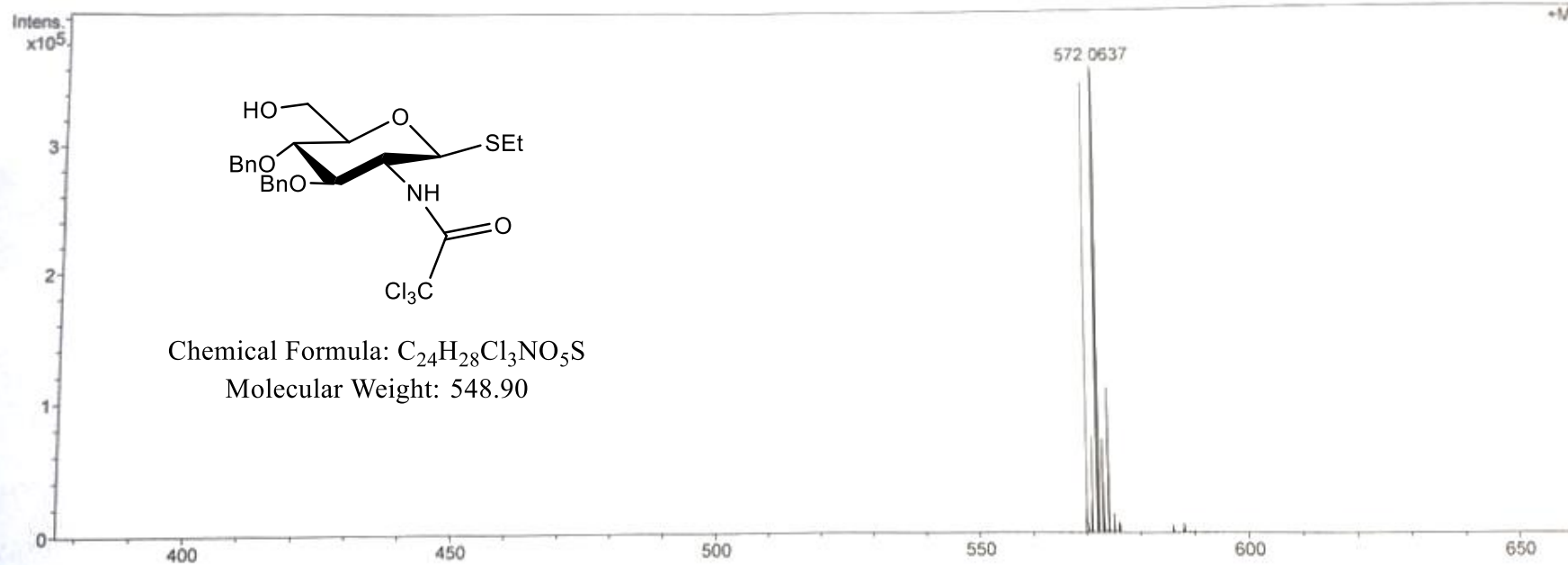
Figure A. 1- Fmoc Protected 6-aminocaproic Acid

**Analysis Information**

Acquisition Date

29/01/2016 10:55:56

Analysis Filename maf56903ks\_P1-C-8\_01\_63638.d  
Method 600p\_meoh1260\_2c1s.m  
Submission Name maf56903ks  
Instrument micrOTOF  
ESI Positive



Chemical Formula:  $C_{24}H_{28}Cl_3NO_5S$   
Molecular Weight: 548.90

Meas. m/z	#	Formula	m/z	err [ppm]	err [mDa]	mSigma	Mean err [ppm]
570.0664	1	C <sub>24</sub> H <sub>28</sub> Cl <sub>3</sub> NNaO <sub>5</sub> S	570.0646	-3.1	-1.8	46.2	-3.1

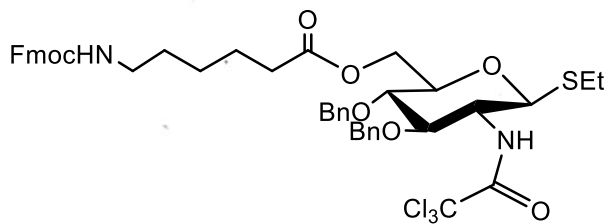
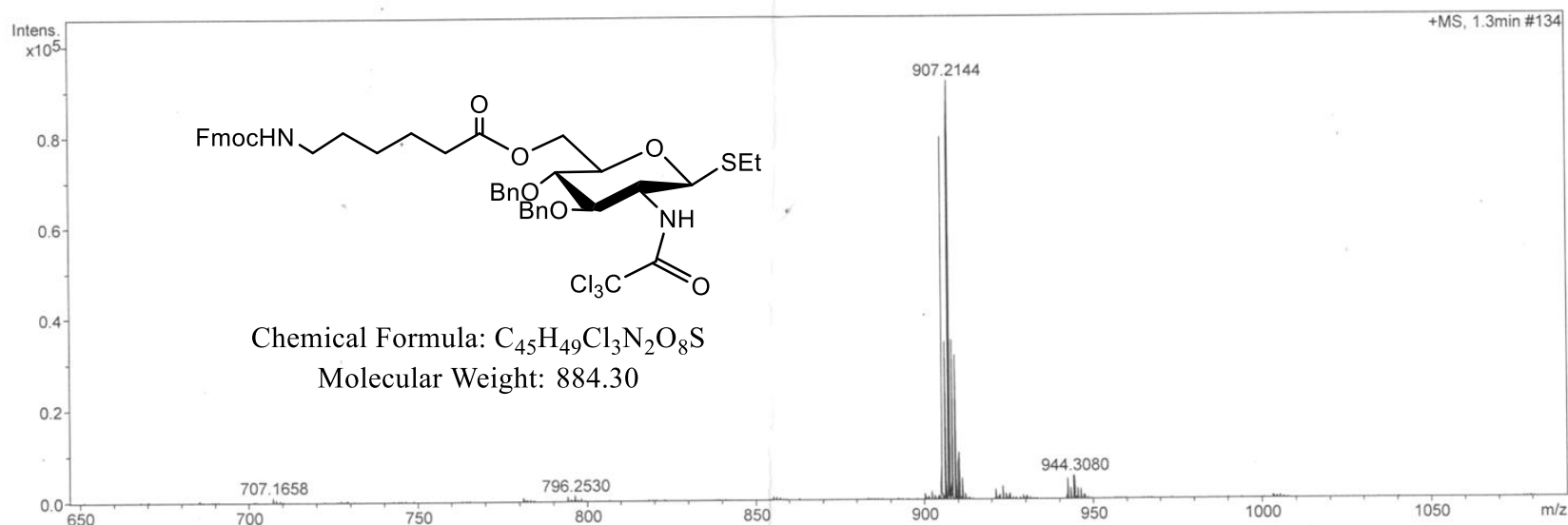
Figure A. 2- Fmoc Deprotected NAG Building Block

Analysis Information

Acquisition Date

09/03/2016 13:37:20

Analysis Filename maf57839ks\_P1-C-8\_01\_64854.d  
 Method 800px\_meoh1260\_2c1s.m  
 Submission Name maf57839ks  
 Instrument micrOTOF  
 ESI Positive



Chemical Formula: C<sub>45</sub>H<sub>49</sub>Cl<sub>3</sub>N<sub>2</sub>O<sub>8</sub>S  
 Molecular Weight: 884.30

Meas. m/z	#	Formula	m/z	err [ppm]	err [mDa]	mSigma	Mean err [ppm]
905.2154	1	C 45 H 49 Cl 3 N 2 Na O 8 S	905.2167	1.5	1.3	55.7	0.0

Figure A. 3- Fmoc 6-Aminocaproic Acid Tagged NAG Building Block

Analysis Information

Analysis Filename maf57920ks\_P1-F-2\_01\_64934.d  
Method 600p\_mech1260\_2c1s.m  
Submission Name maf57920ks  
Instrument micrOTOF  
ESI Positive

Acquisition Date

11/03/2016 15:01:40

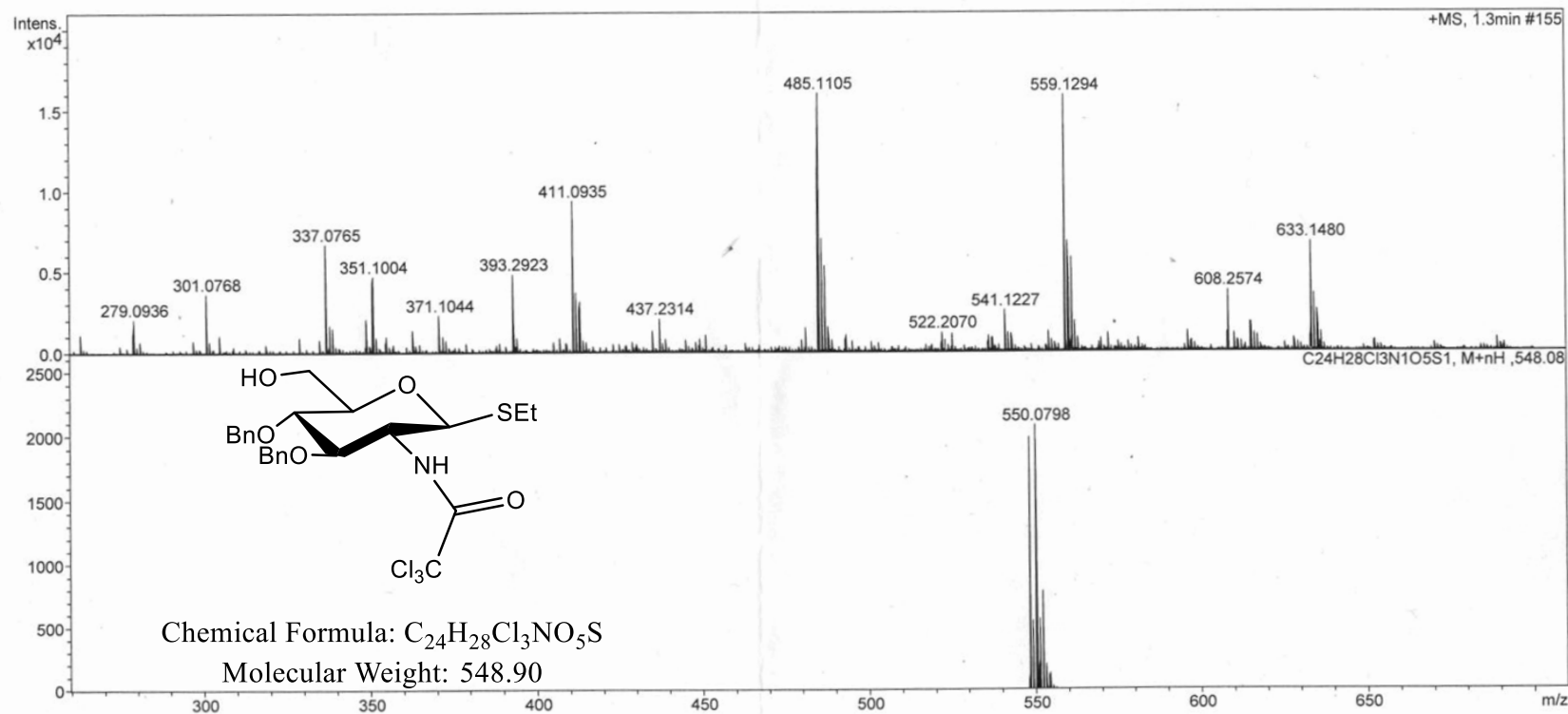
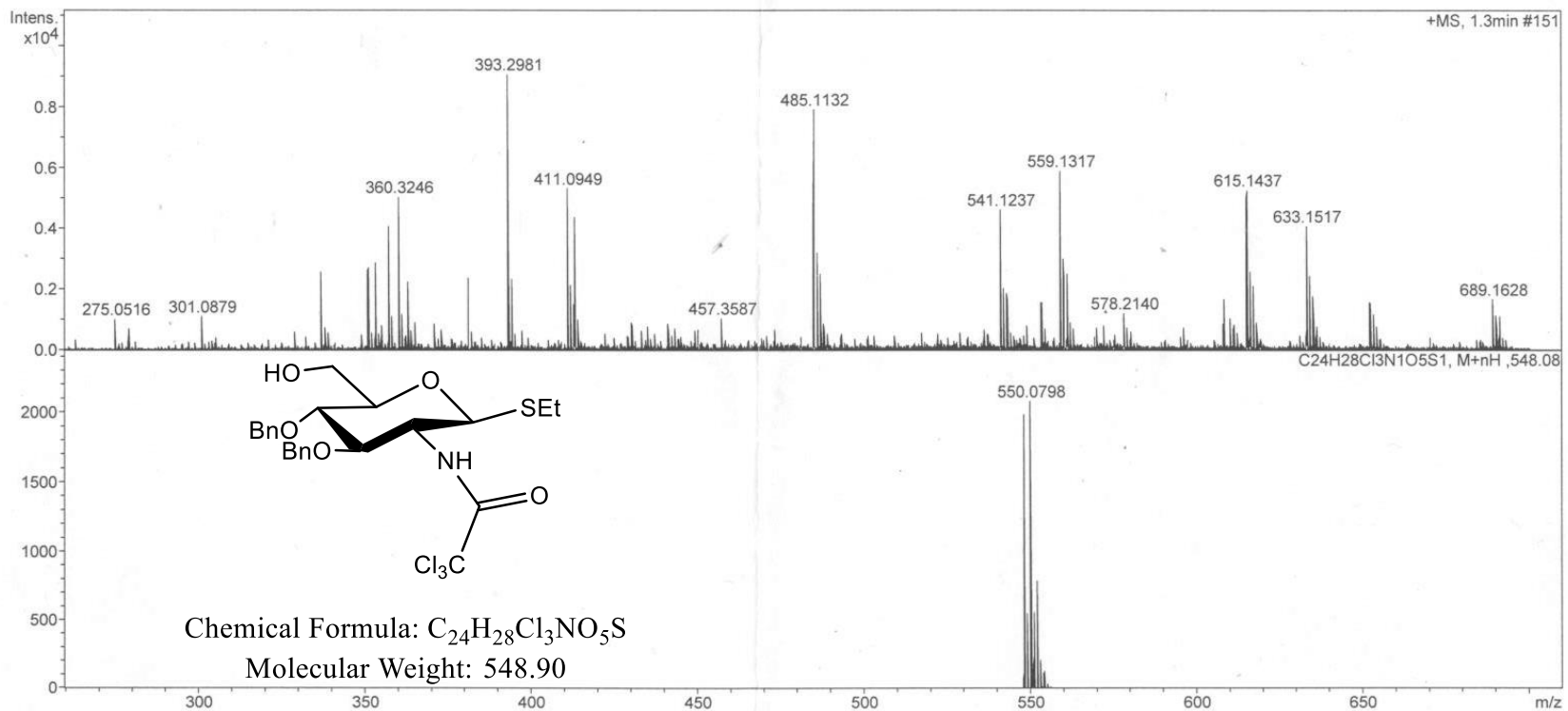


Figure A. 4- Recovery of NAG Building Block by Chlorocarbonyl Polystyrene Beads- Cartridge A

**Analysis Information**

Analysis Filename maf57921ks\_P1-F-3\_01\_64935.d  
Method 600p\_meoh1260\_2c1s.m  
Submission Name maf57921ks  
Instrument micrOTOF  
ESI Positive

Acquisition Date 11/03/2016 15:04:38

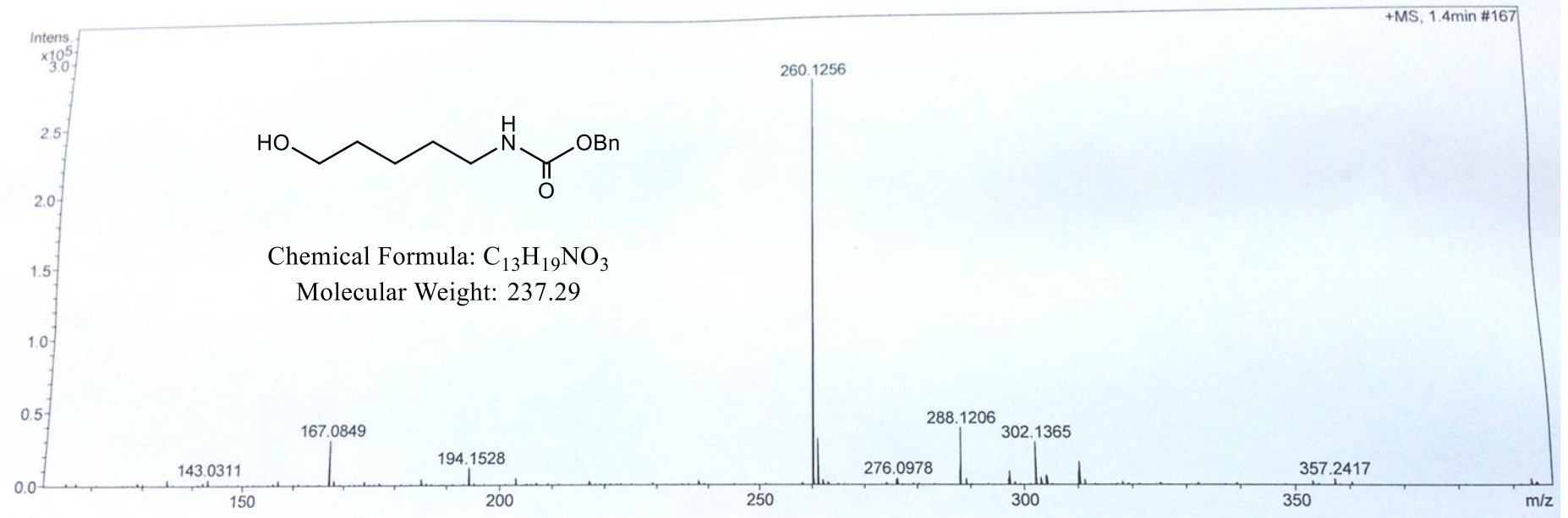


**Figure A. 5- Recovery of NAG Building Block by Chlorocarbonyl Polystyrene Beads- Cartridge B**

Analysis Information

Analysis Filename maf57898ks\_P1-D-1\_01\_64910.d  
Method 400p\_meoh1260\_2c1s.m  
Submission Name maf57898ks  
Instrument micrOTOF  
ESI Positive

Acquisition Date 10/03/2016 16:02:43



Meas. m/z	#	Formula	m/z	err [ppm]	err [mDa]	mSigma	Mean err [ppm]
260.1256	1	C 13 H 19 N Na O 3	260.1257	0.5	0.1	19.8	0.4

Figure A. 6- Photocleavage of Resin

## BIBLIOGRAPHY

- ALEXANDER, J. W. & FISHER, M. W. 1970. Vaccination for *Pseudomonas aeruginosa*. *Am J Surg*, 120, 512.
- ALEXANDER, S. A., KYI, C. & SCHIESSER, C. H. 2015. Nitroxides as anti-biofilm compounds for the treatment of *Pseudomonas aeruginosa* and mixed-culture biofilms. *Org Biomol Chem*, 13, 4751-9.
- ALKAWASH, M. A., SOOTHILL, J. S. & SCHILLER, N. L. 2006. Alginate lyase enhances antibiotic killing of mucoid *Pseudomonas aeruginosa* in biofilms. *Apmis*, 114, 131-138.
- BAHAR, A. A. 2015. *Controlling biofilm and persister cells by targeting cell membranes*. Syracuse University.
- BATHOORN, E., SLEBOS, D.-J., POSTMA, D. S., KOETER, G. H., VAN OOSTERHOUT, A. J. M., VAN DER TOORN, M., BOEZEN, H. M. & KERSTJENS, H. A. M. 2007. Anti-inflammatory effects of inhaled carbon monoxide in patients with COPD: a pilot study. *European Respiratory Journal*, 30, 1131-1137.
- BAYER, A. S., SPEERT, D. P., PARK, S., TU, J., WITT, M., NAST, C. C. & NORMAN, D. C. 1991. Functional role of mucoid exopolysaccharide (alginate) in antibiotic-induced and polymorphonuclear leukocyte-mediated killing of *Pseudomonas aeruginosa*. *Infection and immunity*, 59, 302-308.
- BERRY, A., DEVAULT, J. D. & CHAKRABARTY, A. 1989. High osmolarity is a signal for enhanced algD transcription in mucoid and nonmucoid *Pseudomonas aeruginosa* strains. *Journal of bacteriology*, 171, 2312-2317.
- BHAGIRATH, A. Y., LI, Y., SOMAYAJULA, D., DADASHI, M., BADR, S. & DUAN, K. 2016. Cystic fibrosis lung environment and *Pseudomonas aeruginosa* infection. *BMC Pulmonary Medicine*, 16, 174.
- BHARGAVA, N., SHARMA, P. & CAPALASH, N. 2014. Pyocyanin Stimulates Quorum Sensing-Mediated Tolerance to Oxidative Stress and Increases Persister Cell Populations in *Acinetobacter baumannii*. *Infection and Immunity*, 82, 3417-3425.
- CALIN, O., ELLER, S. & SEEBERGER, P. H. 2013a. Automated polysaccharide synthesis: assembly of a 30mer mannoside. *Angewandte Chemie International Edition*, 52, 5862-5865.
- CALIN, O., ELLER, S. & SEEBERGER, P. H. 2013b. Automated polysaccharide synthesis: assembly of a 30mer mannoside. *Angew Chem Int Ed Engl*, 52, 5862-5.

- CASTELLANI, C., CUPPENS, H., MACEK, M., CASSIMAN, J., KEREM, E., DURIE, P., TULLIS, E., ASSAEL, B., BOMBIERI, C. & BROWN, A. 2008. Consensus on the use and interpretation of cystic fibrosis mutation analysis in clinical practice. *Journal of cystic fibrosis*, 7, 179-196.
- CHAPARRO, C., MAURER, J., GUTIERREZ, C., KRAJEN, M., CHAN, C., WINTON, T., KESHAVJEE, S., SCAVUZZO, M., TULLIS, E., HUTCHEON, M. & KESTEN, S. 2001. Infection with *Burkholderia cepacia* in cystic fibrosis: outcome following lung transplantation. *Am J Respir Crit Care Med*, 163, 43-8.
- CHEN, K. M., CHIANG, M. K., WANG, M., HO, H. C., LU, M. C. & LAI, Y. C. 2014. The role of *pgaC* in *Klebsiella pneumoniae* virulence and biofilm formation. *Microb Pathog*, 77, 89-99.
- CHMIEL, J. F. & KONSTAN, M. W. 2005. Anti-inflammatory medications for cystic fibrosis lung disease. *Treatments in respiratory medicine*, 4, 255-273.
- COLLOT, M., ELLER, S., WEISHAUPT, M. & SEEBERGER, P. H. 2013. Glycosylation efficiencies on different solid supports using a hydrogenolysis-labile linker. *Beilstein journal of organic chemistry*, 9, 97-105.
- COX, C. D. 1986. Role of pyocyanin in the acquisition of iron from transferrin. *Infection and immunity*, 52, 263-270.
- DAMRON, F. H. & GOLDBERG, J. B. 2012. Proteolytic regulation of alginate overproduction in *Pseudomonas aeruginosa*. *Molecular microbiology*, 84, 595-607.
- DAS, T. & MANEFIELD, M. 2012. Pyocyanin promotes extracellular DNA release in *Pseudomonas aeruginosa*. *PLoS One*, 7, e46718.
- DAVIES, J. C. 2002. *Pseudomonas aeruginosa* in cystic fibrosis: pathogenesis and persistence. *Paediatric Respiratory Reviews*, 3, 128-134.
- DAVIES, J. C. & RUBIN, B. K. Emerging and unusual gram-negative infections in cystic fibrosis. *Seminars in respiratory and critical care medicine*, 2007. Copyright© 2007 by Thieme Medical Publishers, Inc., 333 Seventh Avenue, New York, NY 10001, USA., 312-321.
- DAVIS, B. G. & FAIRBANKS, A. J. 2002. Carbohydrate chemistry. *Oxford Chemistry Primers*, 99, ALL-ALL.
- DE BOECK, K., ZOLIN, A., CUPPENS, H., OLESEN, H. V. & VIVIANI, L. 2014. The relative frequency of CFTR mutation classes in European patients with cystic fibrosis. *Journal of Cystic Fibrosis*, 13, 403-409.



- DESMARD, M., DAVIDGE, K. S., BOUVET, O., MORIN, D., ROUX, D., FORESTI, R., RICARD, J. D., DENAMUR, E., POOLE, R. K. & MONTRAVERS, P. 2009. A carbon monoxide-releasing molecule (CORM-3) exerts bactericidal activity against *Pseudomonas aeruginosa* and improves survival in an animal model of bacteraemia. *The FASEB Journal*, 23, 1023-1031.
- DESMARD, M., FORESTI, R., MORIN, D., DAGOUASSAT, M., BERDEAUX, A., DENAMUR, E., CROOK, S. H., MANN, B. E., SCAPENS, D. & MONTRAVERS, P. 2012. Differential antibacterial activity against *Pseudomonas aeruginosa* by carbon monoxide-releasing molecules. *Antioxidants & redox signaling*, 16, 153-163.
- DIAZ DE RIENZO, M. A., STEVENSON, P. S., MARCHANT, R. & BANAT, I. M. 2016. *Pseudomonas aeruginosa* biofilm disruption using microbial surfactants. *J Appl Microbiol*, 120, 868-76.
- DÖRING, G., FLUME, P., HEIJERMAN, H., ELBORN, J. S. & CONSENSUS STUDY, G. 2012. Treatment of lung infection in patients with cystic fibrosis: current and future strategies. *Journal of Cystic Fibrosis*, 11, 461-479.
- DREVINEK, P. & MAHENTHIRALINGAM, E. 2010. *Burkholderia cenocepacia* in cystic fibrosis: epidemiology and molecular mechanisms of virulence. *Clinical Microbiology and Infection*, 16, 821-830.
- ECKFORD, P. D., LI, C., RAMJESINGH, M. & BEAR, C. E. 2012. Cystic fibrosis transmembrane conductance regulator (CFTR) potentiator VX-770 (ivacaftor) opens the defective channel gate of mutant CFTR in a phosphorylation-dependent but ATP-independent manner. *Journal of Biological Chemistry*, 287, 36639-36649.
- EDVAR ONSOYEN, R. M. 2008. *Use of alginate oligomers in combating biofilms*
- ELLER, S., COLLOT, M., YIN, J., HAHM, H. S. & SEEBERGER, P. H. 2013. Automated Solid - Phase Synthesis of Chondroitin Sulfate Glycosaminoglycans. *Angewandte Chemie International Edition*, 52, 5858-5861.
- FARJAH, A., OWLIA, P., SIADAT, S. D., MOUSAVI, S. F., ARDESTANI, M. S. & MOHAMMADPOUR, H. K. 2015. Immunological evaluation of an alginate - based conjugate as a vaccine candidate against *Pseudomonas aeruginosa*. *Apmis*, 123, 175-183.
- FORDE, É., HUMPHREYS, H., GREENE, C. M., FITZGERALD-HUGHES, D. & DEVOCELLE, M. 2014. Potential of host defense peptide prodrugs as neutrophil elastase-dependent anti-infective agents for cystic fibrosis. *Antimicrobial agents and chemotherapy*, 58, 978-985.

- FRASER-REID, B. O., TATSUTA, K. & THIEM, J. 2012. *Glycoscience: Chemistry and chemical biology I–III*, Springer Science & Business Media.
- FUSE, K., FUJIMURA, S., KIKUCHI, T., GOMI, K., IIDA, Y., NUKIWA, T. & WATANABE, A. 2013. Reduction of virulence factor pyocyanin production in multidrug-resistant *Pseudomonas aeruginosa*. *Journal of Infection and Chemotherapy*, 19, 82-88.
- GAD, S. C. 2007. *Handbook of pharmaceutical biotechnology*, John Wiley & Sons.
- GENING, M. L., MAIRA-LITRÁN, T., KROPEC, A., SKURNIK, D., GROUT, M., TSVETKOV, Y. E., NIFANTIEV, N. E. & PIER, G. B. 2010. Synthetic  $\beta$ -(1 $\rightarrow$ 6)-linked N-acetylated and nonacetylated oligoglucosamines used to produce conjugate vaccines for bacterial pathogens. *Infection and immunity*, 78, 764-772.
- GOSS, C. H. & MUHLEBACH, M. S. 2011. Review: *Staphylococcus aureus* and MRSA in cystic fibrosis. *Journal of Cystic Fibrosis*, 10, 298-306.
- GOSS, C. H., OTTO, K., AITKEN, M. L. & RUBENFELD, G. D. 2002. Detecting *Stenotrophomonas maltophilia* Does Not Reduce Survival of Patients with Cystic Fibrosis. *American Journal of Respiratory and Critical Care Medicine*, 166, 356-361.
- GULLAND, A. 2016. Cystic fibrosis drug is not cost effective, says NICE. *BMJ: British Medical Journal*, 353.
- GUO, J. & YE, X.-S. 2010. Protecting groups in carbohydrate chemistry: influence on stereoselectivity of Glycosylations. *Molecules*, 15, 7235-7265.
- HAO, Y., KUANG, Z., XU, Y., WALLING, B. E. & LAU, G. W. 2013. Pyocyanin-induced mucin production is associated with redox modification of FOXA2. *Respiratory research*, 14, 82.
- HASSANI, H. H., HASAN, H. M., AL-SAAD, A., ALI, A. M. & MUHAMMAD, M. H. 2012. A comparative study on cytotoxicity and apoptotic activity of pyocyanin produced by wild type and mutant strains of *Pseudomonas aeruginosa*. *Eur J Exp Biol*, 2, 1389-1394.
- HEIDI, L. 2012. Drug bests cystic-fibrosis mutation. *Nature*, 482, 145.
- HEIJERMAN, H., WESTERMAN, E., CONWAY, S. & TOUW, D. 2009a. Inhaled medication and inhalation devices for lung disease in patients with cystic fibrosis: A European consensus. *Journal of Cystic Fibrosis*, 8, 295-315.
- HEIJERMAN, H., WESTERMAN, E., CONWAY, S., TOUW, D. & GERD DÖRING FOR THE CONSENSUS WORKING, G. 2009b. Inhaled medication and inhalation devices for

- lung disease in patients with cystic fibrosis: a European consensus. *Journal of Cystic Fibrosis*, 8, 295-315.
- HELTSHE, S. L., MAYER-HAMBLETT, N., BURNS, J. L., KHAN, U., BAINES, A., RAMSEY, B. W. & ROWE, S. M. 2014. Pseudomonas aeruginosa in cystic fibrosis patients with G551D-CFTR treated with ivacaftor. *Clinical Infectious Diseases*, ciu944.
- HØIBY, N. 2002. Understanding bacterial biofilms in patients with cystic fibrosis: current and innovative approaches to potential therapies. *Journal of Cystic Fibrosis*, 1, 249-254.
- HOIBY, N., CIOFU, O. & BJARNSHOLT, T. 2010. Pseudomonas aeruginosa biofilms in cystic fibrosis. *Future Microbiol*, 5, 1663-74.
- HOOK, B. D. A., DOHLE, W., HIRST, P. R., PICKWORTH, M., BERRY, M. B. & BOOKER-MILBURN, K. I. 2005. A practical flow reactor for continuous organic photochemistry. *The Journal of organic chemistry*, 70, 7558-7564.
- HORSLEY, A., JONES, A. M. & LORD, R. 2016. Antibiotic treatment for Burkholderia cepacia complex in people with cystic fibrosis experiencing a pulmonary exacerbation. *Cochrane Database Syst Rev*, Cd009529.
- HRAIECH, S., BRÉGEON, F. & ROLAIN, J.-M. 2015. Bacteriophage-based therapy in cystic fibrosis-associated Pseudomonas aeruginosa infections: rationale and current status. *Drug design, development and therapy*, 9, 3653.
- HURT, K. & BILTON, D. 2012. Cystic fibrosis. *Medicine*, 40, 273-276.
- IZANO, E. A., AMARANTE, M. A., KHER, W. B. & KAPLAN, J. B. 2008. Differential roles of poly-N-acetylglucosamine surface polysaccharide and extracellular DNA in Staphylococcus aureus and Staphylococcus epidermidis biofilms. *Applied and environmental microbiology*, 74, 470-476.
- J., B. L. 1980. *Carbonyl Frequencies*, Netherlands, Dordrecht, Springer
- JENNINGS, H. J. 1990. Capsular Polysaccharides as Vaccine Candidates. In: JANN, K. & JANN, B. (eds.) *Bacterial Capsules*. Berlin, Heidelberg: Springer Berlin Heidelberg.
- JOHANSEN, H. K. & GØTZSCHE, P. C. 2015. Vaccines for preventing infection with Pseudomonas aeruginosa in cystic fibrosis. *The Cochrane Library*.
- KALDOR, S. W., SIEGEL, M. G., FRITZ, J. E., DRESSMAN, B. A. & HAHN, P. J. 1996. Use of solid supported nucleophiles and electrophiles for the purification of non-peptide small molecule libraries. *Tetrahedron letters*, 37, 7193-7196.
- KANDASAMY, J., HUREVICH, M. & SEEBERGER, P. H. 2013. Automated solid phase synthesis of oligoarabinofuranosides. *Chemical Communications*, 49, 4453-4455.

- KHAN, S., TØNDERVIK, A., SLETTA, H., KLINKENBERG, G., EMANUEL, C., ONSØYEN, E., MYRVOLD, R., HOWE, R. A., WALSH, T. R. & HILL, K. E. 2012. Overcoming drug resistance with alginate oligosaccharides able to potentiate the action of selected antibiotics. *Antimicrobial agents and chemotherapy*, 56, 5134-5141.
- KLARE, W., DAS, T., IBUGO, A., BUCKLE, E., MANEFIELD, M. & MANOS, J. 2016. Glutathione-Disrupted Biofilms of Clinical *Pseudomonas aeruginosa* Strains Exhibit an Enhanced Antibiotic Effect and a Novel Biofilm Transcriptome. *Antimicrobial agents and chemotherapy*, 60, 4539-4551.
- KREINDLER, J. L. 2010. Cystic fibrosis: Exploiting its genetic basis in the hunt for new therapies. *Pharmacology & therapeutics*, 125, 219-229.
- KRÖCK, L., ESPOSITO, D., CASTAGNER, B., WANG, C.-C., BINDSCHÄDLER, P. & SEEBERGER, P. H. 2012. Streamlined access to conjugation-ready glycans by automated synthesis. *Chemical Science*, 3, 1617-1622.
- KUK, K. & TAYLOR-COUSAR, J. L. 2015. Lumacaftor and ivacaftor in the management of patients with cystic fibrosis: current evidence and future prospects. *Therapeutic advances in respiratory disease*, 9, 313-326.
- LAM, J., CHAN, R., LAM, K. & COSTERTON, J. W. 1980. Production of mucoid microcolonies by *Pseudomonas aeruginosa* within infected lungs in cystic fibrosis. *Infection and immunity*, 28, 546-556.
- LANG, Y., ZHAO, X., LIU, L. & YU, G. 2014. Applications of Mass Spectrometry to Structural Analysis of Marine Oligosaccharides. *Marine Drugs*, 12, 4005-4030.
- LEBEAUX, D., GHIGO, J.-M. & BELOIN, C. 2014. Biofilm-Related Infections: Bridging the Gap between Clinical Management and Fundamental Aspects of Recalcitrance toward Antibiotics. *Microbiology and Molecular Biology Reviews : MMBR*, 78, 510-543.
- LIMOLI, D. H., WHITFIELD, G. B., KITAO, T., IVEY, M. L., DAVIS, M. R., GRAHL, N., HOGAN, D. A., RAHME, L. G., HOWELL, P. L. & O'TOOLE, G. A. 2017. *Pseudomonas aeruginosa* Alginate Overproduction Promotes Coexistence with *Staphylococcus aureus* in a Model of Cystic Fibrosis Respiratory Infection. *mBio*, 8, e00186-17.
- LIN, M. H., SHU, J. C., LIN, L. P., CHONG, K. Y., CHENG, Y. W., DU, J. F. & LIU, S.-T. 2015. Elucidating the Crucial Role of Poly N-Acetylglucosamine from *Staphylococcus aureus* in Cellular Adhesion and Pathogenesis. *PLoS ONE*, 10, e0124216.
- LINARES, J. F., GUSTAFSSON, I., BAQUERO, F. & MARTINEZ, J. L. 2006. Antibiotics as intermicrobial signaling agents instead of weapons. *Proceedings of the National Academy of Sciences*, 103, 19484-19489.

- LUNDGREN, B. R., THORNTON, W., DORNAN, M. H., VILLEGAS-PENARANDA, L. R., BODDY, C. N. & NOMURA, C. T. 2013. Gene PA2449 is essential for glycine metabolism and pyocyanin biosynthesis in *Pseudomonas aeruginosa* PAO1. *Journal of bacteriology*, 195, 2087-2100.
- MARKS, M. I. 1990. Clinical significance of *Staphylococcus aureus* in cystic fibrosis. *Infection*, 18, 53-6.
- MASUELLI, M. A. & ILLANES, C. 2014. Review of the characterization of sodium alginate by intrinsic viscosity measurements. Comparative analysis between conventional and single point methods. *Int. J. BioMater. Sci. Eng*, 1, 1-11.
- MAYER, M. 2016. Lumacaftor-ivacaftor (Orkambi) for cystic fibrosis: behind the 'breakthrough'. *Evidence Based Medicine*, 21, 83-86.
- MILLER, L. C., O'LOUGHLIN, C. T., ZHANG, Z., SIRYAPORN, A., SILPE, J. E., BASSLER, B. L. & SEMMELHACK, M. F. 2015. Development of Potent Inhibitors of Pyocyanin Production in *Pseudomonas aeruginosa*. *Journal of Medicinal Chemistry*, 58, 1298-1306.
- MIRANI, Z. A. & JAMIL, N. 2011. Effect of sub-lethal doses of vancomycin and oxacillin on biofilm formation by vancomycin intermediate resistant *Staphylococcus aureus*. *J Basic Microbiol*, 51, 191-5.
- MIZUGUCHI, S., CAPRETTA, A., SUEHIRO, S., NISHIYAMA, N., LUKE, P., POTTER, R. F., FRASER, D. D. & CEPINSKAS, G. 2010. Carbon monoxide-releasing molecule CORM-3 suppresses vascular endothelial cell SOD-1/SOD-2 activity while up-regulating the cell surface levels of SOD-3 in a heparin-dependent manner. *Free Radical Biology and Medicine*, 49, 1534-1541.
- MOIGNE, V. L., GAILLARD, J. L. & HERRMANN, J. L. 2016. Vaccine strategies against bacterial pathogens in cystic fibrosis patients. *Médecine et Maladies Infectieuses*, 46, 5.
- MOTTERLINI, R. & OTTERBEIN, L. E. 2010. The therapeutic potential of carbon monoxide. *Nature reviews Drug discovery*, 9, 728-743.
- MULLER, M. & MERRETT, N. D. 2014. Pyocyanin Production by *Pseudomonas aeruginosa* Confers Resistance to Ionic Silver. *Antimicrobial Agents and Chemotherapy*, 58, 5492-5499.
- MURRAY, T. S., OKEGBE, C., GAO, Y., KAZMIERCZAK, B. I., MOTTERLINI, R., DIETRICH, L. E. P. & BRUSCIA, E. M. 2012. The carbon monoxide releasing molecule CORM-2 attenuates *Pseudomonas aeruginosa* biofilm formation. *PLoS One*, 7, e35499.

- MUTLUOGLU, M. & UZUN, G. 2011. Pseudomonas infection in a postoperative foot wound. *Canadian Medical Association Journal*, 183, E499-E499.
- NEISES, B. & STEGLICH, W. 1978. Simple method for the esterification of carboxylic acids. *Angewandte Chemie International Edition in English*, 17, 522-524.
- NILSSON, K. G. I. 1988. Enzymatic synthesis of oligosaccharides. *Trends in Biotechnology*, 6, 256-264.
- NOAH, T. L., IVINS, S. S., ABODE, K. A., STEWART, P. W., MICHELSON, P. H., HARRIS, W. T., HENRY, M. M. & LEIGH, M. W. 2010. Inhaled versus systemic antibiotics and airway inflammation in children with cystic fibrosis and Pseudomonas. *Pediatric pulmonology*, 45, 281-290.
- NOBRE, L. S., AL-SHAHROUR, F., DOPAZO, J. & SARAIVA, L. M. 2009. Exploring the antimicrobial action of a carbon monoxide-releasing compound through whole-genome transcription profiling of Escherichia coli. *Microbiology*, 155, 813-824.
- NOBRE, L. S., SEIXAS, J. D., ROMÃO, C. C. & SARAIVA, L. M. 2007. Antimicrobial action of carbon monoxide-releasing compounds. *Antimicrobial agents and chemotherapy*, 51, 4303-4307.
- OTTERBEIN, L. E. 2002. Carbon monoxide: innovative anti-inflammatory properties of an age-old gas molecule. *Antioxidants and Redox Signaling*, 4, 309-319.
- OTTERBEIN, L. E., BACH, F. H., ALAM, J., SOARES, M., LU, H. T., WYSK, M., DAVIS, R. J., FLAVELL, R. A. & CHOI, A. M. K. 2000. Carbon monoxide has anti-inflammatory effects involving the mitogen-activated protein kinase pathway. *Nature medicine*, 6, 422-428.
- PLANTE, O. J., BUCHWALD, S. L. & SEEBERGER, P. H. 2000. Halobenzyl ethers as protecting groups for organic synthesis. *Journal of the American Chemical Society*, 122, 7148-7149.
- PLANTE, O. J., PALMACCI, E. R. & SEEBERGER, P. H. 2001. Automated Solid-Phase Synthesis of Oligosaccharides. *Science*, 291, 1523-1527.
- POWELL, L. C., PRITCHARD, M. F., EMANUEL, C., ONSØYEN, E., RYE, P. D., WRIGHT, C. J., HILL, K. E. & THOMAS, D. W. 2014. A nanoscale characterization of the interaction of a novel alginate oligomer with the cell surface and motility of Pseudomonas aeruginosa. *American journal of respiratory cell and molecular biology*, 50, 483-492.
- PRIEBE, G. P. & GOLDBERG, J. B. 2014. Vaccines for Pseudomonas aeruginosa: A long and winding road. *Expert review of vaccines*, 13, 507-519.

- RATJEN, F., DÖRING, G. & NIKOLAIZIK, W. H. 2001. Effect of inhaled tobramycin on early *Pseudomonas aeruginosa* colonisation in patients with cystic fibrosis. *The Lancet*, 358, 983-984.
- RENNA, M., SCHAFFNER, C., BROWN, K., SHANG, S., TAMAYO, M. H., HEGYI, K., GRIMSEY, N. J., CUSENS, D., COULTER, S. & COOPER, J. 2011. Azithromycin blocks autophagy and may predispose cystic fibrosis patients to mycobacterial infection. *The Journal of clinical investigation*, 121, 3554-3563.
- ROBERTS, J. L., KHAN, S., EMANUEL, C., POWELL, L. C., PRITCHARD, M., ONSØYEN, E., MYRVOLD, R., THOMAS, D. W. & HILL, K. E. 2013. An in vitro study of alginate oligomer therapies on oral biofilms. *Journal of dentistry*, 41, 892-899.
- RYTER, S. W. & CHOI, A. M. K. 2006. Therapeutic applications of carbon monoxide in lung disease. *Current Opinion in Pharmacology*, 6, 257-262.
- SCHATZSCHNEIDER, U. 2015. Novel lead structures and activation mechanisms for CO - releasing molecules (CORMs). *British journal of pharmacology*, 172, 1638-1650.
- SCHNEIDER, E. K., AZAD, M. A., HAN, M.-L., ZHOU, Q. T., WANG, J., HUANG, J. X., COOPER, M. A., DOI, Y., BAKER, M. A. & BERGEN, P. J. 2016. An 'unlikely'pair: The antimicrobial synergy of polymyxin B in combination with the cystic fibrosis trans-membrane conductance regulator drugs KALYDECO and ORKAMBI. *ACS Infectious Diseases*.
- SCHRAM, C. A. 2012. Atypical cystic fibrosis Identification in the primary care setting. *Canadian Family Physician*, 58, 1341-1345.
- SCHÜLIN, T. 2002. In vitro activity of the aerosolized agents colistin and tobramycin and five intravenous agents against *Pseudomonas aeruginosa* isolated from cystic fibrosis patients in southwestern Germany. *Journal of Antimicrobial Chemotherapy*, 49, 403-406.
- SEEBERGER, P. H. 2004. *Solid support oligosaccharide synthesis and combinatorial carbohydrate libraries*, John Wiley & Sons.
- SEEBERGER, P. H., FINNEY, N., RABUKA, D. & BERTOZZI, C. R. 2009. Chemical and enzymatic synthesis of glycans and glycoconjugates.
- SEEBERGER, P. H. & HAASE, W.-C. 2000. Solid-phase oligosaccharide synthesis and combinatorial carbohydrate libraries. *Chemical reviews*, 100, 4349-4394.
- SHAH, P. L., SCOTT, S. F., KNIGHT, R. A., MARRIOTT, C., RANASINHA, C. & HODSON, M. E. 1996. In vivo effects of recombinant human DNase I on sputum in patients with cystic fibrosis. *Thorax*, 51, 119-125.

- SHAH, V. S., MEYERHOLZ, D. K., TANG, X. X., REZNIKOV, L., ALAIWA, M. A., ERNST, S. E., KARP, P. H., WOHLFORD-LENANE, C. L., HEILMANN, K. P. & LEIDINGER, M. R. 2016. Airway acidification initiates host defense abnormalities in cystic fibrosis mice. *Science*, 351, 503-507.
- SHAWAR, R. M., MACLEOD, D. L., GARBER, R. L., BURNS, J. L., STAPP, J. R., CLAUSEN, C. R. & TANAKA, S. K. 1999. Activities of tobramycin and six other antibiotics against *Pseudomonas aeruginosa* isolates from patients with cystic fibrosis. *Antimicrobial agents and chemotherapy*, 43, 2877-2880.
- SMITH, E. E., BUCKLEY, D. G., WU, Z., SAENPHIMMACHAK, C., HOFFMAN, L. R., D'ARGENIO, D. A., MILLER, S. I., RAMSEY, B. W., SPEERT, D. P. & MOSKOWITZ, S. M. 2006. Genetic adaptation by *Pseudomonas aeruginosa* to the airways of cystic fibrosis patients. *Proceedings of the National Academy of Sciences*, 103, 8487-8492.
- SMITH, R. S. & IGLEWSKI, B. H. 2003. *Pseudomonas aeruginosa* quorum sensing as a potential antimicrobial target. *Journal of Clinical Investigation*, 112, 1460-1465.
- SRIRAMULU, D. 2013. Evolution and impact of bacterial drug resistance in the context of cystic fibrosis disease and nosocomial settings. *Microbiology insights*, 6, 29.
- STAMELLOU, E., STORZ, D., BOTOV, S., NTASIS, E., WEDEL, J., SOLLAZZO, S., KRÄMER, B., VAN SON, W., SEELEN, M. & SCHMALZ, H. 2014. Different design of enzyme-triggered CO-releasing molecules (ET-CORMs) reveals quantitative differences in biological activities in terms of toxicity and inflammation. *Redox biology*, 2, 739-748.
- STANTON, B. A. 2017. Adverse Effects of *Pseudomonas aeruginosa* on CFTR Chloride Secretion and the Host Immune Response. *American Journal of Physiology-Cell Physiology*, ajpcell. 00373.2016.
- STEEN, R. 2017. *An investigation into pyocyanin-triggered carbon monoxide-releasing molecules*. Masters by Research, University of York.
- THEILACKER, C., COLEMAN, F. T., MUESCHENBORN, S., LLOSA, N., GROUT, M. & PIER, G. B. 2003. Construction and characterization of a *Pseudomonas aeruginosa* mucoid exopolysaccharide-alginate conjugate vaccine. *Infection and immunity*, 71, 3875-3884.
- TINAJERO-TREJO, M., RANA, N., NAGEL, C., JESSE, H. E., SMITH, T. W., WAREHAM, L. K., HIPPLER, M., SCHATZSCHNEIDER, U. & POOLE, R. K. 2016. Antimicrobial Activity of the Manganese Photoactivated Carbon Monoxide-Releasing Molecule [Mn (CO) 3



- (tpa-κ3 N)]+ Against a Pathogenic Escherichia coli that Causes Urinary Infections. *Antioxidants & redox signaling*, 24, 765-780.
- TROXLER, R. B., HOOVER, W. C., BRITTON, L. J., GERWIN, A. M. & ROWE, S. M. 2012. Clearance of initial mucoid Pseudomonas aeruginosa in patients with cystic fibrosis. *Pediatric pulmonology*, 47, 1113-1122.
- TURNER, K. H., WESSEL, A. K., PALMER, G. C., MURRAY, J. L. & WHITELEY, M. 2015. Essential genome of Pseudomonas aeruginosa in cystic fibrosis sputum. *Proceedings of the National Academy of Sciences*, 112, 4110-4115.
- USHER, L. R., LAWSON, R. A., GEARY, I., TAYLOR, C. J., BINGLE, C. D., TAYLOR, G. W. & WHYTE, M. K. B. 2002. Induction of neutrophil apoptosis by the Pseudomonas aeruginosa exotoxin pyocyanin: a potential mechanism of persistent infection. *The Journal of Immunology*, 168, 1861-1868.
- WEAVER, L. G., SINGH, Y., BLANCHFIELD, J. T. & BURN, P. L. 2013. A simple iterative method for the synthesis of  $\beta$ -(1 → 6)-glucosamine oligosaccharides. *Carbohydrate Research*, 371, 68-76.
- WILSCHANSKI, M., ZIELENSKI, J., MARKIEWICZ, D., TSUI, L.-C., COREY, M., LEVISON, H. & DURIE, P. R. 1995. Correlation of sweat chloride concentration with classes of the cystic fibrosis transmembrane conductance regulator gene mutations. *The Journal of Pediatrics*, 127, 705-710.
- WINSTANLEY, C. & FOTHERGILL, J. L. 2009. The role of quorum sensing in chronic cystic fibrosis Pseudomonas aeruginosa infections. *FEMS microbiology letters*, 290, 1-9.
- WOOD, A. J. J. & RAMSEY, B. W. 1996. Management of pulmonary disease in patients with cystic fibrosis. *New England Journal of Medicine*, 335, 179-188.
- WU, P. E. & JUURLINK, D. N. 2014. Carbon monoxide poisoning. *Canadian Medical Association Journal*, 186, 611-611.
- YAKANDAWALA, N., GAWANDE, P. V., LOVETRI, K., CARDONA, S. T., ROMEO, T., NITZ, M. & MADHYASTHA, S. 2011. Characterization of the poly- $\beta$ -1, 6-N-acetylglucosamine polysaccharide component of Burkholderia biofilms. *Applied and environmental microbiology*, 77, 8303-8309.
- YAN, G. L., GUO, Y. M., YUAN, J. M., LIU, D. & ZHANG, B. K. 2011. Sodium alginate oligosaccharides from brown algae inhibit Salmonella Enteritidis colonization in broiler chickens. *Poultry science*, 90, 1441-1448.
- YOON, S. S., HENNIGAN, R. F., HILLIARD, G. M., OCHSNER, U. A., PARVATIYAR, K., KAMANI, M. C., ALLEN, H. L., DEKIEVIT, T. R., GARDNER, P. R. & SCHWAB, U. 2002.

- Pseudomonas aeruginosa* anaerobic respiration in biofilms: relationships to cystic fibrosis pathogenesis. *Developmental cell*, 3, 593-603.
- ZHANG, L. & MAH, T.-F. 2008. Involvement of a novel efflux system in biofilm-specific resistance to antibiotics. *Journal of bacteriology*, 190, 4447-4452.
- ZHANG, W. Q., ATKIN, A. J., THATCHER, R. J., WHITWOOD, A. C., FAIRLAMB, I. J. & LYNAM, J. M. 2009. Diversity and design of metal-based carbon monoxide-releasing molecules (CO-RMs) in aqueous systems: revealing the essential trends. *Dalton Trans*, 4351-8.
- ZHAO, J., SCHLOSS, P. D., KALIKIN, L. M., CARMODY, L. A., FOSTER, B. K., PETROSINO, J. F., CAVALCOLI, J. D., VANDEVANTER, D. R., MURRAY, S. & LI, J. Z. 2012. Decade-long bacterial community dynamics in cystic fibrosis airways. *Proceedings of the National Academy of Sciences*, 109, 5809-5814.
- ZHU, X. & SCHMIDT, R. R. 2009. New Principles for Glycoside - Bond Formation. *Angewandte Chemie International Edition*, 48, 1900-1934.
- ZOBI, F. 2013. CO and CO-releasing molecules in medicinal chemistry. *Future medicinal chemistry*, 5, 175-188.